Nuclear Medicine Communications

Abstracts

British Nuclear Medicine Society Spring Meeting 2022

Nuclear Medicine Communications 2022, **43:** 577–623

01. Radiolabelling, biodistribution and in-vivo imaging of [^{99m}Tc] NaTcO4 labelled sialic acid in rat induced tumour: a preclinical study

Ravi Ranjan Kumar[a,b], Devinder Kumar Dhawan[c], Vijayata Dani Chadha[d]
[a]*Alliance Medical Ltd, Southwest, United Kingdom.*
[b]*Panjab University, Chandigarh, India.*
[c]*Panjab University, Dept. Of Biophysics, Chandigarh, India.*
[d]*Panjab University, Centre for Nuclear Medicine, Chandigarh, India*

Purpose: Sialic acids are family of 9-carbon amino sugars containing polyfunctional oxygen rich ligand and located on terminal positions of cell surface. More recent evidence shown that the exogenous sialic acid supplemented in culture medium were effectively taken up in various tumour cells. However, to date the use of sialic acid for in-vivo tumour imaging in animals has been largely unexplored. In the present study, N-acetyl neuraminic acid (Neu5Ac) and it is most common type of sialic acid was radiolabeled with gamma emitter [^{99m}Tc] NaTcO4 bio evaluation was performed.

Material and Methods: We followed a direct radiolabelling protocol for radiolabelling of [^{99m}Tc] NaTcO4 with Neu5Ac. HPLC and mass spectra studies were performed to confirm the binding of [^{99m}Tc] NaTcO4 with Neu5Ac. Biodistribution and imaging of [^{99m}Tc] Tc- Neu5Ac in normal and tumour bearing rats were performed.

Results: Radiolabelling of Neu5Ac with [^{99m}Tc] NaTcO4 was obtained with a maximum labelling yield of 93.6%. HPLC results showed single peak appeared with retention time 7.34 minutes while cold Neu5Ac peak appeared at retention time 7.83 minutes. In ESI-MS characterization, the mass spectrum of the cold Neu5Ac and radio complex mixture showed at (m/z)+ mass 332. Whereas radio complex of [^{99m}Tc]Tc-Neu5Ac showed while another peak was observed at 424 and 731. Biodistribution and scintigraphic studies exhibited accumulation of activity in the colon of tumour bearing rats

Conclusions: In conclusion [^{99m}Tc] Tc- Neu5Ac accumulates in in-vivo cancer tissue and has potential to be exploited further for its role in tumour imaging.

02. Optimisation and implementation of scandium-44 and manganese-52 production at King's College London

Veronika Rosecker[a], Esra Korpe[a], Karin Michaelsen Nielsen[a], David Parker[b], Graeme J Stasiuk[a], Philip Blower[a]
[a]*Department of Imaging Chemistry & Biology, School of Biomedical Engineering & Imaging Sciences, King's College London, London, United Kingdom.*
[b]*School of Physics and Astronomy, University of Birmingham, Birmingham, United Kingdom*

Scandium-44 ($t_{½}$: 3.97 h) has similar chemical and decay characteristics to the widely used gallium-68 in PET imaging, but its longer half-life allows off-site production/shipping and imaging over a longer time span. Together with the β^+-emitting scandium-47 ($t_{½}$: 3.35 d) it is a very promising true theragnostic pair. ^{44}Sc is cyclotron-produced by <16 MeV proton bombardment of calcium and purified by cation exchange resin with strong affinity for scandium (v.d.Meulen NP. 2015, 42:745-751. Nucl.Med. Biol.). Our preliminary results show >95% recovery of Sc with trace amounts of Ca after one separation cycle. Herein we present a first radioanalytical characterisation of our cyclotron target and optimised radiochemical separation to implement ^{44}Sc PET.

Interest in manganese-52 ($t_{½}$: 5.59 d) has increased due to its potential use in dual-imaging for PET/MR imaging, its importance in *in vivo* tracking of slow pharmacokinetic processes and imaging of manganese dependent biological processes. ^{52}Mn is cyclotron-produced either by 8-17 MeV proton bombardment of chromium (Barrett KE. 2021, 96-97:19-26. Nucl.Med.Biol.) or by 35-40 MeV α-bombardment of vanadium (Ali BM. 2018, 90:1-9. Pramana-J.Phys.), yielding 86% and 64% of the theoretical yield at low current (15 μA and 2.5 μA), respectively, in our hands. While the latter route can yield a higher radionuclidic purity product, it is limited to alpha beam cyclotrons such as the MC40 at the University of Birmingham. With our smart target design and irradiation and separation process optimisation for both production routes the yield and purity can be fine-tuned. First results towards the implementation of ^{52}Mn production at KCL will be presented.

DOI: 10.1097/MNM.0000000000001555

03. Targeting microbial siderophore receptors: first GMP formulation of [^{68}Ga]Ga-DFO for PET imaging of microbial infection

Afnan Darwesh[a], Maggie Cooper[a], Victoria Gibson[b], Sally Barrington[a], Morad Sallam[b], Amita Patel[b], Vincenzo Abbate[a], Asma Akter[a], Michelle Ma[a], Julia Blower[a], Philip Blower[a]
[a]*King's College London, London, United Kingdom.*
[b]*Guy's and St. Thomas' NHS Foundation Trust, London, United Kingdom*

Purpose: Vascular stents are introduced into patients' arteries to treat arterial blockages or aneurysms. Stents can become infected with bacteria, requiring antimicrobial treatment and/or stent removal and, consequently, significant morbidity and mortality, which could be mitigated by early detection and identification of the infection. Bacteria obtain the iron (Fe) they require to proliferate by secreting siderophores that sequester Fe(III) from their environment and assimilating it via their cell-surface receptors. Gallium(III) (Ga(III)), having similar chemical properties to Fe(III), also binds to siderophores to give isostructural species that are also assimilated. We therefore hypothesise that siderophores, such as desferrioxamine (DFO), radiolabelled with gallium-68, can in principle be used to image and diagnose bacterial infection of vascular stents.

Method: We developed a simple GMP-compatible radiosynthesis of [^{68}Ga]Ga-DFO using GMP-grade reagents overcoming several barriers to translation. We developed GMP compliant analysis methods using thin layer chromatography supported by validation against an HPLC method and tested stability in serum and urine. In vivo biodistribution of [^{68}Ga]Ga-DFO in healthy mice was investigated.

Results: Radiochemical purity (RCP) was consistently ≥ 95% when using ^{68}Ga chloride eluted from a Galli Ad® (IRE) generator and GMP grade sodium acetate buffer. However, RCP fell to 90-95% when using a GalliaPharm® (Eckert & Ziegler) where the elution volume is greater. The product was stable for >3 hr, sterile and endotoxin free.

Conclusion: a GMP compliant method for translation of [^{68}Ga]Ga-DFO to a clinical setting was achieved and the product is now in clinical evaluation for infection imaging of vascular stents.

04. Development of Vape Devices for use in PET ventilation studies

Glenn Woolley[a,b], George Herbert[b], Dave Roberts[b], Juozas Domarkas[b], Graham Wright[a], Steve Archibald[b]
[a]*Hull University Teaching Hospitals NHS, Hull, United Kingdom.*
[b]*University of Hull, Hull, United Kingdom*

Introduction: Conventional aerosol delivery devices, such as nebulisers, produce low outputs requiring large amounts of activity for clinical imaging. Vapes represent an under explored alternative drug delivery system which could address the performance limitations of other devices. Positron emission tomography (PET) has been previously employed to validate novel drug delivery systems. The purpose of this study is to develop and test the characteristics of a novel vape device to deliver a radioactive PET aerosol.

Methods: Variable temperature control vapes were employed with rebuildable atomisers to allow for control over device parameters. A bespoke automated rig was fabricated for the vape to ensure reproducibility. The vape liquid was prepared comprising vegetable glycerol, propylene glycol and [^{18}F]NaF. The vape was compared to a jet nebuliser using an ^{18}F tracer to provide direct comparison. Flow rate, percentage of glycerol and vape duration were all varied to determine optimal parameters.

Results: Glycerol percentage and flow rate appeared to have little effect on device output whereas vape duration and burn sequence had significant effect. Compared to jet nebulisers, vapes show a vastly improved output (13.2% vs 0.3% activity output per second).

Conclusions: Vapes offer a novel accessible delivery system for aerosols, providing higher device output than traditional nebulisers, reducing the required activity and minimising radiation dose to staff. Device parameters were varied to understand their influence on device performance and optimise output parameters for further investigation.

05. Phantom Evaluation of Device-less Respiratory Gating for PET-CT Scanning

Priten Khagram, Neva Patel, Laura Perry, Luis Alves, Zarni Win, Chloe Bowen
Imperial College Healthcare NHS Trust, London, United Kingdom

Purpose: Phantom studies were performed to evaluate the effectiveness of device-less respiratory Data Driven Gating (DDG) algorithm for [^{18}F]FDG PET-CTstudies acquired on a Biograph Vision 600 digital scanner.

Method: An IEC phantom was filled with a 10:1 ratio and placed on a platform restricted to superior-inferior (SI) movement. The mean and maximum activity concentrations of the spheres in the stationary and non-stationary scans were compared. A similar evaluation was performed with a CIRS Dynamic Thorax Motion Phantom containing one of three fillable spherical inserts of volumes 8ml, 2ml or 0.5ml in a non-fillable lung-equivalent background. The phantom motion mimics patient breathing

and combines rotational, SI and AP (anterior-posterior) movements. The CIRS phantom was scanned in 5mm increments from 0-20mm in the SI direction with 5mm AP motion.

Results: Motion in the SI and AP directions caused a decrease in the recovered activity concentration of all spheres and in some cases displayed a PET-CTmisalignment. Applying DDG to the IEC data showed increased recovery of 14-25% across the spheres when compared to non-DDG reconstructions. The CIRS spheres which were subject to a greater range of motion showed a 20-40%, 5-14% and up to 6% increased recovery in the mean activity concentration for the 8ml, 2ml and 0.5ml spheres respectively.

Conclusions: Device-less DDG has been shown to be more effective in recovering the activity concentration of spheres in moving phantoms when compared to non-DDG.

Future work will include retrospective evaluation of clinical effectiveness of DDG using patient data.

06. First Experiences using Siemens' Deviceless Respiratory Gating Software – "OncoFreeze"

Miles Milner, Dr Mary-Frances Dempsey, Dr Sandy Small
West of Scotland PET Centre, Dept of Nuclear Medicine, Gartnavel General Hospital, Glasgow, United Kingdom

Background: Respiratory motion can cause large artefacts in lung and upper abdomen [^{18}F]FDG PET-CT oncology studies.

An existing solution is to gate list mode data over a respiration waveform generated by an external device. An image created only from the quiescent respiratory frame can be used as a motion corrected image.

An alternative is data-driven gating (DDG) which monitors the periodic motion of radioactivity in the patient attributable to respiratory motion. Siemens' Oncofreeze DDG uses a novel, device free technique to extract a respiratory signal directly from the acquired PET data to remove respiratory motion without rejecting counts.

Materials and Methods: We designed a phantom study that moved a NEMA phantom in the Z direction with a ±5mm amplitude sinusoidal waveform. PET images of a static phantom were compared to an image of a moving phantom and an OncoFreeze motion corrected image.

Key Results: The accuracy of the measured sphere volume, diameter in the Z plane, the SUVmean and SUVmax of the "hot spheres" in the NEMA phantom were improved when OncoFreeze motion correction was applied compared to a motion blurred image.

There was evidence that OncoFreeze corrects the measured sphere diameter in the X & Y planes of the motion corrected phantom images.

Conclusion: Our study demonstrated that using OncoFreeze improves the accuracy of some image metrics in the NEMA phantom when sinusoidal motion was applied.

Further work is needed to confirm if there is a correction in sphere diameter in planes without applied motion when using OncoFreeze.

07. Preliminary evaluation of Data-Driven Respiratory Gating on PET-CT data acquired in continuous bed motion using elastic-motion correction image reconstruction for three oncology tracers

Jose M Anton-Rodriguez[a,b], Peter Julyan[a], Jan Walukiewic[a], Heather Williams[a]
[a]*The Christie NHS Foundation Trust, Manchester, United Kingdom.*
[b]*University of Manchester, Manchester, United Kingdom*

Respiratory motion during whole-body PET acquisition can compromise quantification and image quality. We assessed a new data-driven-gating (DDG) (Büther F. 2020,61:1520-1527, JNM) and image reconstruction method referred to as elastic-motion-correction (EMC) reconstruction, which incorporates motion parameters of all respiratory gates into iterative reconstruction algorithm to produce a motion-free single image (Hong I. 2016, IEEE-NSS-MIC).

Patient scans of nine/five/five [^{18}F]FDG/[^{68}Ga]DOTA-TOC/[^{18}F]PSMA acquired on a Biograph-mCT (Siemens-Healthcare) in continuous-bed-motion (CBM) list-mode (LM) were assessed using a research version package of a DDG for CBM-LM and EMC. SUV_{max}, SUV_{peak} and tumour volume (V40% SUV_{max}-threshold) were obtained on images without motion correction (no-MC) and EMC on lesions located thorax to pelvis (28 in total) and a 30 mm diameter VOI in the liver was used to obtain mean and signal-to-noise measurements.

Analysis of no-MC vs EMC we found an increase of SUVs of 37% and 16% for SUV_{max} and SUV_{peak} respectively, an overall decrease of V40% of 32%, increase of liver uniformity of 19% but with an overall increase of 7% of SNR-SUV_{max} (all analysis with $R^2 \geq 0.9$).

Preliminary results showed that this device-free respiratory motion correction approach can be used on scans with different routinely used oncology PET tracers with images returned showing a general increase of SUVs

and SNR-SUV_{max} and reduction of lesions volumes with some penalty of increased noise. Extension to a larger cohort of cases with an assessment of diagnostic image quality will be performed to assess the clinical utility of this DDG approach.

08. Does the addition of TrueX point spread function to the OSEM algorithm reproduce comparable Deauville scores to OSEM alone?

Jonjo Miller, Neil Davis, Beverley Holman, Thomas Wagner, Cindy Leung, Deborah Pencharz, Teresa Szyszko
Royal Free Hospital Department of Nuclear Medicine, London, United Kingdom

Purpose: The Deauville scoring system quantifies response to treatment in lymphoma in the reporting of [^{18}F]FDG PET-CT. Its evidence base was produced using iterative reconstruction methods. Recently, manufacturers have added point spread function (PSF) modelling. Recorded uptake is not directly comparable between iterative and PSF reconstructions (Kuhnert G, et al. 2016, 43:249–258. Eur. J. Nucl. Med. Mol. Imaging., Quak E, et al. 2014;99:e84–e85. Haematologica.). QClear PSF has been shown to alter the reported Deauville score such that the metabolic response of 4-10% of scans was downgraded from complete metabolic response (CMR) to a partial response (PR) (Wyrzykowski M et al. 2020;10(1):99. EJNMMI Res.).

Methods: We aimed to determine if Deauville scores calculated with TrueX were comparable to those produced by iterative alone, in 134 studies of patients with diffuse large B-cell lymphoma (DLBCL), Hodgkin's (HD) or follicular lymphoma (FL) completed between 01/01/2019 - 31/02/2020.

Results: Deauville scores increased in 16 instances, and reduced in 5 instances, with TrueX vs Iterative alone. 7 studies were reclassified as a PR to treatment (Deauville 4) rather than CMR (Deauville 3); potentially leading to unnecessary further treatment. However, kappa scores were 0.893 with HD, 0.737 with DLBCL and 0.766 with FL, showing substantial agreement between the two methods.

Conclusion: Using TrueX rather than iterative reconstruction can alter Deauville scores in a manner which may cause harm to patients and is not evidence based.

09. Investigating the effect of image reconstruction on image quality in [^{68}Ga]Ga-DOTA-TOC PET-CT imaging

Emily Aveyard[a], Lisa Rowley[a], James Cullis[b]
[a]*University Hospitals Coventry and Warwickshire NHS Trust, Coventry, United Kingdom.*
[b]*University Hospitals Birmingham NHS Foundation Trust, Birmingham, United Kingdom*

Purpose of study: [^{68}Ga]Ga-DOTA-TOC PET-CTis clinically indicated for neuroendocrine tumour imaging. The value of the noise penalisation coefficient β in the Q.Clear reconstruction to enhance contrast-to-noise ratio (CNR), signal-to-noise ratio (SNR), and signal-to-background ratio (SBR) was investigated.

Method: A NEMA IQ phantom containing [^{68}Ga]Ga-DOTA-TOC was scanned using varying sphere-to-background concentration ratios. Scans were reconstructed using VuePoint HD (VPHD), VuePoint FX (VPFX) and Q.Clear (QCFX) (β250–1000). Contrast recovery and background variability were measured to calculate CNR. 11 clinical [^{68}Ga]Ga-DOTA-TOC PET-CTscans were reconstructed with VPHD, VPFX and QCFX (β250–500). Lesion and liver standardised uptake values SUV_{max}, SUV_{mean} and SUV_{sd} were measured to determine SNR and SBR. 4 experienced clinicians scored image quality of reconstructed images as "Excellent", "Good", "Acceptable", or "Poor".

Summary of results: In phantom studies, a statistically significant improvement ($p < 0.0001$) in CNR was observed for QCFX (β250–500) over VPHD and VPFX. CNR increased with β across all phantom acquisitions. In patient studies, statistically significant increases in normalised lesion SUV_{max} ($p < 0.001$), SUV_{mean} and SBR ($p < 0.01$) were observed for QCFX (β250–500) over VPHD and VPFX. β250 gave the highest values of SUV and SBR. Noise (liver SUV_{sd}) did not vary between β250–450. Clinician review scored β250 as poor, and β500 as excellent.

Conclusions: Q.Clear gives enhanced CNR and SBR over VuePoint HD and VuePoint FX. However, CNR improves with increased β, whilst SBR is enhanced at decreased β. Visual assessment of image quality by experienced clinicians indicates an optimal value of β500 for [^{68}Ga]Ga-DOTA-TOC PET-CTimaging.

10. Emerging role of [^{18}F]FDG-PET-CT in patients with breast cancer

Lyn Zimmo[a], Nitasha Singh[a], Stefan Voo[b], Charles Zammit[a], Sarah Westwell[a], Malcolm Reed[c], Sabina Dizdarevic[a]
[a]*Brighton and Sussex University Hospital, Brighton, United Kingdom.*
[b]*University College Hospital, London, United Kingdom.*
[c]*Brighton and Sussex Medical School, Brighton, United Kingdom*

Aim: To evaluate evolving clinical indications for [^{18}F] FDG-PET-CT in patients with breast cancer in our Cancer Network.

Method: Retrospective cohort study of 159 patients with breast cancer who underwent PET-CT 01 January 2019 to 31 December 2020 (maximum follow-up 2 years; mean 356 days). Clinical indications were compared with the current Royal College of Radiologists and Royal College of Physicians 2016 guidelines for PET-CT: i)dense breasts ii)brachial plexopathy iii)therapeutic baseline iv) chemotherapy response. Evolving scan indications were subcategorised and assessed against current published evidence.

Results: 175 scans were performed in 159 patients. 75/175(43%) were in accordance with the 2016 guidelines. No scan was performed for (i); 4/175(2%) scans for (ii), 31/175(18%) for (iii) and 40/175(23%) for (iv). 100/175(57%) scans were requested for evolving indications: 13/100(13%) for v)increasing biochemical markers (CA-125 or ESR) and equivocal imaging; 13/100(13%) for vi)biopsy guidance; 71/100(71%) for vii)inflammatory versus malignant disease; 2/100(2%) for viii)iodinated contrast allergy and 1/100(1%) for ix)primary of unknown origin presumed breast.

At follow up, 24/159(15%) patients were deceased; 87%(21/24) with positive versus 12.5%(3/24) with negative scans.

Conclusion: New indications for PET-CT in the assessment of breast cancer have emerged since the published 2016 guidelines with strong evidence base (v, viii and ix) for incorporation into the 2022 updated guidelines. PET-CT is also a valuable problem-solving tool in complex patients (vi, vii). Larger multi-centre studies however are needed to assess the full clinical and prognostic value of [18F]FDG-PET-CT in breast cancer patients.

11. Clinical value of scanning the legs of myeloma patients with [^{18}F]FDG PET-CT

Sachin Modi, Thomas Wagner
Department of Nuclear Medicine, Royal Free Hospital, London, United Kingdom

Introduction: Guidelines for myeloma imaging typically recommend whole body [^{18}F]FDG PET-CT. However, it is not clear if imaging the lower limbs changes management. If scanning the legs does not change patient management, reducing the scanning field would reduce scanning time and improve patient experience. Our aim was to assess if PET-CT scans for myeloma staging and follow-up demonstrated findings in the legs, and if these findings affected clinical management.

Methods: A retrospective review of whole body [^{18}F]FDG PET-CT reports was performed for myeloma scans undertaken between 2015 and 2020, excluding patients with known lesions or symptoms in the legs. Each report was examined to determine the presence of findings in the lower limbs, and whether findings affected management.

Results: 258 scans were identified. 75 (29%) had findings in the lower limbs; 33 (13%) had findings below the knees and 57 (22%) had findings between the knees and upper thighs. 20 (8%) had findings related to myeloma. The remainder were due to non-myelomatous findings.

A total of 4 (2%) scans had findings with potential relevance to patient management, of which 3 (1%) were related to myeloma management. All findings affecting myeloma management were at the level of the knee or above.

Conclusion: [^{18}F]FDG PET-CT for imaging myeloma patients did not identify findings relevant to management of myeloma below the knees. We therefore propose that scanning from vertex to knees is a safe, efficient and reasonable alternative for imaging myeloma patients.

12. The value of "one-stop shop" service using contrast enhanced CT and PET-CT in the management of patients with lymphoma

Ana Matos[a,b], Dr Mary Dempsey[a,b], Dr David Colville[c], Dr Sandy Small[a,b]
[a]*West of Scotland PET Centre, Gartnavel General Hospital, NHS Greater Glasgow and Clyde, Glasgow, United Kingdom.*
[b]*Department of Clinical Physics & Bioengineering, NHS Greater Glasgow and Clyde, Glasgow, United Kingdom.*
[c]*Diagnostic Imaging Services, NHS Greater Glasgow and Clyde, Glasgow, United Kingdom*

Haematology clinical pathways outline many steps from referral to diagnosis, staging, treatment and follow-up of patients with lymphoma, including serial PET-CT and contrast enhanced CT (ceCT). Efforts have been made by the regional haematology team and PET-CT department to implement a "one-stop shop" service to eliminate waiting times between both studies. The purpose of this study was to explore the practical impact of the newly implemented service.

Introduction of "one-stop shop" service presented numerous challenges, including imaging protocol development, image optimisation, review of referral processes and booking systems. Robust staff training using a new imaging technique was crucial for the successful implementation of the service. Agreement on referral criteria, vetting and reporting was also vital to deliver the service in a timely manner.

To date, thirty-seven lymphoma patients underwent a routine [^{18}F]FDG PET-CT immediately followed by ceCT. Studies were performed for staging/re-staging (n=11) and end of treatment (n=26) purposes. One of the main benefits of performing both studies on the same day was to reduce delays in determining final response and decrease hospital attendances. The new service has also reduced the number of intravenous cannulations performed per patient. Performing PET-CT and ceCT on the same day allowed similar patient positioning in both scans improving image interpretation and reporters' confidence. Patient dose was also reduced when compared to other diagnostic CT scanners.

Introducing a "one-stop shop" service PET-CT and ceCT presented many challenges, nevertheless it contributed to staff role development and improved the standards of care delivered to patients with lymphoma.

13. Fast Track Pathways for Giant Cell Arteritis: Evaluation of [^{18}F]FDG positron emission tomography-computed tomography (PET-CT) as an early diagnostic tool at University College London Hospital, NHS Trust

Dalia Ludwig[a], Stefan Voo[b,c], Vanessa Morris[a]
[a]*Department for Rheumatology, University College London Hospital, London, United Kingdom.*
[b]*Institute of Nuclear Medicine, University College London Hospital, London, United Kingdom.*
[c]*Biomedical Research Centre, NIHR, University College London Hospital, London, United Kingdom*

Giant Cell Arteritis (GCA) is a medium and large vessel vasculitis causing irreversible blindness in 20-50% of patients. Prompt diagnosis using a fast-track pathway (FTP) increases diagnostic confidence and reduces disease-associated morbidity. Delays in investigations reduces test sensitivity leading to inappropriate steroid treatment. Tocilizumab (IL-6 blockade) is a licensed treatment but needs well documented investigations to permit usage. Temporal artery biopsy (TAB) was the diagnostic gold standard but is costly, invasive and lacks sensitivity. Temporal artery ultrasound (TAUS) is an effective diagnostic tool. [^{18}F]FDG PET-CT can detect large vessel involvement.

Our GCA-FTP combines early specialist assessment and diagnostics including PET-CT, designed around the British Society for Rheumatology GCA guidelines and Royal College of Physicians/BNMS recommendations. 40 patients with confirmed GCA pre-FTP and 49 on the FTP (29/49 confirmed GCA) are reported. 65% of patients pre-FTP had TAB, only 25% in the FTP. 7.5% had TAUS pre-FTP and 86% in the FTP. Average time to TAB was 6 days pre- and post-FTP with approximately 2-week delay for histopathology. Time to TAUS pre-FTP was 2 days and 1 day in FTP. No patients (0%) had PET-CT pre-FTP, 92% in FTP. Average time to PET-CT was 2.5 days. 38% of patients had negative or inconclusive ultrasound and/or negative biopsy but confirmed vasculitis on PET-CT. 55% of this cohort had vertebral involvement only.

TAUS with PET-CT allows for high diagnostic accuracy without the need for biopsy. PET-CT helps to capture all patients with GCA and satisfy NHS England criteria for tocilizumab.

14. Optimising the energy window for SeHCAT counting using Geant4 Monte Carlo simulations

Gregory James, Joseph O'Brien, Bill Thomson
Sandwell and West Birmingham Hospitals NHS Trust, Birmingham, United Kingdom

Aim: The inclusion of Compton scattered events can be helpful in wholebody counting (Notghi A et al. Nucl Med Commun 2011; **32**:960-6). The geometric mean is also used to account for relative changes in counts due to attenuation. The aim of this study is to establish which energy window(s) give the most reliable results for SeHCAT counting.

Method: A humanoid water phantom and intrinsic gamma camera detectors were modelled using a validated Geant4 Monte Carlo code. A selenium-75 point source was simulated at different locations inside the abdomen of the phantom. The geometric mean counts were measured relative to the source position at the origin (x=0, y=0) for different combinations of energy windows banded as follows: 30-110 keV, 110-170 keV, 170-230 keV, 230-300 keV, 300-360 keV and 360-450 keV.

Results: The table shows the percentage difference in SeHCAT retention relative to a central source position:

Energy Window	Median difference from central position [IQR]
All Photopeaks	+1.0% [-0.2% to +6.0%]
2 upper Photopeaks	+6.2% [+3.0% to +15.5%]
Energy > 170keV	+1.1% [-0.2% to +6.0%]
2 upper Compton bands	-2.4% [-6.3% to -0.2%]
Whole Spectrum	-3.7% [-8.3% to -1.9%]

Conclusion: Energy windows inclusive of Compton regions generally performed better than photopeak windows. Energy windows centred on the top two photopeaks of selenium-75 performed very poorly with an average overestimation of +6.2%. On balance, we propose counting all events (Compton and photopeaks) above 170keV. This energy band avoids interference from technetium-99m sources, and the inclusion of Compton scattered events reduces the variation in geometric mean counts from changes in source position.

15. Optimising SeHCAT studies: A window of opportunity?

Tamar Willson, Richard Meades
Royal Free London NHS Foundation Trust, London, United Kingdom

Many centres perform SeHCAT retention acquisition using one energy window covering the 265 and 279 keV photopeaks. This excludes the majority of photons available to count from the SeHCAT capsule. In their 2011 technical note, the Birmingham City group recommended acquiring all counts that exceed 160 keV, in order to include the Compton scatter from the higher energy photons but exclude any potential counts from stray cobalt-57 or technetium-99m sources which may be in the vicinity. (Notghi A. et al. Nucl Med Commun 2011; **32**:960-6)

We propose placing one window over the 136 keV photopeak (111-159 keV) and a second wider window (160-296keV) to encompass the higher energy photons and their Compton scatter. Logistical steps must still be taken to avoid the presence of stray sources, however calculating SeHCAT retention independently using the two windows and comparing the values provides a quality control method to detect stray source influence in the lower window. Summing the counts from these wider windows significantly improves the counting sensitivity which may be translated into reduced scanning time.

Based on spectra acquired from a SeHCAT capsule inside a water-filled phantom at two metres to an intrinsic gamma camera head, we calculate that 47% of the full spectrum counts were captured using these proposed windows. The >160 keV window collected 17% of the counts and the 242-296 keV window collected only 7%. The counts excluded by many departments therefore represent a significant opportunity to shorten scanning time, which is of particular interest in the setting of increased numbers of referrals for the SeHCAT test.

16. Development of a Novel Technique for Measurement of Bile Acid Retention (SeHCAT) via Scintillation Probe

Kieran Hamilton, Andrew Bussey, Dionne Limmer, Mark Richardson, Adam Baker
James Cook University Hospital, Middlesbrough, United Kingdom

Purpose: To develop an alternative method of measuring bile acid retention (SeHCAT studies), improving departmental capacity by reducing burden on gamma camera time.

Methods: A Radhound Scintillation SS500 contamination probe was mounted to a bespoke stand coupled with a RS Electronics RSiLDM-30 rangefinder. The survey meter serves as both a laser guide for patient positioning and to measure probe-patient distance, yielding reproducible positioning between measurements. Patients' external count rates were measured using the gamma camera (current standard practice) and with the probe. Agreement between calculated retentions from both techniques will validate the probe's use as an appropriate measuring device. A measured retention of ≤15%, is considered as malabsorption and patients are managed accordingly.

Results: Across the entire range of retentions measured (~0-75%), the mean difference between the two techniques was: 1.90 ± 1.92% (n=45). However, over the clinically relevant range of 10 – 20% retentions, the mean difference was 0.99 ± 0.86% (n=10). Over the entire range sampled, the Pearson correlation coefficient is 0.99, indicating a strong positive correlation between the retentions calculated from both techniques. The differences calculated retentions from the two techniques are more pronounced at higher retention values (>40%), where the increased uncertainty has no bearing on the diagnostic outcome.

Conclusion: As this study continues, a continued acceptable correlation between the measured retention in both techniques will validate the novel probe method. This has wider ranging implications; this technique offers a logistically efficient and cost-effective means for Nuclear Medicine departments to perform bile acid retention (SeHCAT) studies.

17. SeHCAT energy windows and the effect of patient attenuation on background measurements

Tom Sanderson, Robert Harding
Nottingham University Hospitals NHS Trust, Nottingham, United Kingdom

We have investigated the effect of SeHCAT energy window configuration on the variation of measured retention with geometric source location, and also the effect of patient attenuation on background measurements.

A phantom study was performed with a SeHCAT capsule located at varying positions within a large Perspex cylinder at both Day 0 and Day 7. This was repeated with two different energy window configurations, a 'photopeaks only' set-up (121, 136, 265, and 403 keV ± 10%), and a 'higher peaks+scatter' set-up (160-430 keV) as recommended by the BNMS SeHCAT masterclass in 2019. Subsequently, using only the 'higher peaks+scatter' windows, simultaneous anterior and posterior background measurements with the patient in position on

the couch were taken for 18 patients, and compared with background measurements made without the patient present.

The phantom study demonstrated a reduced variation in retention with source location when using the 'higher peaks+scatter' set-up. The patient background study found that the posterior count decreased, and the anterior count increased when the patient was present on the couch, with an increasing effect at higher patient weights. The effect on calculated retention was low (<0.5% absolute difference at patient weights <120 kg) but increased to a maximum of 2.9% for a 147 kg patient.

Using a 160-430 keV energy window reduces variations in measured SeHCAT retention with varying geometric source location. Patient attenuation influences anterior and posterior background measurements, but this was only found to be clinically significant at patient weights >120 kg.

18. Impact on SeHCAT Bile Acid Retention Measures with a Pre-capsule Patient Background Image

Louise Macdonald[a,b], Sarah Williams[a,b,c], Carolyn Paterson[a,b], Alison Bolster[a,b,c], Gillian Ainslie-Mclaren[a,b]

[a]*Department of Clinical Physics and Bioengineering, Glasgow, United Kingdom.*
[b]*Department of Nuclear Medicine, Northeast sector, Glasgow, United Kingdom.*
[c]*College of Medical, Veterinary and Life Sciences, University of Glasgow, Glasgow, United Kingdom*

Introduction: SeHCAT studies are performed to assess for bile acid malabsorption by administering a capsule of 0.37MBq SeHCAT. Patients are imaged on day 1 post-administration and day 7 to assess tracer retention. Patients with poor bile acid retention (BAR) have relatively low counts on day 7 and there is potential for "overcorrection", when background subtraction returns a negative count value.

Methods: To overcome this problem we introduced the acquisition of a patient background image, taken on day 1 pre-administration (see figure 1), alongside the room background acquisition. These changes were made on the assumption that background counts would be lower with the patient in the field of view and may be proportionate to patient size. The ratio of the day 1 room background and patient background images can be applied to the room background image on day 7.

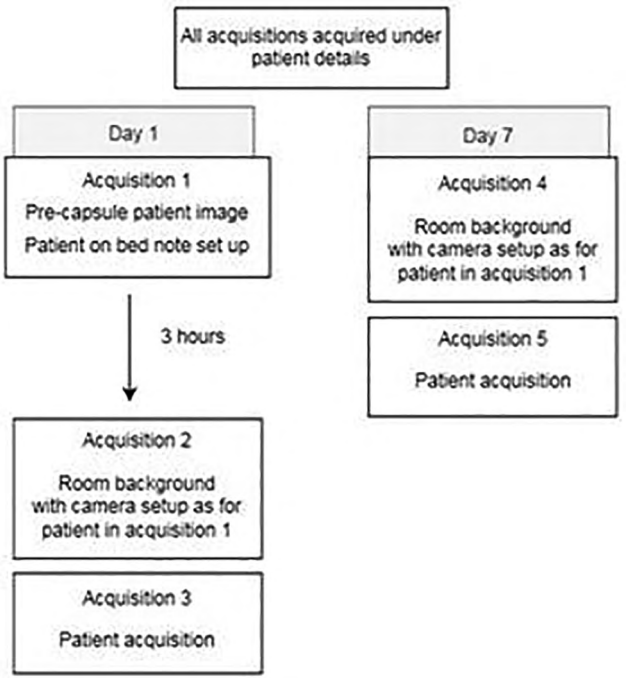

For this study, a dataset of 24 retrospective patients were analysed. BAR measures were calculated using two methods; method one used room background correction whereas method two used a combination of room and patient background correction. Results were compared, taking into account the impact of other factors including BMI and camera positioning.

Results and Conclusions:

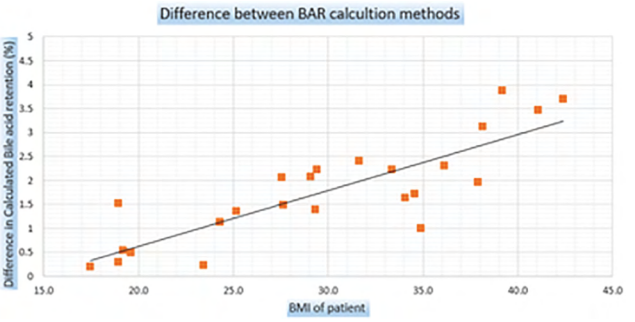

Initial findings suggest patients with higher BMI have a larger percentage difference between the two BAR calculation methods, with consistently higher results when using the room and patient background correction.

19. Survey of surgical trainees' experience with bile acid malabsorption and (75SeHCAT) scan

Marwa Al-Azzawi[a], Alison Bolster[a], Lynsey Devlin[b], Sally Darnbourough[b], Sai Han[a]
[a]*Glasgow Royal Infirmary, Glasgow, United Kingdom.*
[b]*Beatson West of Scotland Cancer Centre, Glasgow, United Kingdom*

Background: Bile acid malabsorption (BAM) is a common condition and one of the differentials for chronic loose stool. BSG guidelines recommend investigating patients with suspected BAM with a 75SeHCAT scan. The study aimed to find the experience of surgical registrars with BAM and 75SeHCAT scans

Methods: An online survey of 10 questions were sent to surgical registrars at 2 hospitals.

Results: 18 responses were returned. 60% of the registrars were involved routinely in seeing patients with chronic loose stool. The majority of registrars considered BAM as one of the differentials. When diagnosing BAM, half of the group would start with empirical treatment while the other half would request a 75SeHCAT scan. 70% of the group weren't aware that pelvic radiotherapy is one of the risk factors in developing BAM. It was found that only 15% of the group were able to request 75SeHCAT scans without any difficulties.

Conclusion: With the increased prevalence of BAM, especially in surgical patients, we need to raise the awareness among surgical registrars of the risk factors for developing BAM, and the availability of SeHCAT scans that would aid in confirming a diagnosis, to make sure patients get prompt treatment and avoid unnecessary investigations.

20. Patients with positive 75SeHCAT scans: A single health board experience

Marwa Al-Azzawi[a], Sally Darnborough[b], Lynsey Devlin[b], Alison Bolster[a], Sai Han[a]
[a]*Glasgow Royal Infirmary, Glasgow, United Kingdom.*
[b]*Beatson West of Scotland Cancer Centre, Glasgow, United Kingdom*

Aim: To identify patients with a positive 75SeHCAT scan and review their symptoms of bile acid malabsorption (BAM) and risk factors.

Methods: All positive 75SeHCAT scans that were done at our trust from January 2015 to March 2020. Were included.

Results: A total of 40 patients had a positive result. The mean age at diagnosis was 50y. 75% (n=30) of patients were females. The mean duration of symptoms was 4 years (range: 1-11 years). Patients reported an average of 9 bowel movement a day (range: 3-20 movement/day). The majority of scans with a positive result were requested by the gastroenterology team, followed by the oncology team as part of the "pelvic radiotherapy late effects service", followed by the surgical team.

75% (n=30) had a severe BAM (retention <5%). 40% (n=15) had a previous pelvic radiotherapy, while 30% (n=12) had a previous cholecystectomy. 35% (n=14) had been labelled as IBS prior to their 75SeHCAT scan results. Excluding the patients with previous radiotherapy, the patients had an average of 4 clinic (range: 1-10 clinic) prior to getting a 75SeHCAT scan requested, due to the difficulties in obtaining one in the trust.

Conclusion: 75SeHCAT scan is a useful test in diagnosing BAM. It is important to identify patients who have the risk factors for developing BAM and investigate them accordingly.

21. Solid gastric emptying scintigraphy in children with rumination syndrome

Lorenzo Biassoni, Rita Meshaka, Maria Giovanna Puoti, Kornelia Nikaki, Keith Lindley, Matilde Pescarin, Marina Easty, Ania Rybak, Osvaldo Borrelli
Great Ormond Street Hospital for Children, London, United Kingdom

Background: The underlying pathophysiological mechanisms of rumination syndrome are still not entirely elucidated. Low basal lower oesophageal sphincter (LES) pressure and straining episodes during transient LES relaxations are thought to facilitate rumination. No data are available on the role of gastric emptying in these patients. Our aim was to review the pattern of solid meal gastric emptying (GE) of in children with rumination syndrome.

Methods: A consecutive case series of children with confirmed rumination and solid meal GE scintigraphy at diagnosis were reviewed retrospectively. Solid GE Scintigraphy was performed according to latest SNMMI guidelines, with a standardized [99mTc]Tc-labelled test feed. GE was analysed as the percentage of radioactivity retained in the stomach over 4 hours using the geometric mean of the decay-corrected anterior and posterior counts for each time point. Gastric retention of >10% at 4 h was considered evidence of delayed GE of solids.

Results: Fourteen children (male 6; median 13.4 years, range 5.6-15.5) met inclusion criteria. All had evidence of rumination syndrome on high-resolution impedance manometry (two type 1; two type 2; ten more than one type). Eight (57%) patients had delayed GE with a median gastric retention of radiolabelled feed at 4 h of 25% (range 12-50).

Conclusions: In our small series delayed GE occurred in more than half of the children with rumination syndrome, suggesting its role in the pathogenesis of symptoms in a subgroup of patients. Our result might advocate the need of additional pharmacological agent for a successful treatment of the disease.

22. Small-bowel transit scintigraphy in children with paediatric intestinal pseudo-obstruction

Atchariya Chanpong[a,b,c], Elizabeth Morris[d], Marina Easty[d], Bruce Goodwin[c], Ania Rybak[d], Simon Eaton[a], Nikhil Thapar[c], Osvaldo Borrelli[d], Lorenzo Biassoni[d]
[a]*Institute of Child Health, London, United Kingdom.*
[b]*Prince of Songkla University, Songkla, Thailand.*
[c]*Queensland Children's Hospital, Brisbane, Australia.*
[d]*Great Ormond Street Hospital for Children, London, United Kingdom*

Aim: Paediatric intestinal pseudo-obstruction (PIPO) is a severe gastrointestinal (GI) motility disorder characterized by intestinal obstruction in the absence of luminal occlusion. The diagnosis relies on the clinical picture and functional tests, including a measure of small bowel dysmotility. Small bowel scintigraphy (SBS) has potential to objectively measure small bowel transit (SBT) and is currently not validated in children. We have tested feasibility of SBS in children with GI dysmotility.

Method: Patients with suspected GI dysmotility underwent solid and/or liquid gastric emptying scintigraphy (GES) prospectively; images were acquired for up to 8 hours from ingestion. The percentage of colonic filling at 6 hours was compared as an index of SBT in PIPO versus non-PIPO and correlated against antro-duodenal manometry scores.

Results: Twenty-two patients with PIPO (41% male), 41 with non-PIPO (41% male) were included. PIPO patients had a significantly lower colonic filling at 6 hours compared to non-PIPO patients with both liquid (25% vs 83%; P=0.001) and solid SBS (7% vs 64%; P=0.016). Patients with myopathic PIPO showed slower SBT than patients with neuropathic PIPO, both with liquid (4% vs 50%; P=0.032) and solid test feeds (2% vs 17%; P=0.639). There was a significant negative correlation between SBT and ADM scores (r=-0.417, P=0.009).

Conclusion: This limited series suggests that SBS is a feasible method to objectively test small bowel transit in PIPO; it correlates with ADM (an invasive test) and may help differentiate myopathic versus neuropathic PIPO.

23. Kinetic and Static Analysis of ^{82}Rb Uptake in Patients with Non-Small Cell Lung Carcinoma

Cameron Anderson, Andrew Thornton, Kjell Erlandsson, John C Dickson, Ashley M Groves
Institute of Nuclear Medicine, University College London Hospitals NHS Foundation Trust, London, United Kingdom

Introduction: The aim of this study was to characterise ^{82}Rb rubidium chloride ([^{82}Rb]$RbCl_2$) uptake in patients with non-small cell lung carcinoma (NSCLC) and correlate dynamic and static PET imaging metrics.

Methods: 10 patients with lesions confirmed to be NSCLC underwent dynamic PET-CT imaging for 6.5 minutes post injection of 1300-1900MBq [^{82}Rb]$RbCl_2$, with static images formed from the last 4.5 minutes of the acquisition. 1TC1k, 1TC2k, 2TC3k and 2TC4k kinetic models with differing numbers of tissue compartments (TC) and rate constants (K_1-k_4) were fit to tumour time activity curves, with the quality of fit determined through Akaike Information Criteria (AIC) analysis. Spectral Analysis, which does not require a compartmental structure to be imposed, and graphical analysis, assuming reversible uptake (Logan plots) and irreversible uptake (Patlak plots) was undertaken. Static analysis consisted of tumour standard uptake values (SUVs).

Results: 8 of 10 lesions were best described (i.e., had the lowest AIC value) by an irreversible 2TC3k model, indicating reversible uptake into an initial compartment and subsequent irreversible trapping in a second compartment. Spectral analysis indicated irreversible components in 8 of the 10 lesions. Visual inspection revealed data was well fit with Patlak plots compared to Logan plots, further supporting irreversibility of uptake. There was a significant correlation between net influx ($K_i=(K_1*k_3)/(k_2+k_3)$) and static imaging metrics SUV_{max} ($R = 0.68$, $p = 0.03$) and SUV_{mean} ($R = 0.69$, $p = 0.03$).

Conclusion: [^{82}Rb]$RbCl_2$ uptake in NSCLC is seemingly best described by a two compartmental irreversible uptake model with net influx rate correlating with SUV.

24. Investigating SPECT-CT Quantification in bone scans with GE's SmartMAR CT Metal Artefact Reduction Algorithm

Robert Harding, Nathan Dickinson
Nottingham University Hospitals NHS Trust, Nottingham, United Kingdom

Aims: Our investigation assessed the impact on image quality and SPECT-CT quantification in bone scans, when reconstructing images using GE's SmartMAR versus our standard CT protocol.

Methods: A phantom study was performed using a nested dual chamber cylindrical phantom. The outer volume was filled with water. A 15ml vial with 100kBq/ml of ^{99m}Tc was immersed in a background of bone mimicking fluid with 10kBq/ml of ^{99m}Tc in the inner chamber. Six SPECT-CT acquisitions were performed with hip, knee, and ankle prostheses present, and with no implant present. Images were reconstructed using CT with and without SmartMAR. The mean activity recovery coefficients of the vial were compared to the scans without an implant. Additionally, 36 patient studies containing metal implants were reconstructed with and without SmartMAR. The impact on image quality was reviewed by two radiologists.

Results: The vial mean recovery coefficients showed noticeable differences between the two reconstructions: Knee: MAR:0.81±0.02 vs NoMAR:0.85±0.02, Hip: MAR:0.74±0.01 vs NoMAR: 0.78±0.03, Ankle: MAR:0.79±0.02 vs NoMAR: 0.89±0.02 and No Implant: MAR:0.81±0.02 vs NoMAR: 0.81±0.02. For the ankle and knee implants, SmartMAR produced recovery coefficients in agreement with the scans containing no implant. In the patient study, SmartMAR CT had no perceivable impact on the SPECT reconstruction appearance. However, improvements in CT image quality from SmartMAR increased radiologist reporting confidence (in 27% and 44% of cases) when metal was present.

Conclusions: SmartMAR broadly improves quantification accuracy with minimal impact on the visual appearance of SPECT images. Improvements in CT image quality increased radiologist diagnostic reporting confidence.

25. Optimisation of quantitative bone SPECT-CT imaging using the Siemens xSPECT Quant reconstruction

Frederick Varley, Kuldip Nijran, Chloe Bowen
Imperial College Healthcare NHS Trust, London, United Kingdom

Purpose: To validate and optimise quantitative SPECT-CT for ^{99m}Tc bone studies using the Siemens xSPECT Quant reconstruction

Method: A NEMA IEC image quality phantom was filled with [^{99m}Tc]Tc-HDP and imaged on a Siemens Intevo Bold system. Acquisition and reconstruction parameters were varied. Image quality and accuracy were measured using signal-to-noise ratio, percentage contrast, resolution accuracy, and the recovery coefficients of the generated Standard Uptake Values (SUVs). This was repeated using a custom phantom containing K_2HPO_4 bone-equivalent solution and clinically relevant activity concentrations to more closely mimic realistic attenuation and scatter in bone.

Results: In terms of the recovery coefficients of the recovered SUVs, the optimal reconstruction was found to be 4 subsets, 96 iterations, although reconstructions with similarly high multiples of iterations and subsets also performed well. In terms of image quality parameters, the optimum reconstruction, found by ranking reconstructions relative each other, was 3 subsets, 48 iterations. These were consistent across both the IEC phantom and the custom phantom. Acquisition parameters of the highest matrix size and longest time-per-view gave the highest quality images in terms of both accuracy and image quality.

Conclusion: Optimum parameters for the Siemens xSPECT Quant reconstruction have been established for ^{99m}Tc bone studies using phantom data. Evaluation of the impact of this optimisation on clinical data is to be performed before clinical use.

26. Use of the CT scout view (topogram) for accurate attenuation correction and quantification of nuclear medicine planar studies: Patient Data

Gregory James, Joseph O'Brien, Bill Thomson
Sandwell and West Birmingham Hospitals NHS Trust, Birmingham, United Kingdom

Aim: Planar studies can benefit from attenuation correction to give absolute quantification of radiotracer. Past techniques of using radionuclide transmission sources have been problematic (Ostertag, et al.,1989). With SPECT-CT gamma camera systems becoming commonplace, this study will examine whether the CT scout view (topogram) can be used for accurate attenuation correction and quantification of planar studies.

Method: 138 patients with a known activity of radiotracer uptake were invited to take part in the study. This included gastric emptying (N=39), HIDA (N=38), colonic transit (N=23), V/Q (N=24) and Lymphoscintigram (N=14) patients. A geometric mean image was acquired for each patient followed immediately by a CT topogram (140kVp, 20mA). We have previously shown there is a direct relationship between the topogram pixel value and the equivalent thickness of water (total attenuation). The geometric mean images were corrected for attenuation on a pixel-by-pixel basis using the derived thickness, T (cm), from the topogram and a linear attenuation coefficient of μ=0.12cm^{-1}. The activity of tracer uptake was then derived using the in-air sensitivity factor (cps/MBq) and compared to the known activity administered to the patient.

Results: The mean difference between the derived tracer activity and the true activity was -0.3% ± 0.4% (95% CI: -10.1% to +9.5%). This is not significantly different from zero bias (p=0.429).

Conclusion: The CT scout view allows pixel-by-pixel attenuation correction of geometric mean images. It is a quick and simple technique to obtain absolute tracer uptake to within ±10% (95% CI) with a low additional radiation dose (<0.1mSv).

27. A quantitative phantom comparison of GE LEHR and LEHRS collimators for planar ^{99m}Tc imaging

Sarah Woods, Ian Armstrong
Manchester University NHS Foundation Trust, Manchester, United Kingdom

By employing thinner septa, new LEHRS collimators from GE report to offer improved sensitivity over previous LEHR collimators without loss of image quality. This work aims to evaluate sensitivity and distance-dependent planar image quality to verify this.

A GE Optima 640 with LEHR and NMCT860 with LEHRS were evaluated. Planar ^{99m}Tc sensitivity was measured using a 10×10 cm BSI phantom at 10 cm distance. Planar ^{99m}Tc image quality was assessed in 10-million count images of a Williams phantom acquired at 0, 5, 10 and 15 cm from the collimator using a 512 matrix. The signal-to-background ratio (SBR) of the four hot features within the phantom was calculated from the ratio of mean counts in circular regions (7-, 10-, 20- and 40-mm diameter) and the background region mean counts.

Planar sensitivity was 74 and 87 cps/MBq for LEHR and LEHRS respectively, representing a 17% increase for the LEHRS collimators. Across all distances and hot features, the mean absolute percentage difference of SBR between the two collimators was 1.3%, with a maximum absolute difference of 3.0%. This was well within the 6.0% Poisson uncertainty in SBR calculated from the number of counts in the regions. No relation between the SBR percentage differences and the size of hot feature was observed.

This work confirms that LEHRS collimator provide the benefit of a 17% gain in planar sensitivity while maintaining image quality across a clinically relevant range of distances. Additional work evaluating performance in SPECT and other radionuclides is encouraged.

28. Phantom image quality analysis of Clarity 2D image enhancement

Sarah Woods, Ian Armstrong
Manchester University NHS Foundation Trust, Manchester, United Kingdom

Clarity 2D is a post-processing technique from GE, applied to planar images, combining noise reduction with signal enhancement using Lucy-Richardson deconvolution. This aims to reduce noise while preserving or enhancing features. This brief phantom study evaluated image quality with varying amounts of Clarity 2D blending.

10-million count ^{99m}Tc planar images of a Williams phantom were acquired at 0 cm from an LEHRS collimator using a 512 matrix on a GE NMCT 860. Clarity 2D was applied as 0% (original image), 20%, 40% and 60% blending. Background pixel noise (coefficient of variation) and signal-to-background ratio (SBR) of the four hot features within the phantom was calculated from the ratio of both mean (SBR_{mean}) and maximum (SBR_{max}) counts in circular regions (7, 10, 20 and 40mm diameter) and the background mean counts.

Background image noise was 5.8%, 4.9%, 4.1% and 3.1% for 0%, 20%, 40% and 60% Clarity 2D blending respectively. SBR_{mean} increases were most apparent in the 7 and 10mm features with approximately 6% gain with 20% blending and 12% at 40% blending. No further increase was observed with 60% blending. SBR_{max} increased by approximately 13% in the 7 and 10mm features with 40% and 60% blending but fell in the largest feature due to noise suppression. This resulted in a non-monotonic response curve which was attributed to edge-enhancement artefacts, identified from profiles through features.

Even with low blending, Clarity 2D provides planar image enhancement and visualisation of smaller features. Further investigation of the impact on quantitative planar investigations is encouraged.

29. A comparison of SPECT vs planar renal function measurements for DMSA

Asifa Javed, Gregory James, Joseph O'Brien, Bill Thompson
Sandwell and West Birmingham NHS Trust, Birmingham, United Kingdom

Aim: SPECT is useful to improve contrast resolution but has limited use in quantification due to a lack of commercial solutions. The aim of this study is to compare SPECT DMSA relative renal function measurements to values obtained from a geometric mean image.

Method: 44 patients referred for a DMSA scan received standard planar imaging (anterior, posterior, RPO, LPO) followed by a SPECT scan. Geometric mean images were produced from the anterior and posterior images and the relative renal function quantified. The tomographic data were reconstructed with resolution recovery (4 iterations, 10 subsets, Butterworth filter, power=10, critical frequency 0.48). Semi-automated threshold segmentation

was used to define the renal uptake and the relative functions were quantified. A Bland-Altman plot was produced showing the difference between planar and SPECT relative uptake.

Results: For reduced relative renal function, SPECT uptake measurements were lower compared to geometric mean. Conversely, for increased relative renal function, SPECT uptake measurements were higher compared to geometric mean. The mean difference between the planar and SPECT relative function measurements was +1.4% ± 0.5% (95% CI: -4.8% to +7.5%) with SPECT giving higher functional values on average. Although this shows statistical significance (p=0.006), the differences are considered to be clinically insignificant.

Conclusion: The data show that there is no significant clinical difference between the relative function obtained from SPECT DMSA compared to geometric mean. It may be possible to change acquisition techniques from planar to SPECT without loss of accuracy in relative function measurements.

30. A Closer Look at Nuclear Medicine Workforce Shortages

Joana do Mar Machado[a], Joseph Purden[b], André Nunes[c], Carla Abreu[d], Christopher Mayes[e], Mónica Martins[f]
[a]*King's College London, London, United Kingdom.*
[b]*Swansea University, Swansea, United Kingdom.*
[c]*Guy's and St Thomas' NHS Foundation Trust, London, United Kingdom.*
[d]*The Royal Marsden NHS Foundation Trust, London, United Kingdom.*
[e]*Royal Liverpool and Broadgreen University Hospitals NHS Trust, Liverpool, United Kingdom.*
[f]*Singleton Hospital, Swansea Bay University Health Board, Swansea, United Kingdom*

The issue of Nuclear Medicine (NM) staff shortages is not declining and instead, it is likely to worsen in the immediate future. This study sets out the analysis of the NM workforce in the UK, establishing the workforce's size and vacancy rate, and addressing challenges faced by departments.

Between October 2020 and July 2021, the RTN BNMS group carried out a survey of the NM workforce which referred to NM Technologists and radiographers, including responses from thirty-eight providers of NM and PET-CTimaging in the UK.

Participants reported a considerable proportion of vacancies (34), and 55.9% have been vacant for 6 months or more. Another issue is workforce ageing with 21.1% of staff within 5 years of expected retirement. Moreover, the fast integration of new technology advances and the increased workload demand leads staff to cover multiple areas/modalities, where around 34.9% and 35.2% of professionals also supported Radiopharmacy and PET/CT, respectively. Another challenge is the uncertainty of Brexit and the considerable reliance on non-UK nationals, with 30.6% of the respondent workforce being non-UK nationals.

Our study suggests that action must be taken as a matter of urgency. At the time of writing this abstract, work is being undertaken by the RTN group to add the NM workforce to the shortage occupation list. The path to repairing this situation is not an easy one. Still, a significant increase in dedicated long-term funding for education and training could help to tackle the worsening of workforce crisis.

31. The Nuclear Medicine Technologist will see you now

Lidia Jasinska[a], Christopher Marquis[b], Phillipa Williams[a]
[a]*UHS, Southampton, United Kingdom.*
[b]*University of Cumbria, Lancaster, United Kingdom*

Background: It has been estimated that an additional 3500 radiographers alone are needed over the next 5 years. Assistant Practitioners, Advanced Practitioners and Radiologists equals further 2500 positions. A major expansion in the imaging workforce is a must to fulfil the increasing demand for radiology services. Recruitment within existing radiology workforce and training in Nuclear Medicine had proven insufficient. Development of Apprenticeship for Nuclear Medicine degree at Cumbria University was essential. Registration with The Academy for Healthcare Science (AHCS) was guaranteed upon completion.

Methods used: Data analysis from the first University intake in 2017 through 2018, 2019 and the very challenging 2020 cohort of apprentices.

Assessment of the recruitment process including candidate background, experience and education.

Students' journey and feedback from their degree level 6 studies.

Data for the number of graduating students across cohorts.

Retention data of newly qualified professionals in training departments.

Summary: Recruiting candidates internally, ensuring they have a healthcare experience, facilitate retention post qualification.

Fulfilment of University requirements regarding UCAS points proves to be a valuable tool to ensure studies completion.

UHS alone managed to recruit four candidates. Two already qualified with 1st hons degree and working at band 5 level and the other two are determined to progress within the profession upon graduation.

Conclusion: It had been proved that candidates with prior healthcare experience are more likely to successfully complete studies. They perform well within the role and progress guaranteeing retention. Structured training with university input ensured highly qualified workforce registered with AHCS.

32. Learning from Excellence (LfE): Appreciate Enquiry as one Development Tool for Providing Training

Ross Williamson, Alice Nicol
NHS Greater Glasgow & Clyde, Glasgow, United Kingdom

Learning from Excellence (LfE) is a program which is being developed in healthcare to promote learning from what works well, in addition to established learning from when things do not go so well. Local Nuclear Medicine staff are exploring the application of LfE in delivery of Clinical Technologist staff training.

NHS Greater Glasgow and Clyde (NHSGGC) is a large organisation with four sectors and have more than forty Nuclear Medicine Technologist staff, with a long history of training. Staffing levels are being challenged with increased staff turnover, including retirements. We have been tasked with creating well-trained Technologists for the future using the IPEM Training scheme, coupled with our local competency-based training.

Appreciative enquiry is a tool recommended in LfE and it is being used for learning in the context of training by the Technical Service Managers who are working together to deliver a standardised training programme for NHSGGC. Recent changes include a set Band 5 recruitment & interview panel being created to identify the best existing & future applicants as new trainees. The multi-disciplinary panel has various backgrounds and specialist Nuclear Medicine experience.

Appreciative enquiry is also being used within the staff management teams and with the trainees themselves, aiming to develop all areas of the local training scheme including post-training interviews. Buy-in from all sectors was essential, aiming to create a positive, supportive environment for trainees.

This presentation will describe the first steps of LfE in local Nuclear Medicine services, focusing on strengthening the delivery of Technologist training.

33. Audit of Activity Residues for DAT, Parathyroid and GFR Examinations

Lara Bonney[a], Daniel McGowan[a,b]
[a]*Oxford University Hospitals NHS Foundation Trust, Oxford, United Kingdom.*
[b]*University of Oxford, Oxford, United Kingdom*

To fulfil requirements under IRMER 2017 a record of the patient administered activity must be held. At OUH the dispensed activity (DA) is recorded for this purpose. Quantitative SPECT requires accurate knowledge of the net administered activity, including for subtraction of residue remaining in the syringe/administration device following administration. Following implementation of quantitative SPECT, residue data was recorded for DAT ([^{123}I]I-Ioflupane) and parathyroid ([^{99m}Tc]Tc-MIBI) examinations. Data was also recorded for GFR ([^{99m}Tc]Tc-DTPA) examinations over a 12-month period.

The net activity administered (DA minus residue) was extracted from Gold Client (Hermes Medical Solutions AB), and the DA extracted from the RIS. GFR data was extracted from the processing spreadsheet. This avoided the increased errors associated with manual data extraction. The relative residue size (as a percentage of the DA) was compared between examinations.

Total study size was 498. Average DAT residue (n=255) 5.8MBq, (3.2% of DA), average GFR residue (n=100) 0.64MBq, (7.0% of DA), average Parathyroid residue (n=143), 46MBq, (6.6% of DA). Comparing administrations flushed with saline (DAT and Parathyroid) against those not flushed (GFR) showed no significant difference between the two groups ($p=0.27$). Comparing studies dispensed in approximately 2.5ml (DAT) to those dispensed in approximately 1.25ml (GFR and Parathyroid) showed a significant difference ($p<0.001$).

Residues were found to average less than 10% of the DA for each study considered, this is relevant to dose audits and DRLs. The data suggests that the relative residue size is volume limited with larger percentage activity residues occurring for more concentrated doses.

34. Speeding up SPECT scans using "Acquire During Step" mode

Tim Melhuish
University Hospital Southampton NHS Trust, Southampton, United Kingdom

Aim: With an increased demand for whole-body SPECT imaging at University Hospital Southampton NHS Foundation Trust (UHS), we explored the use of 'Acquire

During Step' (ADS) mode, offered by the equipment as an alternative to Step and Shoot (S&S), to reduce the time required to perform a SPECT scan.

Method: Phantoms were scanned on a Siemens Symbia Intevo Bold in both S&S and ADS modes so that image quality and contrast recovery could be compared for the two modes.

A Jaszczak phantom filled with ~200MBq Tc99m, fillable spheres with 4:1 sphere: background activity concentration ratio was scanned in both modes, using equal time per projection and analysed visually and quantitatively.

Results: Phantom results:

1.Image quality (Jaszczak phantom) results are very similar in both modes with the same number of rod segments and spheres clearly visible when reconstructed in Flash 3D (F3D) and xSPECT.

2.Tomographic uniformity is very similar in both modes

3.Quantification of the spheres using Siemens "xSPECT Quant" revealed contrast recovery to be very similar in both modes

Conclusion: ADS mode saves around 3 minutes per SPECT, compared to S&S, for 120 projections (60 per head). This is saved from the time it takes the camera to move from one angle to the next. Resolution, uniformity and contrast recovery was found to be equivalent in both modes.

A SPECT Spatial Resolution phantom will be scanned to compare spatial resolution and, if comparable, ADS mode will be implemented widely at UHS.

35. Introducing tracer injections through Portacaths

Indre Vaitkute, Katharine Chalmers, Sorcha Curry, Armidita Jacob
King's College London, London, United Kingdom

Aim: To assess potential challenges of using a portacath for tracer administration such as: gaining portacath access; determining how much saline flush is needed in order to achieve the lowest tracer residual in the line and the port; recognising the signs of extravasation and managing leaked radioactive substance should the cannula be incorrectly prepared; correct injection procedure and port de-access.

Methods: Experiments were performed where a chest phantom was fitted with a correctly and an incorrectly prepared portacath. The first portacath was flushed with varying volumes of saline and a PET-CTscan was performed to check the images for residual in the line.

Results: Different volumes of saline flush were used in the experiment, and it showed that the optimum volume in order to achieve the lowest residual in the line is 20mL. An attempt to use the incorrectly prepared port for tracer injection was unsuccessful.

Conclusion: It has been proven that 20 ml saline flush after FDG injection is sufficient, as it has minimal residual that was deemed negligible by clinician (PET window<4.5). Extravasation of the radiopharmaceuticals usually do not require a specific intervention and it was proven that a manual injection would be unlikely to result in extravasation. In PET-CTCentres where technologists are not trained to use a portacath, a ward nurse would be needed to access the port and flush it with heparinised saline post-injection.

36. Evaluation of the Image Quality in [^{68}Ga]-DOTATOC – a 2-Year Study

Clara Ferreira[a,b], Lisa Rowley[a]
[a]*University Hospital of Coventry and Warwickshire, Coventry, United Kingdom.*
[b]*Centre for Sport, Exercise and Life Sciences - Coventry University, Coventry, United Kingdom*

[^{68}Ga]-DOTATOC imaging is used to detect, stage and follow-up patients with Neuro Endocrine Tumours (NET). Optimisation of image quality is important in ensuring best outcomes for patients. The aims of the study are to assess image quality of [^{68}Ga]-DOTATOC scans at our centre and the best organ to be used for background measurement. This retrospective observational study analysed [^{68}Ga]-DOTATOC scans from 93 patients acquired on a GE-PET-CT 710, following the EANM [^{68}Ga]-DOTA guidelines (2017) and using Q.Clear (β=350) reconstructions. SUVmean was measured for the primary, local nodes (LN) and distant metastasis (DM), and also in healthy liver (HL), left ventricle-cardiac muscle (CM), and blood pool (BP), to use as a background. Contrast-to-noise ratio (CNR) was then calculated using the different backgrounds. Images from 93 patients were analysed, (43 female, 50 male), average age of 65±13.8 years. The average background SUVmean measured in HL (8.68±4.58 kBq/mL) and in CM (4.40±2.83 kBq/mL) was higher than the background measured in BP (2.94±3.03 kBq/mL). The background measured in HL and CM was more variable in patients who have liver and cardiac metastases. The BP measurements were more reliable as BP is less susceptible to develop NETs. The CNR with using BP background was 13.77±10.29 for primary, 7.42±7.51 for LN and 11.05±13.13 for DM, which indicates a high contrast, however the standard deviation was high for DM and LN. The study of [^{68}Ga]-DOTATOC scans indicates high image quality based on the CNR. The BP is the more reliable organ for background measurements.

37. Oncological bone whole body SPECT-CT: a review of additional findings above the clavicles and below the lesser trochanters

Hend Komber, David Little, Stewart Redman, Richard Graham
Royal United Hospitals Bath, Bath, United Kingdom

Background: There is a move towards using whole body single photon emission computed tomography/computed tomography (SPECT-CT) imaging for diagnosing bone metastases. When performed on a dual-headed gamma camera, this may cover from clavicles to proximal femurs due to time constraints. In contrast, the novel 360° CZT scanner can perform a whole body (vertex to toes) SPECT-CT in under 20 minutes. The aim was to explore the rate of additional findings above the clavicles and below the lesser trochanters and assess whether this extended field of view is of clinical benefit.

Methods: Single-centre, retrospective study of 117 consecutive SPECT-CT scans for oncological bone assessment over a four-month period. Analysis of the incidence of additional clinical findings above the clavicles and below the lesser trochanters was performed by two independent readers.

Results: The male: female ratio was 71:46 and mean patient age was 68 years. The distribution of primary malignancies was prostate 65/117 (55.6%), breast 40/117 (34.2%), lung 5/117 (4.3%) and other 7/117 (6.0%). One scan was excluded from the 'above clavicles' group as the patient was not scanned above the clavicles. There were additional findings of malignancy above the clavicles in 16/116 scans (13.8%) and below the lesser trochanters in 16/117 scans (13.7%).

Conclusion: A whole body (vertex to toes) oncological bone SPECT-CT protocol is useful for detection of additional findings of clinical significance above the clavicles and below the lesser trochanters.

38. Whole body SPECT-CT in oncology – how often are findings equivocal?

Hend Komber, Richard Graham, David Little, Stewart Redman
Royal United Hospitals Bath, Bath, United Kingdom

Background: Novel 360° CZT scanners can perform a whole body (vertex to toes) oncological bone single photon emission computed tomography/computed tomography (SPECT-CT) in under 20 minutes. The aim was to explore the rate of equivocal skeletal findings and assess the level of certainty in the radiological report.

Methods: Single-centre, retrospective study of 117 consecutive SPECT-CT scans for oncological bone assessment over a four-month period. Scans were analysed for the presence of active malignant skeletal disease and classified according to the level of radiological certainty. Analysis was performed by two independent readers.

Results: The male: female ratio was 71:46 and mean patient age was 68 years. Active malignant skeletal disease was found in 31.6% patients with 97.3% cases having a high level of radiological certainty (consistent with (>90% probability of disease). No active malignant skeletal disease was found in 61.5% patients with 95.8% cases having a high level of radiological certainty (consistent with (>90% probability of benign findings). 7/117 (6.0%) patients had indeterminate findings of active malignant skeletal disease - representing the overall rate of equivocal findings for whole body SPECT-CT. All seven patients had further follow up imaging or biopsy.

Conclusion: A whole body (vertex to toes) oncological bone SPECT-CT protocol results in a low rate of equivocal findings (6%) and can differentiate presence of active malignant skeletal disease with high level of reporter certainty.

39. Oncological bone whole body SPECT-CT: a review of incidental findings

Hend Komber, Stewart Redman, Richard Graham, David Little
Royal United Hospitals Bath, Bath, United Kingdom

Background: Novel 360° CZT scanners can perform a whole body (vertex to toes) oncological bone single photon emission computed tomography/computed tomography (SPECT-CT) in under 20 minutes. The aim was to explore the rate of incidental findings reported and assess the likely clinical significance.

Methods: Single-centre, retrospective study of 117 consecutive SPECT-CT scans for oncological bone assessment over a four-month period. Scans were analysed for the frequency of incidental unexpected clinical findings, as follows: 'no incidental findings', incidental findings 'of clinical significance in current clinical episode', 'of possible clinical significance in future clinical episodes' or 'of likely no clinical significance'. Analysis was performed by two independent readers.

Results: The male: female ratio was 71:46 and the mean patient age was 68 years. The distribution of the data was as follows: 'no incidental findings' = 50/117 (42.7%), incidental findings 'of clinical significance in current clinical episode' = 13/117 (11.1%), 'of possible clinical significance in future clinical episodes' = 48/117 (41.0%) and 'of likely no clinical significance' = 6/117 (5.1%). Incidental findings 'of clinical significance in current clinical episode' included new malignancy in 11/117 (9.4%), severe

vertebral degeneration in 2/117 (1.7%) and hydronephrosis in 2/117 (1.7%).

Conclusion: A whole body (vertex to toes) oncological bone SPECT-CT protocol is useful for detection of incidental findings of clinical significance, including those of new malignancy.

40. Clinical utility of perfusion only SPECT-CT (Q-SPECT-CT) for diagnosing pulmonary embolism (PE) in patients with a moderate-to-high pre-test probability of PE during the COVID-19 pandemic: a retrospective, single centre study

Bernadith Marimon[a,b], Mubarik Arshad[b,a], Stefan Voo[b,a,c]
[a]*Whittington Hospital NHS Trust, London, United Kingdom.*
[b]*University College London Hospitals NHS Foundation Trust, London, United Kingdom.*
[c]*Biomedical Research Centre, NIHR, UCLH, London, United Kingdom*

Background: Following BNMS' recommendations during the COVID-19 pandemic, we have fully amended our protocols and performed perfusion only Q-SPECT-CT for all patients referred for suspected PE. The aim was to reduce the risk of aerosolization of respiratory droplets and adhere to new infection control requirements. This is an audit on the diagnostic efficacy of the altered Q-SPECT-CT imaging in detecting PE.

Material and Methods: Sequential patients with clinical suspicion of PE who were referred for nuclear medicine evaluation between March 2020 and March 2021 were included in the study (n=60). All patients underwent Q-SPECT-CT unless pregnant (Q-SPECT only). Imaging results were correlated with the follow-up clinical data.

Results: All patients had a moderate-to-high pre-test probability for PE (mean Wells score 2.8, range 2-4). There were 13 PE positive scans in this cohort, all of which were reported in high confidence. None of the patients who had the perfusion study without the ventilation had inconclusive result (i.e., needing CTPA for further assessment).

Of the 60 patients imaged with Q-SPECT-CT, 6 (10%) patients had a positive COVID-19 infection. Q-SPECT-CT was positive in 4/60 (7%) of patients, all of which were COVID-19 positive. Distribution of pulmonary emboli was bilateral and subsegmental. Ancillary acute findings on Q-SPECT-CT included bilateral parenchymal ground glass opacities (n=5) and pleural effusions (n=2). None of the scans was rendered indeterminate or in need of ventilation images.

Conclusion: Q-SPECT-CT alone has clinical utility for diagnosing PE in patients with moderate-to-high pre-test probability for PE, including pregnant or COVID-19 patients.

41. Validation of a semi-automated V/Q SPECT Pulmonary Embolism Quantification Method

Bodiyabaduge Harini Fernando[a,b], Lefteris Livieratos[a,b], Julia Charlotte Fowler[a,b]
[a]*King's College London, London, United Kingdom.*
[b]*Guy's and St Thomas' Hospitals NHS Foundation Trust, London, United Kingdom*

Background: Quantification of the percentage of Pulmonary Embolism (%PEQ) burden may be helpful to guide patient triage to different treatment and follow up strategies in future.

Aim: To develop, validate a semi-automated method for %PEQ from VQ SPECT-CT datasets.

Methodology: 100 consecutive PE positive V/Q-SPECT-CT studies, using [^{81m}Kr] as the ventilation agent were retrospectively analysed.

Two image sets were derived from raw projection data with differing post processing parameters, the first using the current departmental clinical reconstruction protocol (DCR) (S16,I4,GF1), the second using a previous phantom optimised reconstruction protocol (POR) (S16,I16 GF0).

For each dataset the gold-standard %PEQ was derived utilising the SPECT-CT hybrid image with visual identification of segmental/subsegmental VQ mismatches being summated, guided by broncho-pulmonary segmental maps.

For each DCR and POR dataset two semi-automated systems were used to derive %PEQ, firstly using the Hermes generated quotient image data (QID method), secondly using separate SPECT V and Q volumetrically derived data (VDD method) applying thresholds identified from previous phantom experiments.

Resulting %PEQs were compared to the gold-standard %PEQs using Pearson correlation and Bland Altman plots.

Results: The closest correlation was achieved by using the POR protocol, with VDD method R^2=0.89, bias 1%, SD 7% and QID method R^2=0.8, bias 4%, SD 7%. The average time taken to achieve %PEQ from QID: 4 minutes vs VDD: 5 minutes.

Conclusion: The POR protocol VDD method gave the closest correlation to the gold-standard %PEQ and is our recommended semi-automated method as it only adds a minute to the process.

42. Additional value of multiphase thin slice 4D-CT in SPECT-CT [^{99m}Tc]Sestamibi imaging in patients with primary hyperparathyroidism-a useful 3D roadmap for surgeons

Randeep Kulshrestha, Nirav Kaneria, Ayah Nawwar
University Hospitals Bristol & Weston NHS Foundation Trust, Bristol, United Kingdom

Purpose: To evaluate the added value of the multi-phase high resolution CT in the SPECT-CT study by investigating correlation in relation to the SPECT planar static images and SPECT-CT as well as the prior ultrasound thyroid scan.

Method: A retrospective review was performed on 16 patients who had undergone 4D SPECT-CT with dynamic high-resolution CT from its implementation in Autumn of 2019 to currently. The proportion of patients who had correlative imaging with dynamic enhanced CT was evaluated.

Results: 7 of 16 patients, the positive dynamic CT correlated with the planar SPECT and/or SPECT-CT, and also the prior positive thyroid ultrasound. In 5 of 16 patients the negative dynamic CT correlated with the negative planar SPECT and SPECT-CT and of these 4/16 correlated with a negative prior ultrasound. 4 of 16 cases did not correlate and of these, 1 of 16 had a positive dynamic CT with a negative SPECT/SPECT-CT (possibly early washout) and positive prior ultrasound. 3 of 16 patients had a negative ultrasound, and a positive enhancing lesion on 4D-CT which correlated on SPECT-CT.

Conclusion: Dynamic multi-phase CT showed very good correlation with both SPECT and SPECT-CT (15/16=94%) as well as ultrasound (13/16=81.2%) and is fairly accurately correlated with these modalities in 12 of 16 patients as either positive or negative (75%). In many cases it localises the precise anatomical location of the suspected parathyroid adenoma, providing an accurate 3D roadmap for the surgeons.

Reference: Chazen JL, AJNR Am J Neuroradiol. 2012 Mar;33(3):429-33 Am J Neuroradiol.

43. Establishing a normal thyroid to background reference range values for [^{99m}Tc]Pertechnetate in a single centre population using fusion of SPECT scans and CT studies

Rohit Srinivasan[a], Shuaib Siddiqui[a], Christopher Sibley-Allen[a], Alexander James Fowler[b], Julia Charlotte Fowler[a]
[a]*Guy's and St. Thomas' NHS Foundation Trust, London, United Kingdom.*
[b]*Barts & the London School of Medicine and Dentistry, Queen Mary University of London, London, United Kingdom*

Background: There can be technical problems with thyroid uptake quantification for example if there is extravasated activity. A thyroid: background (T:B) ratio can be a helpful alternative and has been successful in other centres when carried out on planar datasets compared to an established normal range.

Purpose of the study: To determine whether [^{99m}Tc] Pertechnetate SPECT datasets can be used to establish a normal T:B ratio reference range for our patient population.

Methods: We retrospectively processed 97 consecutive low dose (40MBq) thyroid SPECT scans, which had been performed as part of parathyroid scintigraphy protocol for biochemically euthyroid patients. Hermes Hybrid Recon Neurology v3.2 was used to create reprojected planar images from Thyroid SPECT and separately acquired CT datasets. Regions of interest (ROI) were drawn around the thyroid(T) then dragged to nearby background(B) to allow the T:B ratio to be calculated (T-B)/B.

Results: The results of the T:B ratio were not normally distributed, which appears to be secondary to skewing of the background using Shapiro-Wilk methodology.

Conclusion: This dataset and method does not appear useful for establishing a normal distribution for our population, with particular issue with non-normality of background counts. These results appear anomalous, considered possibly due to the reprocessing of non-hybrid acquired SPECT-CT datasets, noise reflecting the low injected dose activity or the use of SPECT data. We will be testing these causes further.

44. [^{99m}Tc]DPD initial study of ATTR cardiac amyloidosis diagnosis and correlation with cardiac MR and transthoracic echocardiogram

Randeep Kulshrestha, Nirav Kaneria, Ayah Nawwar
University Hospitals Bristol & Weston NHS Foundation Trust, Bristol, United Kingdom

Purpose: To investigate the outcome of [^{99m}Tc]DPD study for ATTR cardiac amyloidosis, and to see if the severity score correlated with the findings of cardiac MR and transthoracic echocardiography.

Method: Retrospective review x14 patients who had a [^{99m}Tc]DPD scan for cardiac amyloid. Outcome of the test was recorded as either negative for ATTR cardiac amyloidosis (score 0 or 1), or positive for ATTR cardiac amyloidosis (score of 2 or 3). Correlation of the result was made with a prior echocardiogram and cardiac MR.

Results: 8/14 patients were either grades 2 or 3 score, hence had a high likelihood of ATTR cardiac amyloidosis. 6/14 patients had a grade 0 score and were negative for ATTR cardiac amyloidosis. Of the 8/14, 6/7(86%) patients who were positive, had prior echocardiograms and/or cardiac MR showing concentric left ventricular hypertrophy (LVH), reduced left ventricular systolic function, and

reduced left ventricular ejection fraction (LVEF). Of the 6/14 negative patients, 4/6 (66.7%) showed prior severe LVH and reduced LVEF.

Conclusion: [^{99m}Tc]DPD reliably differentiated ATTR cardiac amyloidosis from patients without, based on prior echocardiography and cardiac MRI (6 of 7 patients). Patients who were negative on [^{99m}Tc]DPD DPD but showed positive prior imaging features of cardiac amyloid may have light chain cardiac amyloidosis or another form of cardiomyopathy. Distinguishing the different types of cardiac amyloidosis including ATTR cardiac amyloid (both hereditary and senile wild type), from light chain AL cardiac amyloid is important as each form are treated differently, and new genetic therapies can now be offered.

45. Determining the normal standardised uptake value (SUV) in bone and the optimal SUV scale for reporting using [^{99m}Tc] Tc-HMDP with a 360° CZT SPECT-CT scanner

Jordi Mathew[a], Stewart Redman[b], David Little[b], Sarah Cade[b], Richard Graham[b]
[a]*Universtiy of Bristol, Bristol, United Kingdom.*
[b]*Royal United Hospitals Bath, Bath, United Kingdom*

Background and aims: The aim of this study was to determine normal Standardised Uptake Values (SUV) in bone when using a novel 360°CZT SPECT-CT gamma camera and to determine the optimal default SUV scale to use when reporting.

Methods: Single centre, retrospective study of ~80 consecutive whole-body SPECT-CTs. SUVs are adjusted for patient body weight (SUVbw). SUVmax and SUV mean were sampled from; T1, T8, L1 and L5 vertebrae, femur, anterior superior iliac spine (ASIS), posterior superior iliac spine (PSIS) and bladder. Each vertebrae had three 10mm diameter spherical VOIs drawn (left medulla + cortex, central medulla. and right medulla + cortex). VOIs were centrally placed at the ASIS and PSIS. The femoral VOI was placed in the shaft. The bladder VOI was placed centrally.

4 SUV scales (0-10, 0-15, 0-20 and 0-25) were ranked in order of preference by 2 radiologists and scored on acceptability for reporting.

Results: Results from ~80 patients:

T1 mean SUVmax: 6.34, 6.20, 6.01 T8 mean SUVmax: 5.87, 6.60, 6.09 L1 mean SUVmax: 4.99, 5.72, 4.82 L5 mean SUVmax: 5.61, 5.13, 5.80 Mean SUVmax ASIS: 7.60 Mean SUVmax PSIS: 5.48 Mean SUVmax Femur: 2.37 Mean SUVmax Bladder: 27.94

Results from initial 10 pilot patients determined that a scale of 0-15 SUV was ranked as the best default scale for reporting.

Conclusion: The mean normal SUVmax in the vertebrae, ASIS and PSIS lie between 2-10 (excluding outliers). The 0-15 SUV scale may be ideal for use as the default when reporting SPECT-CT bone scans.

46. UK Audit of national variation in calculated radiation doses due to radionuclide exposure

Anthony Murray[a], Matthew Memmott[b]
[a]*Bradford Teaching Hospitals NHS Foundation Trust, Bradford, United Kingdom.*
[b]*Manchester University NHS Foundation Trust, Manchester, United Kingdom*

Introduction: It is a core requirement of IRR17 compliance for risk assessments and the investigation of accidental exposure scenarios that the magnitude of doses likely to be encountered are evaluated. A national audit was undertaken to investigate the variation in dose estimations for a range of foreseeable accidental exposure scenarios in nuclear medicine (NM).

Methods: Participants were asked to estimate the levels of exposure in 15 foreseeable scenarios; covering whole-body and extremity exposures from external sources, internal exposure and exposures from skin (surface contamination and needle-stick injury) and eye contamination. Questions were intentionally simplified to reduce variation from assumptions made by the participants and to focus more on the underlying gross systematic variation.

Results: Twenty-seven centres participated. There was generally a very wide variation in the estimated exposures across all the categories of exposures, apart from internal exposure estimates. Whilst there was no ground truth for each individual question, the variation in results itself often exceeded the relevant threshold for classification and annual dose limits. The majority of variation was due to differences in methods, models and assumptions used by each participant.

Conclusion: This audit raises questions around how IRR17 compliance can be universally demonstrated with such wide national variation. It evidences the need for a more standardised practice in NM radionuclide exposure estimates through national consensus guidelines or standards etc.

47. Optimising cylinder model dimensions for VARSKIN to simulate a droplet of radioactive skin contamination using Geant4 Monte Carlo code

Gregory James, Joseph O'Brien, Bill Thomson
Sandwell and West Birmingham Hospitals NHS Trust, Birmingham, United Kingdom

Aim: VARSKIN provides a convenient way of calculating skin dose from predefined geometries, but the models are limited to concentric shapes such as discs and cylinders. The aim of this study is to use Geant4 Monte Carlo code to independently compare the cylindrical geometries in VARSKIN to more realistic droplet models obtained from photography.

Method: Geant4 was used to model various droplets of radioactive liquid on the skin based on photographs. The dose rates were recorded to the sensitive basal layer 70μm beneath the surface for three droplet volumes (10, 30 and 50μl) and 26 radionuclides, giving a wide range of electron and photon energies. Four different cylinders were considered for each droplet volume as approximations to the 'true' droplet model. The dose rates from the cylinder models were then compared against the dose rates from the 'true' droplet models.

Results: The table gives the optimum cylinder dimensions that best approximate a true droplet shape for each volume. The mean bias and 95% CI from the true droplet model is quoted.

Conclusion: Using the cylinder dimensions (above) in software packages such as VARSKIN, dose rates from radioactive skin contamination are expected to be within ±7.4% of a 'true' droplet model at 95% CI.

	10 μl	30 μl	50 μl
Radius, r	1.26 mm	2.02 mm	2.51 mm
Height, h	2.01 mm	2.35 mm	2.53 mm
Mean bias:	-0.5% ± 0.7% (p=0.443)	0.3% ± 0.7% (p=0.652)	-0.5% ± 0.6% (p=0.383)
95% CI:	-7.4% → 6.4%	-6.8% → 7.4%	-6.3% → 5.3%

48. Potential Skin Doses from [^{223}Ra] and [^{211}At] from the daughter products' alpha emissions

Bill Thomson, Greg James, Joe O'Brien
Physics and Nuclear medicine, City Hospital, Birmingham, United Kingdom

Aim: The primary alpha emissions of ^{223}Ra and ^{211}At are 5.78 MeV and 5.87MeV respectively, which penetrate 45μm so do not reach the skin basal layer (average 70μm). So, the contamination alpha dose is often considered zero. However, there are higher energy alphas from decay-chain products. The skin dose from these is considered using VARSKIN+ software.

Method: VARSKIN+ was used to determine contamination skin doses at 70μm separately for each of the decay-chain radionuclides of ^{223}Ra {^{219}Rn, ^{215}Po, ^{211}Pb, ^{211}Bi, ^{211}Po and ^{207}Tl} and ^{211}At {^{211}Po and ^{207}Bi}. (VARSKIN+ allows consideration of the complete decay-chain, but currently has errors). In particular, ^{215}Po has 7.39MeV alphas and ^{211}Po has 7.345MeV alphas (range 74μm). The electron and photon doses were for a 1cm^2 area contamination, and VARSKIN+ gives alpha doses for a point source contamination.

Results: For ^{223}Ra only, skin doserate is 0.011mSv/hr/kBq (electrons/gammas). The decay products' doses are 2.95mSv/hr/kBq (electron/gammas, x270 higher), and 5590mSv/hr/kBq from alphas (x524,000 higher).

For ^{211}At only, skin doserate is 0.006mSv/hr/kBq (electrons/gammas). The decay products' doses are 6.4E-05mSv/hr/kBq (electron/gammas, negligible) and 1839mSv/hr/kBq from alphas (x306,000 higher).

For [^{223}Ra](including decay chain), 5.4kBq on skin for 1-minute gives 500mSv; for ^{211}At the activity is 16kBq.

Conclusion: Skin dose from ^{223}Ra and ^{211}At is dominated (>99.9%) by the alpha dose from their decay chains. Staff should be aware of this and use appropriate PPE to minimise potential skin contamination, and also ensure that the potential for patient skin contamination during administration is minimised.

49. Variation in retrospective patient specific external dose rate and subsequent radiation restrictions following five [^{177}Lu]Lu-PSMA therapy cycles in an outpatient setting

Anne-Marie Stapleton[a,b], Nathaniel Scott[b], Yong Du[b,c]
[a]*Royal Surrey NHS Foundation Trust, Guildford, United Kingdom.*
[b]*GenesisCare, Windsor, United Kingdom.*
[c]*Royal Marsden Hospital, London, United Kingdom*

Purpose of study: External dose rates from radionuclide therapy patients often pose radiation risks to those around them. This risk is patient and situation specific. Therefore, standardised radiation restrictions can cause either unnecessary patient inconvenience or insufficient radiation protection of the public. This study examined inter-cycle variations in one patient's external dose rate for multiple cycles of [^{177}Lu]Lu-PSMA therapy. This case report discusses individualisation of [^{177}Lu]Lu-PSMA radiation restrictions.

Methods: A patient regularly self-measured their external dose rate over multiple days following 6 consecutive administration cycles of [^{177}Lu]Lu-PSMA. Bi-exponential curves were fitted to the >150 data points. External dose rate variations were calculated from this data. These were combined with typical patient contact patterns to calculate individualised radiation restrictions.

Results: Early patient contact has the largest impact on resultant doses to others, therefore an initial isolation period significantly reduces the subsequent restrictions necessary to meet dose constraints. In this patient,

bi-exponential fits to external dose rate data showed significant inter-cycle variability resulting in different restriction requirements. This suggests restrictions should be cycle and patient specific but can utilise patient measured data.

Conclusions: Individualised and cycle specific radiation restrictions can be calculated for patients undergoing [^{177}Lu]Lu-PSMA therapy to fit a range of dose constraints, given their expected contact patterns and self-measured external dose rate decay curves.

50. The use of semi-automatic dispensing in PET imaging

Sorcha Curry[a], Lewis Davies[a], Aidan Griffiths[b], Sofia Periera[a], John Joemon[a], Armidita Jacobs[a], Jane MacKewn[a]
[a]*King's College London, London, United Kingdom.*
[b]*GSTT, London, United Kingdom*

Introduction: Staff extremity dose from manually dispensing PET tracer can be high. To reduce this, the Amercare Automated Dispenser (ADD) was introduced to the PET Centre. It uses volume-based input for controlled filling and emptying of syringes. It was first optimised followed by audit of performance in clinical use.

Method: Initial setup of the ADD was performed by comparing volumes of saline dispensed against weighing scale measurements. An extremity dosemeter was used to measure dose received at the fingertip and base during injection process. An audit of its use for routine dispensing was performed.

Results: Following setup of the ADD, its use resulted in dose reduction from 140μSv to 86μSv (39%) at fingertip and 50μSv to 22μSv (56%) at base of finger during the injection process. The monthly finger dose recorded on the passive extremity dosemeters supplied by our approved dosimetry service was reduced by 35% on average. The ADD gave an average deviation from requested activity of 7% and a second attempt needed 22% of the time. The calibration step performed on each vial is the largest source of error. 2021 ring badges readings are still 28% lower than before use of ADD.

Conclusion: Both extremity dosemeter and passive dosemeter results showed a substantial reduction in staff finger dose. The audit showed good accuracy and reliability providing the vial calibration step was performed correctly; however, occasional adjustment of the setup is required. The results seen on introduction of the ADD have been maintained after 2 years of use.

51. Staff Dose Reduction Using an Automated Infusion Device in a PET-CT Department: Variations due to Operator Technique

Amy McCredie[a,b], Ana Matos[a,b], Alastair Gemmell[a,b], Sandy Small[a,b]
[a]*West of Scotland PET Centre, Gartnavel General Hospital, NHS GGC, Glasgow, United Kingdom.*
[b]*Department of Clinical Physics & Bioengineering, NHS GGC, Glasgow, United Kingdom*

Aim: The purpose of this study was to evaluate staff whole-body radiation dose, comparing manual dose administration via an automatic dose dispenser (ADD – Von Gahlen, Netherlands) and lead syringe shield versus an automatic dose injector (IntegoTM MEDRAD, Inc.), for [^{18}F]FDG and [^{18}F]PSMA-1007 studies. The Intego^{TM} was introduced to the department due to an increase in patient load and staff radiation dose levels.

Methods: Over a six-month period, ten operators were asked to record their electronic personal dosimeter (EPD) dose (in μSv) before and after manual administration (ADD) and use of IntegoTM. The administered activity and any factors affecting the administration were also recorded. These readings were collated and normalised per MBq of ^{18}F to account for difference in activity due to weight-based administration.

Results and Discussion: The mean whole-body dose to staff for the ADD was 0.0043±0.0025 μSv/MBq and for Intego^{TM} 0.0017±0.0011 μSv/MBq, representing an average 60% reduction in dose. Mann-Whitney U test was statistically significant ($p<0.001$). Technologist B had the largest mean dose reduction of 81%, versus Technologist J with the smallest mean dose reduction of 21%, the difference was attributed to operator technique. The two main causes of increased operator dose were time and distance from source.

Conclusion: Intego^{TM} greatly reduces the staff whole-body dose during administration of ^{18}F when compared with manual administration. Variation in operator technique contributes to differences in dose reduction, showing that continued staff training and review of techniques is crucial for further improvements in dose reduction.

52. Breastfeeding interruption following Lung V/Q: Is it necessary during early lactation?

Thomas Biggans, Ed Hockaday, Glen Gardner, Clare Monaghan
NHS Tayside, Dundee, United Kingdom

Purpose: Current guidance to interrupt breastfeeding is based on limited data with very little published information relevant to the colostrum phase. The aim of this work was to estimate potential doses to infants from breastfeeding patients who underwent a Lung V/Q scan <96 hours post-partum.

Methods: Following administration, milk samples were collected. The activity concentration of each sample was measured using a gamma counter of known counting efficiency.

Fractional ingestion was determined using the method set out by (Mountford et al., 1999, 50:89-111. App. Rad. Iso.) assuming a feed volume of 142 ml at 4-hour intervals. Effective dose assuming no interruption was evaluated using the coefficient presented by (Stabin et al., 2000, 41(5):863-873. J. Nucl. Med.).

Results: 2 patients within 24 hours post-partum provided samples with an average peak activity concentration of 0.5 kBq/ml (Range 0.1 – 0.9). The average estimated effective dose to the foetus was 0.06 mSv (0.02 – 0.09).

4 patients between 48 and 72 hours post-partum provided samples with an average peak activity concentration of 14.2 kBq/ml (8.5 – 20.5). The average estimated effective dose to the foetus was 0.97 mSv (0.59 – 1.51). The average effective half-life was 4.2 hours (3.9 – 4.3).

Conclusion: These results are comparable to those found in the literature in particular the order of magnitude difference between those within and outwith 24 hours of giving birth. The limited data suggests that breastfeeding interruption is not required if < 24 hours post-partum.

53. Colloid Scintigraphy for Splenosis - a Case Series

Neil Thomson, Humayun Bashir, Liviu Stanisor, Gordon Ellul
Kent and Canterbury Hospital, Canterbury, United Kingdom

Splenosis is the result of splenic tissue breaking off of the main organ and auto-transplanting (heterotopic autotransplantation) at another site inside the body. It most commonly occurs as a result of traumatic splenic rupture or abdominal surgery. [^{99m}Tc]Tc-colloid scintigraphy is useful in deciphering the reticulo-endothelial origins of difficult-to-characterize soft tissue lesions, identified on cross-sectional radiological imaging i.e., CT

A review of [^{99m}Tc]Tc-nanocolloid SPECT-CT scans performed at the Kent and Canterbury Hospital in 2020 and 2021 was undertaken with a pictorial review of the cases with splenosis.

Seven [^{99m}Tc]Tc-colloid SPECT-CT scans were performed at the department for splenosis. Four females and three males. Median age was 76 (range 52 - 77). Four patients were referred for characterization of incidental lesions picked on CT done for unrelated causes. Two patients had undergone prior CTs, and one patient had an [^{18}F]FDG PET-CT for abdominal symptoms and suspected malignancy. One patient had history of trauma to spleen while one had a post-trauma splenectomy.

[^{99m}Tc]Tc-colloid SPECT-CT identified 3 patients with solitary splenules and 1 patient, with history of post-trauma splenectomy, showed 5 splenules spread across the abdomino-pelvic cavity. In the remaining 3 patients, colloid scintigraphy helped rule out splenosis. One of these proved to be lymphoma (stage IIIS) on follow-up [^{18}F]FDG PET-CT, one (sub-diaphragmatic location) regressed on CT and one lesion in the tail of pancreas remained indeterminate even after MRI and Octreotide imaging.

In conclusion, [^{99m}Tc]Tc-colloid scintigraphy is the functional imaging of choice for splenosis.

54. Improving our support to breastfeeding nuclear medicine patients

Rachel Bidder[a], Christine Turner[a], Wendy Jones[b], Catherine Humphreys[a], Gaynor Jones[a]
[a]*Swansea Bay University Health Board, Swansea, United Kingdom.*
[b]*Breastfeeding and Medication Pharmacist, United Kingdom, United Kingdom*

Radiopharmaceuticals administered to breastfeeding patients may excrete into breast milk. Consequently, nuclear medicine professionals are required to give radiation protection instructions in order to minimise the radiation exposure of the breastfeeding infant as per the ARSAC Notes for Guidance (2022). Instructions was provided in the form of breastfeeding interruption times, but no information was given if breastfeeding expertise was required in the event of mastitis developing following the interruption of breastfeeding.

The aim of our work was to review and improve the current support given to breastfeeding patients undergoing ^{99m}Tc based nuclear medicine procedures.

A patient leaflet entitled 'information for breastfeeding patient having a ^{99m}Tc diagnostic study was prepared which includes breastfeeding interruption times for several ^{99m}Tc based studies including lung perfusion and sentinel lymph node procedures. The leaflet was reviewed by both our local neonatal infant feeding lead and a breastfeeding and medication pharmacist.

A patient leaflet for breastfeeding patients was developed following a thorough review by breastfeeding experts. The leaflet now contains information on how to store breast milk safely, suggestions for what could be done with the breast milk once the radioactivity has decayed and contact information for the local breastfeeding expert.

Healthcare professionals have a duty to protect the breastfeeding relationship to support the health of the patient and the breastfeeding infant.

We have successfully updated our information for breast-feeding patients ensuring that the information is correct and evidenced based.

Furthermore, we have encouraged our local MR and CT colleagues to undergo a similar review.

55. Half-time [^{123}I]Ioflupane DaTSCAN acquisitions show no statistically significant effect on quantification

Sebastian Janner[a], Christopher Sibley-Allen[b], Richard Fernandez[b], Lefteris Livieratos[c]
[a]*Royal Brompton Hospital, London, United Kingdom.*
[b]*Guy's and St Thomas' Hospitals, London, United Kingdom.*
[c]*King's College London, London, United Kingdom*

[^{123}I]Ioflupane DaTSCAN are a lengthy acquisition taking up to an hour whilst the patient remains still – a challenge for patients with motor symptoms. This study investigated the impact of reducing acquisition times (minimising potential intrascan patient motion) on image quantification, while optimising reconstruction for the reduced-count images.

Projection data for 29 patients referred for [^{123}I]Ioflupane DaTSCAN (a typical quarterly workload at a large tertiary centre) were Poisson re-sampled using HERMES Hybrid Recon Neurology v3.2, simulating reduced-count scans equivalent to 50% and 75% reductions in scanning time. SPECT images were reconstructed using 16 iterations, 4 subsets with a 0.7cm^{-1} FWHM Gaussian post-filter and were quantified by SBR ratio/Z-score against the ENC-DAT database, over 4 RoIs using HERMES BRASS Brain Analysis v2.6. Reconstructions of 50% reduced-count data with 12 iterations or a 1cm^{-1} FWHM Gaussian post-filter were also assessed.

A 50% count reduction had no statistically significant effect ($p \geq 0.13$) on image quantification when compared to full-count scans; nor did reducing to 12 iterations. Increasing the Gaussian post-filter size had a statistically significant effect ($p \leq 0.03$) on image quantification which makes classification as abnormal more likely (6% of results changed from normal to abnormal). A 75% count reduction resulted in a statistically significant effect ($p \leq 0.013$) on quantification which could increase the rate of under-diagnosis (7% of results changed from abnormal to normal).

We conclude that shortening acquisition times by 50% appears to have no statistically significant effect on DaTSCAN quantification and may help reduce potential patient motion artefacts.

56. Use of Personal Protective Equipment against ^{219}Rn emitted from ^{223}Ra Therapy patients

Michael Draper[a], Richard Fernandez[b], Philomena Geraghty[b], David Gallacher[b]
[a]*Kings College London, London, United Kingdom.*
[b]*Guy's & St. Thomas' NHS Foundation Trust, London, United Kingdom*

Radium-223 dichloride solution ([^{223}Ra]RaCl$_2$), is injected intravenously for palliative treatment of prostate cancer in patients with bone metastases. Administration is perceived as straightforward; however, studies have shown that following administration exhaled breath from patients may contain radioactive Radium-223 progeny [Parker C., et al. 2013, 213-223 N Engl J Med; Ooe, K., et al. 2019, 6-13. EJNMMI Phys.].

This study aimed to assess the radiation exposure of at-risk groups such as patient family members and hospital staff.

At this large teaching hospital, ^{223} Ra administration is performed by a dedicated therapy nurse, overseen by a Clinical Scientist. Over 6 months, 22 administrations were randomly selected for assessment. In line with Covid-19 guidance, all patients wore surgical facemasks (SFMs). Staff additionally wore eye protection (visor/goggles).

Personal contamination monitoring of staff was performed following each administration using dedicated scintillation monitors. PPE were processed into samples and counted (gamma and liquid scintillant) using a sample counter.

Sample counting measured radioactive contamination on all patient SFMs (n=20). For staff 65% of SFMs (n=43) and 57% of visors/goggles were contaminated. 67% (n=3) of patient family members' SFMs were contaminated. Gamma spectroscopy and activity concentrations will be presented.

PPE worn by staff and patients were found to be contaminated by exhaled ^{219} Rn. This has significant implications for administration of this UK wide routine therapy. In particular, this study supports the continued use of face masks for patients and staff in order to minimise inhalation of ^{219} Rn and its progeny. Considerations of public dose, adequate ventilation and appropriate waste disposal is required.

57. The impact of [^{18}F]FDG-PET imaging in early stage, locally advanced breast cancer patients referred for neo-adjuvant chemotherapy: a retrospective, cross-sectional, multi-centre study

Alexandra Dudek[a], Sophie Merrick[b], Emma Spurrell[c], Lauramay Davis[a], Irfan Kayani[a], Jamshed Bomanji[a], Rebecca Roylance[b], Stefan Voo[a,d]
[a]*Institute of Nuclear Medicine, University College London Hospitals NHS Foundation Trust (UCLH), London, United Kingdom.*
[b]*Department of Medical Oncology, UCLH, London, United Kingdom.*

[c]*Department of Medical Oncology, Whittington Hospital NHS Trust, London, United Kingdom.*
[d]*Biomedical Research Centre, NIHR, UCLH, London, United Kingdom*

Background: Despite its increasing role in breast cancer imaging, the impact of [^{18}F]FDG-PET in early, locally advanced breast cancer (LABC) staging remains unclear. High-grade tumoural phenotypes exhibit a strong metastatic potential even in early stages of disease, which is often underdiagnosed on conventional imaging (US, CT, MRI). We evaluated the yield of [^{18}F]FDG-PET, as a sensitive metabolic imaging modality, in high-grade LABC patients prior to neo-adjuvant chemotherapy.

Methods: 30 consecutive patients with LABC on conventional imaging (clinical stage IIA, IIB, IIIA-T3N1) and histologically proven high-grade tumours, who were referred for neo-adjuvant chemotherapy, were included in the study. All patients underwent [^{18}F]FDG-PET imaging, in addition to conventional imaging. The prognostic impact of PET findings was analysed.

Results: PET changed the clinical stage in 46.7% (14/30) patients. It showed unsuspected N3 nodal disease (infraclavicular, supraclavicular, or internal mammary nodes) in 37% (11/30) and in-transit locoregional soft-tissue or distant metastases in 10% (3/30) cases, which were not appreciable on conventional imaging. It confirmed 13% muscle chest wall (4/30), 57% overlying skin (17/30) and 30% areolar involvement (9/30).

Conclusion: [^{18}F]FDG PET scanning is not yet part of the routine staging in early stage LABC referred for neo-adjuvant chemotherapy. However, the diagnostic impact of [^{18}F]FDG PET in patients with clinical stage IIA or higher seems significant and could hold powerful prognostic implications.

58. Chelator-Free Radiolabelling and Purification of Graphene Oxide Nanosheets of Different Lateral Sizes

Harry Grover[a,b], Dhifaf Jasim[b], Beverley Ellis[a], Kostas Kostarelos[b]
[a]*Department of Nuclear Medicine, Manchester University NHS Foundation Trust, Manchester, United Kingdom.*
[b]*Nanomedicine Laboratory, National Graphene Institute and Faculty of Biology, Medicine & Health, The University of Manchester, Manchester, United Kingdom*

Introduction & Aims: Graphene oxide (GO) has many potential biomedical applications due to its versatile chemistry and biocompatibility; for example, the accumulation of GO in the spleen makes it an attractive candidate for targeted splenic drug delivery (Kostarelos K. et al., 2020, 14:10168-10186. ACS Nano). Understanding the biodistribution of GO is a key challenge in evaluating its potential in clinical applications.

Previously, biodistribution has been studied by chelating a radiometal with a macrocycle covalently bonded to the GO. However, chelators can affect the properties of the nanomaterial, and thus its biodistribution. Therefore, there is a need to develop chelator-free radiolabelling strategies of GO to measure biodistribution.

Methods: In-111 was deposited on the surface of three different sized GO sheets: ultrasmall (US), small (S), and large (L) GO under mild reduction conditions. The materials were purified using solid phase extraction and analysed chromatographically. Stability in mouse serum was assessed over 24 hours.

Results: The method gave labelled GO constructs with initial radiolabelling efficiencies of 35.5 ± 10.8%, 32.8 ± 6.4%, and 33.6 ± 7.3%, respectively. Purification yielded samples with purities of 75.3 ± 9.7%, 80.8 ± 10.9% and 74.6 ± 15.4%. Stability studies showed an initial decrease in RCP of 7.8 ± 2.0% after 1 hour, then a slower decrease of 21.3 ± 8.3% over 23 hours.

Conclusion: GO was radiolabelled using a chelator-free method and purified which will allow reliable biodistribution studies. The improved radiolabelling method of GO will facilitate the radiolabelling of other graphene-based materials with diverse biomedical applications.

59. Quantitative [^{123}I] Ioflupane DaTSCAN single photon computed tomography-computed tomography (SPECT-CT) in Parkinsonism

Elena Missir Missir[a], Patrick Begley[b], Jessop Maryam[b], Singh Nitasha[b], Helena McMeekin[c], Mark Aplin[b], Puja Parekh[a], Malgorzata Raczek[a], Sabina Dizdarevic[b,a]
[a]*Brighton and Sussex Medical School, Brighton, United Kingdom.*
[b]*University Hospitals Sussex NHS Foundation Trust, Brighton, United Kingdom.*
[c]*Hermes Medical, London, United Kingdom*

Aim: [^{123}I] Ioflupane (DaTSCAN) binds to the presynaptic dopamine transporter (DaT) but also has a tenfold lower affinity for the serotonin transporter (SERT) on 5-HT neurons (Ziebell M. 2010, 51:1885-1891. J. Nucl. Med.). Our aim was to quantify absolute uptake in striatal and extra-striatal regions using SPECT-CT and improve DaTSCAN image quality.

Method: Twenty-six patients with parkinsonism underwent DaTSCAN SPECT-CT prospectively. The scans were visually analysed independently by two experienced reporters. Specific binding ratios (SBRs) from Chang attenuation corrected SPECT were obtained

using GE DaTQuant. Normalised Concentrations (NC) and Specific Uptakes (NSU) from measured attenuation, and modelled scatter corrected SPECT-CT were obtained using HERMES HybridRecon and Affinity, and modified EARL volumes of interest.

Results: Striatal NSU and SBR positively correlate (R=0.65-0.88, p=0.00). SBR, NC, and NSU boxplots differentiated between scans without evidence of dopaminergic deficit (SWEDD) and abnormal scans. Interestingly, body weight inversely correlated with NC values in extra-striatal regions [frontal (R=0.81, p=0.00); thalamus (R=0.58, p=0.00); occipital (R=0.69, p=0.00)] and both caudate nuclei (R=0.42, p=0.03 (Right), R=0.52, p=0.01(Left)). Improved visual quality of SPECT-CT versus SPECT images was noted by both reporters for all scans.

Conclusion: DaTSCAN SPECT-CT resulted in more accurate quantification and improved image quality. It enabled quantification of extra-striatal regions, which is not possible with relative SPECT semi-quantification. Larger studies are required to establish the full value of absolute quantification to assess the interplay between DaT and SERT, for diagnosis and monitoring progression of neurodegenerative disease, in patients receiving selective serotonin-reuptake inhibitors and to verify whether serotonin and/or dopamine transporters are dysfunctional in obesity?

60. [^{99m}Tc]Sestamibi SPECT-CT in differentiation of renal masses: The end of diagnostic nephrectomy?

Thomas Biggans[a], Sameer Gangoli[b], Nitasha Singh[c], Prasad Guntur[a], Zeeshan Aslam[a], Lisa O'Brien[b], Maryam Jessop[c], Sabina Dizdarevic[c]
[a]*NHS Tayside, Dundee, United Kingdom.*
[b]*University Hospitals Sussex NHS Foundation Trust, Chichester, United Kingdom.*
[c]*University Hospitals Sussex NHS Foundation Trust, Brighton, United Kingdom*

Purpose: To present the initial UK multicentre clinical experience of renal [^{99m}Tc]Sestamibi SPECT-CT in the differentiation of renal masses.

Methods: A case series of 17 patients from three UK centres. Use of [^{99m}Tc]Sestamibi as a tumour imaging agent is approved by the Administration of Radioactive Substances Advisory Committee (ARSAC). Patients were administered with 900 MBq of [^{99m}Tc]Sestamibi intravenously. SPECT-CT acquisition of the abdomen was conducted 75-90 minutes post injection. Fused images were reconstructed by OSEM with CT-based attenuation correction.

Images were evaluated visually and, in one centre, semi-quantitatively in conjunction with the uptake ratio threshold (Gorin et al., 2015, 69:413-416. Eur. Urol.) by experienced reporters. The uptake ratio was also determined (Rowe et al., 2015, 40(4):309-313. Clin. Nuc. Med.).

Results: Three patients were reported as likely Oncocytoma (high [^{99m}Tc]Sestamibi uptake) with biopsy proven oncocytomas. Fourteen scans were reported as likely RCC: 9 patients had histologically proven RCC, 2 Oncocytoma on biopsy, 1 sample from biopsy was insufficient, 1 patient was too frail to undergo biopsy and 1 patient is awaiting biopsy.

These preliminary results indicate 60% sensitivity and 100% specificity in identifying Oncocytoma.

Conclusion: With consideration of the low number of Oncocytoma, our findings are consistent with the previously published literature. [^{99m}Tc]Sestamibi SPECT-CT is a promising non-invasive technique that has yet to find its place in the diagnostic pathway for renal lesions. Standardisation of protocols and larger multicentre prospective studies are required.

61. Optimisation of the Computed Tomography Component of Hybrid Imaging

Jen Dennis, Jonathan Dixon
NHS Greater Glasgow and Clyde, Glasgow, United Kingdom

Purpose: The use of ionising radiation is commonplace in healthcare with its prevalence increasing as technology develops. While the information provided can be invaluable, the concomitant risk of cancer induction must be considered. This exercise outlines our efforts at optimising the Computed Tomography (CT) components of hybrid imaging in our centre.

Methods used: Using two Siemens Symbia SPECT-CT systems (one 2-slice, one 16-slice) and a Kyoto Kagaku anthropomorphic phantom, a series of thorax and abdomen scans were performed using a range of reference mAs (mAs_{ref}), with, and without, iterative reconstruction (available on the 16-slice system). Additional image reconstructions were performed on a range of convolution kernels.

Images were reviewed both quantitatively and qualitatively. Standardised regions of interest were positioned on each image and the standard deviation was taken as a surrogate for image noise.

Summary of results: The use of iterative reconstruction (IRIS) on the 16-slice scanner resulted in a greater reduction in noise than had been expected. Further investigation is required to assess the extent that mAs_{ref} can be reduced while maintaining the level of noise deemed acceptable on the 2-slice scanner (that does not benefit from iterative reconstruction).

Convolution kernels generally had the expected result in terms of smoothing and noise structure but some of the 'specialist' kernels warrant further investigation.

Inherent differences in hardware between the two- and 16-slice scanners made inter-scanner comparisons difficult.

Conclusion: Although lower than for diagnostic CT scanners, the dose burden from CT components of hybrid imaging can still be reduced through optimisation.

62. Vitamin D and the accuracy of Nuclear Medicine imaging in patients with prosthetic hip and knee joints – a retrospective study

Hannah Chandler[a], Simon King[b], Hassan Hirji[a]
[a]*London Northwest University Healthcare NHS Trust, London, United Kingdom.*
[b]*University Of West England, Bristol, United Kingdom*

Introduction: Nuclear medicine is a well-established modality to assess appearances of infection or loosening of prosthetic-joint replacements. However previous research suggests that loosening and low-grade peri-prosthetic infection can appear very similar. Patients with vitamin D (VD) deficiency have been noted to have poorer outcomes post-surgery for both infection and loosening. Patients with low grade uptake and low VD levels may be mismanaged if imaging is inaccurate. This study evaluated the association between Nuclear Medicine imaging accuracy and VD levels in patients with prosthetic-joint replacements.

Methods: A retrospective single centre cohort study was carried out. 298 cases were collected anonymously including knee and hip prostheses. Findings were split into two categories, matched whereby scan reports agreed with clinical findings and unmatched whereby it did not match (imaging was inaccurate). Chi-squared and Fishers Exact Tests were performed to assess statistical significance.

Results: Analysis shows a very statistically significant association between imaging accuracy of prosthetic-joint replacements and VD level ($p<0.001$). There was no significant difference between prosthesis types. It was found that patients with low VD were 2.61 times more likely to have inaccurate results.

Conclusion and Implications for Practice: There was an association between VD levels and Nuclear Medicine imaging accuracy and imaging results in cases with low VD levels were two times more likely to be inaccurate. Prospective research would be appropriate to further confirm this. VD levels could be used as an indicator for accuracy of imaging results or low VD levels could be managed prior to imaging.

63. Patient-Led Whole-Body Retention Dosimetry in ^{131}I-NaI Molecular Radiotherapy (MRT) for Thyroid Malignancies

Tahani Alkahtani[a,b,c], Lefteris Livieratos[a,b], Valerie Lewington[a,b]
[a]*King's College London, London, United Kingdom.*
[b]*Guy's & St Thomas' Hospitals NHS Foundation Trust, London, United Kingdom.*
[c]*Princess Nourah bint Abdulrahman University, Riyadh, Saudi Arabia*

Introduction/Aim: Sodium Iodide ([^{131}I]-NaI) molecular radiotherapy (MRT) is used to treat hyperthyroidism and thyroid cancer. The outcome of MRT depends on the absorbed radiation dose delivered to target tissues and healthy organs. For practical reasons, post-treatment imaging is rarely performed beyond 48 hours after MRT administration. This limits the reliability of absorbed dose estimates and results in patients being provided with generic radiation safety advice. In this study, we measured the early distribution of ^{131}I-NaI using whole-body imaging. We combined this information with long-term whole-body retention data obtained from patient-led whole-body dose monitoring.

Method: Patients with differentiated thyroid cancer received ^{131}I-NaI (3.7-7.4GBq) for thyroid remnant ablation or post-ablation MRT. Planar whole-body images at 48hr following ^{131}I-NaI administration were acquired to assess early uptake. Patient-led whole-body retention measurements using a hand-held radiation monitor (ATOMTEX model AT6130, Belarus) were used to follow the time course of radioactivity clearance in each patient for four weeks post-therapy.

Results: A significant correlation was shown between patient-led and whole-body imaging derived injected activity (IA) measurements ($r=0.8$, $p<0.05$). A Bland-Altman suggests good agreement between both dosimetry methods.

Conclusion: This study supports the concept of integrating patient-led radiation monitoring into ^{131}I-NaI treatment planning and conveniently allows the collection of retention data for several weeks after MRT administration without the need for repeated hospital attendance. These data will be useful for single-time-point dose calculations, outcome assessment and personalised radiation protection guidance.

64. Towards Treatment Planning in Radioiodine Treatment of Graves' Disease

Paul Gape[a,b], Jan Taprogge[a,b], Lily Peake[a,b], Iain Murray[a,b], Glenn Flux[a,b]
[a]*The Royal Marsden NHS Foundation Trust, Sutton, United Kingdom.*

[b]*The Institute of Cancer Research, Sutton, United Kingdom*

Purpose: There remains a debate as to the optimal treatment for patients with Graves' Disease receiving radioiodine (RAI).

This work aimed to establish population-level relationships between absorbed dose to the thyroid and treatment outcome, and to investigate potential patient-level covariates affecting outcome.

Methods: Data from a systematic review and meta-analysis were used to assess the relationship between absorbed dose and treatment outcome (non-hyperthyroid, euthyroid, hyperthyroid) following RAI. The dose-response relationships were fitted using a two-parameter sigmoidal function, characterized by the absorbed dose at 50% response rate (D_{50}) and a slope parameter (γ).

Patient-level data were analysed in a cohort receiving a planned absorbed dose of 60 Gy to the thyroid. Multivariate logistic regression was performed to determine patient-specific covariates predictive of 12-month outcome.

Results: The non-hyperthyroid and hypothyroid dose-response relationships were well described by the chosen function, with D_{50} = 70 Gy [53 – 87 Gy], 225 Gy [161 – 290 Gy] and γ = 1.40 [0.91 – 1.90], 1.36 [0.73 – 1.98] respectively. The euthyroid response was inferred from these outcomes, giving a maximum euthyroid rate of 38% at 128 Gy.

In the fixed dose cohort, thyroid volume and 24-hour uptake were negatively associated with non-hyperthyroid outcome (p = 0.05, 0.005 respectively). The effective half-life in the thyroid was positively associated with euthyroidism (p < 0.001), and negatively associated with hypothyroidism (p = 0.003).

Conclusions: A clear dose-response relationship was demonstrated between thyroid absorbed dose and treatment outcome. Individual patient covariates influencing outcome were identified in a fixed dose cohort.

65. S-phase enrichment by hydroxyurea treatment enhances [^{177}Lu]Lu-DOTA-TATE uptake *in vitro*

Jordan Cheng[a], Lefteris Livieratos[b], Samantha Terry[a]
[a]*King's College London, London, United Kingdom.*
[b]*Guy's & St Thomas' Hospitals NHS FT, London, United Kingdom*

Purpose: Investigate whether S-phase enrichment with hydroxyurea (HU) treatment of cell cultures affects [^{177}Lu]Lu-DOTA-TATE uptake for potential combination therapy settings.

Methods: S-phase enrichment in asynchronously growing wildtype (U2OS)/transfected (U2OS+SSTR2A) human bone osteosarcoma and rat pancreatic cancer (CA20948) cells was achieved by treatment with 2 mM HU for 17 hours 37°C/5% CO_2. After treatment, excess HU was removed, and cells were allowed to recover for 3 hours. Cells were then either harvested, for cell cycle distribution/SSTR2A expression assessment by flow cytometry, or further incubated with 25 nM [^{177}Lu]Lu-DOTA-TATE for 4 hours at 37°C/5% CO_2 to determine radiopharmaceutical uptake.

Results: HU treatment increased SSTR2A expression by 1.6-fold in U2OS+SSTR2A and 1.2-fold in CA20948 compared to untreated controls. The S-phase was enriched in U2OS+SSTR2A (19.5% G1, 76% S, 4.5% G_2/M) but almost completely diminished in CA20948 (79.6% G1, 1.4% S, 18% G2/M) post HU treatment. Uptake of [^{177}Lu]Lu-DOTA-TATE (mean ± SD Bq/cell) was highest in U2OS+SSTR2A (0.117 ± 0.023), followed by CA20948 (0.025 ± 0.006) then U2OS (0.005 ± 0.003). Uptake was increased 1.6-fold in U2OS+SSTR2A cells after HU treatment (untreated vs HU Bq/cell; 0.117 ± 0.023 vs 0.189 ± 0.042, p = 0.0001) but decreased in CA20948 (untreated vs HU Bq/cell; 0.025 ± 0.006 vs 0.017 ± 0.007, p = 0.0089).

Conclusion: Enrichment of cells in S-phase enhanced [^{177}Lu]Lu-DOTA-TATE localisation within U2OS+SSTR2A cells. There is potential to combine clinical molecular radionuclide therapies, such as [^{177}Lu]Lu-DOTA-TATE, with commonplace chemotherapies that target aspects of the cell cycle to improve therapeutic outcomes.

66. Determining the Dominant Sources of Uncertainty in PET Dosimetry

Paul Gape[a,b], Dominic Rushforth[a,b], Carla Abreu[a,b], Jonathan Gear[a,b], Glenn Flux[a,b]
[a]*The Royal Marsden NHS Foundation Trust, Sutton, United Kingdom.*
[b]*The Institute of Cancer Research, Sutton, United Kingdom*

Purpose: Estimates of absorbed doses in diagnostic nuclear medicine are useful to compare radiation risks with other tracers or modalities, or to plan a therapeutic absorbed dose. However, assessment of uncertainty is not a routine aspect of these calculations.

The aim of this work was to determine the parameters with the greatest influence on the normal organ absorbed dose uncertainty, and therefore identify potential areas for optimisation.

Methods: Image-based dosimetry was performed for seven patients as part of the SOLLID (Simplification

of Low-Level Internal Dosimetry) trial (n = 4 [^{68}Ga]Ga-PSMA, n = 2 [^{68}Ga]Ga-DOTA-TATE, n = 1 [^{18}F-FDG]).

Uncertainties associated with volume delineation, partial volume effect, activity quantification and time-activity curve fitting were calculated in accordance with EANM guidelines. The uncertainty introduced when using model-based S-value was quantified by comparing patient-specific Monte Carlo simulations with reference models within IDAC-Dose 2.1.

Results: Dosimetry was performed for 34 organs.

The dominant contributions to the uncertainty were from the S-value and the fitting of the time-activity curve, with average fractional uncertainty of 15.0% (SD = 10.3%) and 8.8% (SD = 8.5%) respectively. Contributions from volume delineation, recovery factor and activity quantification were consistently smaller, implying that optimising these aspects of the dosimetry chain will not significantly reduce the overall uncertainty.

Conclusions: A systematic analysis of normal organ dosimetry has shown that the dominant contributions to uncertainty in the absorbed dose are from the S-value and the fitting of the time-activity curve, hence this should be the focus of future optimisation.

67. Is Quantitative Post-treatment SPECT-CT Useful to Assess Peptide Receptor Radiotherapy Response in Neuroendocrine Tumours (NETs)?

Tahani Alkahtani[a,b,c], Lefteris Livieratos[a,b], Valerie Lewington[a,b]
[a]*King's College London, London, United Kingdom.*
[b]*Guy's & St Thomas' Hospitals NHS Foundation Trust, London, United Kingdom.*
[c]*Princess Nourah bint Abdulrahman University, Riyadh, Saudi Arabia*

Introduction/Aim: Quantitative [^{68}Ga]Ga-DOTA-TATE-PET-CTimaging has been used to assess response in patients undergoing peptide receptor radiotherapy (PRRT). As standardised uptake values (SUV) can also be calculated from post-treatment [^{177}Lu]Lu-DOTA-TATE-SPECT-CT imaging we have investigated whether serial changes in PET and SPECT-derived SUV are a) correlated and b) might be used as surrogate early response indicators.

Method: We analysed retrospective data from 19 patients with histologically confirmed, unresectable metastatic NETs treated with PRRT x4 cycles. SUVmax, lesion-to-liver (LTL) and lesion-to-spleen (LTS) were measured in 69 individual lesions and 76 normal tissues using [^{68}Ga]-PET-CT(pre- and post-PRRT) and ^{177}Lu-SPECT-CT images (24-hr post-PRRT-cycles 1 and 4). The Wilcoxon Signed-Rank test was applied to test SUV changes and Spearman's correlation.

Results: A significant correlation was shown between SPECT- and PET-derived SUV measurements (r_s=0.8, $p<0.01$). The average SPECT-SUVmax at cycle one PRRT was comparable to PET-SUVmax at baseline before PRRT (30 ± 24 and 35± 18, respectively). Following PRRT, SPECT- and PET-derived SUVmax reduced by 45± 29.6% and 34± 27.5% respectively. LTS and LTL change show a significant, robust positive linear correlation (r_s=0.8, $p<0.05$) using both SPECT and PET. LTL and LTS reduced post-therapy by 40±33.4% and 46±25.6% in SPECT and by -20±35% and -25±29% in PET, respectively.

Conclusion: Measurement of SUV changes derived from quantitative SPECT-CT is feasible to evaluate PRRT response in NETs, is comparable with PET-SUV changes and therefore may provide a useful early response indicator in NET patients undergoing molecular radiotherapy.

68. Correlation of in vitro radiotoxicity induced by Auger electron emitters and Beta minus particles with delivered absorbed dose

Ines M Costa[a], Giuseppe Schettino[b,c], Gilbert O. Fruhwirth[d], Samantha Y.A. Terry[a]
[a]*Department of Imaging Chemistry and Biology, School of Biomedical Engineering and Imaging Sciences, King's College London, London, United Kingdom.*
[b]*Faculty of Engineering and Physical Sciences, University of Surrey, Guildford, United Kingdom.*
[c]*Department of Medical Radiation Sciences, National Physical Laboratory, Teddington, United Kingdom.*
[d]*Imaging Therapies and Cancer Group Comprehensive Cancer Centre, School of Cancer and Pharmaceutical Sciences, King's College London, London, United Kingdom*

Aim: Correlation of radiobiological effects with absorbed dose in Auger-electron (AE) therapy is poorly understood. We aimed to correlate radiotoxicity induced by AE-emitters technetium-99m and iodine-123 with absorbed dose in comparison to β–emitting rhenium-188.

Methods: MDA-MB-231 breast cancer cells expressing the human sodium/iodide symporter (hNIS; MDA-MB-231. hNIS-GFP) were used as model for controlled cellular uptake of radionuclides. Uptake, efflux, and subcellular location of radionuclides were determined to estimate nuclear absorbed dose using MIRD formalism. Radiotoxicity was established using clonogenic assays. Controls included cells treated with decay products or gamma-rays.

Results: [^{99m}Tc]TcO_4^- and [^{123}I]I^- resulted in reduction in survival fraction (SF) following 72h incubation in hNIS-expressing cells only, with 22,419 and 9497 decays/cell required to achieve $SF_{0.37}$, respectively. [^{188}Re]

ReO_4^- reduced SF in hNIS-expressing cells and to a lower extent in MDA-MB-231 cells ($p<0.0001$), with 14,946 decays/cell to achieve $SF_{0.37}$. Dose-response curves of MDA-MB-231.hNIS-GFP cells followed typical linear-quadratic model post-incubation with $[^{188}Re]ReO_4^-$ and gamma-irradiation, with a lower nuclear absorbed dose to achieve $SF_{0.37}$ required for $[^{188}Re]ReO_4^-$ (0.79 Gy vs 2.59 Gy). In contrast, $[^{123}I]I^-$ and $[^{99m}Tc]TcO_4^-$ required a lower estimated dose of 0.61 and 0.68 Gy, respectively, with dose-response curves following a linear-quadratic model with constraint $\beta=0$.

Conclusion: Estimated nuclear absorbed dose indicated a greater therapeutic efficacy of AE-emitters to gamma-rays irradiation and rhenium-188, with iodine-123 requiring a lower dose to diminish cell survival to 37%. Dose-response curves fitted with $\beta=0$ constrain suggested AE-emitter-radiotoxicity being caused mainly by lethal damage, contrary to typical observed dose-response curves for gamma-rays and rhenium-188 with sub- and lethal damage contributions.

69. [^{18}F]FDG brain PET: Normal activities, asymmetries, and ratios for comparison with patient data

Gil Wright[a], Alexander Hammers[b]
[a]*University of York, York, United Kingdom.*
[b]*King's College London, London, United Kingdom*

Purpose: Physiological appearances of brain [^{18}F]FDG-PET data vary substantially. We developed simple methods to quantify asymmetries and regional activities to aid clinical interpretation.

Methods: T1w-MRI and [^{18}F]FDG-PET from 37 healthy adults from the Lyon MRXFDG normal database (Mérida I et al. 2021, 11:91. Eur. J. Nucl. Med. Mol. Imaging Res.) were aligned along the anterior commissure-posterior commissure (AC-PC), interhemispheric fissure, and tilt-corrected.

We assessed brain torque and asymmetry and sampled activities over five ROIs twice over 1-2 weeks. ROI-drawings took approximately 15 minutes/brain.

Results: Petalia extended further left occipitally (1.6±2.2, max 7.2mm) and right anteriorly (0.6±1.2, max 3.6mm). Posterior orbitofrontal cortex showed leftward protrusion into middle cerebral fossa (24/37; mean1.6±2.0, max 7.2mm).

For the five ROIs, test-retest mean absolute error was 1.4-9.2% for volumes, 1.0-3.8% for activity, and 2.1(±1.5)% for the basal ganglia/neocortex (BG/NC) ratio. Intraclass Correlation Coefficients were 0.885-0.998. Activities in the five ROIs were highly intercorrelated ($r\geq0.9$) but not with the BG/NC ratio ($r<0.1$). Coefficients-of-variation were high for individual ROIs (19-22%) but low for the BG/NC ratio (5%).

Conclusion: We replicated and quantified known asymmetries and describe a novel leftward posterior orbitofrontal lobe asymmetry of similar magnitude, useful for avoiding misattribution of anterior middle cerebral fossa asymmetries.

Despite using simple clinical software and minimal time effort, measures were highly reproducible. The BG/NC ratio was independent of variable and intercorrelated activities and had favourable descriptive statistics, supporting potential suitability for the detection of autoimmune encephalitis (DeLeiris N et al. 2021, doi:10.1007/s00259-021-05507-9. Eur. J. Nucl. Med. Mol. Imaging).

70. Usefulness of [^{18}F]FDG brain PET coregistered to MRI in an epilepsy surgery programme

Ioannis Stavropoulos[a], Nandini Mullatti[b], Rinki Singh[b], Richard Selway[b], Harutomo Hasegawa[b], Jozef Jarosz[b], Franz Brunnhuber[b], Monique Cloherty[c], Istvan Bodi[b], Teresa Szyszko[b,c], Victoria Warbey[b,d], Sally Barrington[b], Robert Elwes[b], Alexander Hammers[b]
[a]*Department of Clinical Neurophysiology, King's College Hospital, London, United Kingdom.*
[b]*King's College Hospital, London, United Kingdom.*
[c]*Royal Free London NHS Foundation Trust, London, United Kingdom.*
[d]*Guy's and St Thomas' NHS Foundation Trust, London, United Kingdom*

Purpose: Epilepsy surgery has evolved from favouring lobectomies towards tailored, smaller resections. [^{18}F]FDG brain PET has been used for over 40 years and currently co-registration to MRI increases precision. We audited the role of FDG PET+MRI in a tertiary epilepsy surgery centre for children and adults.

Methods: For 62 patients with [^{18}F]FDG-PET (35 with normal MRI) discussed in an epilepsy surgery MDT, a presurgical hypothesis was formulated based on history (including semiology), interictal EEG, ictal video-EEG, MRI and Neuropsychology without disclosure of PET. The decision on how to proceed was recorded (operation=OP / intracranial EEG=icEEG / no operation=STOP / Other (further testing and re-discussion)). The PET+MR results were then divulged, and we determined whether they altered the hypothesis/management.

Results: In 23/62 patients (37%), PET+MR did not change management (18 STOP, 3 icEEG, 2 OP).

In 15/62 (24%), there was minor impact: 14 changes to new icEEG target site(s) and 1 clarification of localisation.

Major impact was seen in 24/62 (39%). Of 15 patients deemed inoperable (STOP), 9 had an icEEG recommendation, and 6 to further testing (e.g., SPECT, new MRI). Of 7 scheduled for icEEG, 2 received a direct OP recommendation, 2 required a different icEEG evaluation, 2 further imaging, and 1 to STOP. One patient scheduled for direct OP went for icEEG instead.

Conclusion: MR-coregistered PET changed management in >60% of patients. Of 33/62 initially considered inoperable, 15 could proceed to either icEEG or further testing. In our setting, [^{18}F]FDG PET+MR was a useful presurgical investigation.

71. [^{123}I]Ioflupane progression studies: Does attenuation correction matter?

Alp Notghi, Joseph O'Brien
Sandwell and West Birmingham NHs Trust, Birmingham, United Kingdom

Repeat [^{123}I]Ioflupane studies are used to monitor the progression of disease. In equivocal cases, this can be used to establish diagnosis as annual decline in striatal Specific Binding Ratio (SBR) is higher in PD/PD+/DLB (>6%), compared to the normal decline with age (<1%). We assessed to see if SBR using Chang attenuation correction (AC) improved the distinction of normal from abnormal DaTSCAN.

Method: 21 patients with repeat studies (mean interval 24.1 months SD 14.7, median 18) were included. Images were processed using OSEM 10x10 iterations, with and without AC. Striatal SBR and z-scores (using appropriate local normal reference for AC and NAC) were calculated (GE DaTQUANT software). Paired t-test was used to compare AC and NAC, and one-way anova to compare SBR for normal (N), abnormal (PD), and vascular Parkinson's (VP) patients.

Results: Although the SBR values were higher when AC was performed, there was no difference in %annual change in SBR between AC and NAC (mean change of -3.20 and -3.57 % per annum for NAC and AC respectively, p=0.69). The % annual change was also the same for individual groups with or without AC (p=NS for N, PD and VP).

The power to distinguish the three patient groups (N, PD and VP) was good both with and without AC (p=0.01 & p=0.02 respectively).

Conclusion: When calculating SBR to assess progression of disease, both AC and NAC calculations result in the same % change per annum and can equally be used to assess the change.

72. Qualitative Comparison of different reconstruction techniques for Brain [^{18}F]FDG-PET-CT

Mohamed El-Sayed, Daniel Fakhry-Darian, Lydia Ram, Erin Ross, Simon Hughes
University Hospitals Birmingham NHS Foundation Trust, Birmingham, United Kingdom

Purpose: Iterative Reconstruction (IR) is the standard processing method for Brain [^{18}F]FDG-PET-CT in our institution. In light of advancing reconstruction techniques and different practices between departments, we aim to compare the quality of 5 reconstruction methods; to evaluate our current practice.

Methods: 10 consecutive Brain [^{18}F]FDG-PET-CT were selected from our department's worklist. Our standard protocol was used; 15 minutes acquisition on Siemens Biograph MCT64 PET-CT, 30 minutes after 250MBq [^{18}F]FDG injection. The CT-attenuation corrected scans were anonymised on Hermes, then processed using 5 reconstruction techniques; Filtered Back Projection (FBP), FBP+TOF (Time of Flight), IR, IR+TOF, IR+TOF+PSF (Point-Spread function). 50 resulting datasets were randomised, then scored by 3 readers using 3 quality indicators (1:separation of posterior cingulate gyri,2:separation of putamen & caudate,3:separation of colliculi). Scores (1-4) were provided based on well-defined standards. Results were statistically analysed using ANOVA, paired-T and Fleiss-Kappa tests (SPSS).

Results: IR showed the highest total mean quality scores ($reader_1$=3, $reader_2$=2.4, $reader_3$=2.7) with substantial inter-reader agreement (k=0.681,p<0.001,95%CI 0.48-0.88). IR was not significantly superior to IR+TOF (p=0.086) or FBP+TOF (p=0.110), but these demonstrated less inter-reader agreement. IR was significantly superior to FBP (p=0.013) and IR+TOF+PSF (p<0.001); the latter had the lowest total mean quality scores ($reader_1$=2.2, $reader_2$=1.8, $reader_3$=2) with substantial inter-reader agreement (k=0.612,p<0.001,95%CI 0.41-0.82).

Conclusion: IR is superior to FBP for processing Brain [^{18}F] FDG-PET-CT. In departments where FBP is still used, adding TOF can improve image quality. PSF should not be used with IR, as it degrades image quality.

73. Audit of memory clinic patients receiving indeterminate [^{18}F]FDG PET-CT brain reports in order to establish current care

Jayne Lynch[a], Tiarna Byrne[a], William Murphy[a], Bernadette McGuinness[a,b], Peter Passmore[a,b], Emma Cunningham[a,b]
[a]*Belfast Health and Social Care Trust, Belfast, United Kingdom.*

[b]*Queen's University, Belfast, United Kingdom*

Background: Fluorodeoxyglucose positron emission tomography/computed tomography ([18F]FDG PET/CT) is recommended when diagnostic clinical criteria for early dementia are inadequate, with reduced uptake patterns indicating dementia causing diseases.

This audit of our current practice aimed to identify patients with indeterminate scan results and review clinical follow-up and diagnoses.

Methods: [18F]FDG PET/CTs requested between 01/01/2015 to 31/12/2018 were analysed (n=134). Reports were further reviewed if a) there was any mention of reduced uptake and b) this was insufficient to constitute a typical disease pattern (n=74). These were then categorised into reports with indeterminate (n=22) and negative conclusions (n=52).

Parietal and post-cingulate Z scores were calculated using the CortexID programme and deemed significant if >2. Electronic care records were interrogated between January – March 2021 for clinical follow-up and diagnoses.

Results: All n=22 patients with indeterminate report conclusions had areas of reduced uptake in the temporoparietal regions. At outpatient follow up, 20 had developed dementia (11/20 had parietal z scores >2) and 2 had mild cognitive impairment (with normal z scores).

Furthermore, of n=52 with negative reports, 43/52 had reduced uptake in the temporoparietal regions, 9 with parietal z scores >2. At outpatient follow up, 24/52 had developed dementia, 7 with z scores >2.

Conclusion: The majority of patients with an indeterminate [18F]FDGPET-CTconclusion and patients with a negative conclusion but significant parietal z scores subsequently developed dementia. All patients with 'indeterminate' scans, by their current definition, and parietal z scores >2, should be followed up.

74. Feasibility and initial experience of [18F]FET PET-MR image fusion for evaluation of recurrent primary brain tumours

Habibollah Dadgar
Nuclear Medicine and Molecular imaging centre, RAZAVI hospital, Mashhad, Islamic Republic of Iran

Background: An accurate monitoring technique is crucial in brain tumours to choose the best treatment approach after surgery and/or chemoradiation. Radiological assessment of brain tumours is widely based on the MRI modality in this regard; however, the MRI criteria are unable to precisely tumoral tissue from treatment-related changes. This study was conducted to evaluate whether combined MRI and 18F-FET PET can improve the diagnostic accuracy of the practitioners to discriminate treatment-related changes from true recurrence of brain tumour.

Methods: We retrospectively analysed [18F]FET PET-CTof 11 patients with the histopathologically proven brain tumour that were suspicious for recurrence changes after 3-4 months of surgery. All patients underwent MRI and [18F]FET PET/CT. As a third assessment, fused [18F]FET PET/MRI was also acquired. Finally, the diagnostic accuracy of the applied modalities was compared.

Results: Eleven patients aged 27 to 73 years old with a mean age of 47 ± 13 years were enrolled. According to the results, of 11 cases, 9 cases (82%) showed positive MRI and 6 cases (55%) showed positive PET-CTand PET/MRI. Tumoral recurrence was observed in 6 patients (55%) in the follow-up period. Based on follow-up results, accuracy, sensitivity, specificity, positive predictive value (PPV) and negative predictive value (NPV) were 64%, 85%, 25%, 67%, 50% for MRI alone and 91%, 85%, 100%, 100% and 80% for both PET-CTand PET/MRI, respectively.

Conclusion: This study found that [18F]FET PET-MR image fusion in the management of brain tumours might improve recurrence detection; however, further well-designed studies are needed to verify these preliminary data.

75. Added utility of [67Ga]SPECT-CT to prior high resolution petrous temporal CT and MR IAMs in confirming or excluding skull base osteomyelitis in cases of otitis externa/necrotising otitis externa

Randeep Kulshrestha, Nirav Kaneria, Ayah Nawwar, Julian Kabala
University Hospitals Bristol & Weston NHS Foundation Trust, Bristol, United Kingdom

Purpose: To investigate the added utility of [67Ga]SPECT-CT to prior CT and MR imaging of the skull base/petrous temporal region in patients with suspected otitis externa or necrotising otitis externa.

Method: Retrospective review of x13 patients who had a [67Ga]SPECT scan for suspected necrotising otitis externa and prior imaging with CT of the petrous temporal bones +/- MR internal auditory meati. Epicentre of infection was sought with SPECT-CT and also the value of serial imaging was assessed.

Results: 11 of 13 patients had positive findings on SPECT-CT and 2/13 were confirmed as negative. Of the 11 patients, 2/11 had otitis externa alone, 1/11 had necrotising otitis externa, with no bone involvement, and 8/11 had necrotising otitis externa with bone

involvement/osteomyelitis. All positive cases correlated well with prior CT +/- MR imaging, in one case excluding bone involvement suspected on CT. The epicentre of active infection and distribution/migration of infection was more accurately located with SPECT-CT in 10/13 patients (77%). Serial imaging in 6 patients was carried out to monitor response to treatment or to assess for recurrence and 3/6 showed migration and progression, and 1/6 patients showed a partial treatment response, and 2/6 showed complete resolution.

Conclusion: [^{67}Ga]SPECT-CT showed excellent correlation with both CT and MRI, and in many cases confirmed the exact location and accurately assessed for associated osteomyelitis of the skull base, resulting in a longer course of IV antibiotics. In the 6 patients who had serial imaging, it accurately monitored treatment response.

76. [^{18}F]FDG PET-CT in Anti-Neutrophil Cytoplasmic Antibodies-associated Vasculitis (ANCA-V): prospective, cross-sectional, single centre study

Laura-May Davis[a], Alexandra Dudek[a], Michael Kemna[b], Vanessa Morris[c], Stefan Voo[a,d]
[a]*Institute of Nuclear Medicine, University College London Hospital NHS Foundation Trust, London, United Kingdom.*
[b]*Maastricht University Medical Centre, Maastricht, Netherlands.*
[c]*Department of Rheumatology, University College London Hospital, London, United Kingdom.*
[d]*Biomedical Research Centre, NIHR, UCLH, London, United Kingdom*

Background: Tools for evaluation of activity in patients with anti-neutrophil cytoplasmic antibodies (ANCA)-associated vasculitis (ANCA-V) include scoring clinical manifestations, determination of biochemical parameters of inflammation and obtaining tissue biopsies. These diagnostic tools, however, are sometimes inconclusive.

The aim of this study is to evaluate the added value of PET scans in patients with AAV with suspected disease activity.

Material and Methods: All PET scans made between December 2020 and February 2022 to assess disease activity in biopsy-proven ANCA-V patients were retrospectively included in the study. All scans were examined visually and quantitatively using SUVmax and positive findings which were classified according to their anatomic localisation. Clinical data, hsCRP and ANCA levels both at the same time of scanning and during a follow-up period of at least of 1 year were obtained.

Results: Fifteen scans were performed during a period of suspected active disease. 48 positive sites were found in total, most commonly the nasopharynx (n=11) and the lungs (n=9). Interestingly, 18 clinically occult sites were found, such as the thyroid glands (n=5), aorta (n=4) and bone marrow (n=6).

Conclusion: [^{18}F] FDG PET scans in ANCA-V patients with active disease show positive findings in multiple sites of the body, including sites clinically unsuspected and difficult to assess otherwise. PET scans may offer an added diagnostic value when other evaluations are inconclusive.

77. Use of Delayed Imaging in [^{201}Tl]TlCL Brain SPECT-CT

Louise-Anne Wason[a], Natasha Fullerton[b], Alice Nicol[c]
[a]*Department of Nuclear Medicine, DCPB, New Victoria Hospital, Glasgow, United Kingdom.*
[b]*Department of Neuroradiology, INS, Queen Elizabeth University Hospital, Glasgow, United Kingdom.*
[c]*Department of Nuclear Medicine, DCPB, Queen Elizabeth University Hospital, Glasgow, United Kingdom*

[^{201}Tl]TlCl SPECT-CT can be used to differentiate between non-malignant and malignant processes, and higher from lower grade glial tumours. We aimed to determine if performing delayed imaging in addition to routine early imaging would help differentiate high from low grade glioma, and recurrent glioma from inflammatory processes, including radiation necrosis and pseudo-progression.

Four patients were referred with suspected or known glioma after MRI had identified new tumour or apparent tumour progression. Each underwent SPECT-CT imaging of the head, performed at 10 minutes and 3 hours post administration of 100MBq [^{201}Tl]TlCl.

In two patients with glioblastoma treated previously with radio- and chemotherapy, imaging demonstrated increased focal [^{201}Tl]TlCl uptake on both early and delayed imaging. No [^{201}Tl]TlCl washout on the delayed imaging was seen in one of the patients, and increased delayed uptake in the other, suggesting tumour recurrence rather than pseudo-progression or radiation necrosis.

One patient with newly diagnosed tumour demonstrated no [^{201}Tl]TlCl uptake in early or delayed imaging suggesting no significant volume of high-grade tumour.

One patient with suspected glial tumour demonstrated initially increased [^{201}Tl]TlCl uptake, with washout and decreased uptake on delayed imaging, suggesting a benign process not high-grade tumour.

This initial data demonstrates that performing additional delayed imaging can be useful for management of patients with suspected glioma and suspected radiation

necrosis. An audit of a larger number of patients will follow to determine the usefulness of this technique in the management of glioma patients, particularly with suspected radiation necrosis.

78. New bifunctional chelators for radiolabelling of antibodies with PET imaging radioisotopes

Matthew Farleigh[a], Truc Pham[a], Zilin Yu[a], Jana Kim[a], Kavitha Sunassee[a], George Firth[a], Vijay Chudasama[b], James Baker[b], Nicholas London[c], Charlotte Rivas[a], Michelle Ma[a]
[a]*King's College London, London, United Kingdom.*
[b]*University College London, London, United Kingdom.*
[c]*Imperial College London, London, United Kingdom*

Background: Positron Emission Tomography (PET) imaging with antibody-based contrast agents frequently uses the radioisotopes [^{64}Cu]Cu^{2+} and [^{89}Zr]Zr^{4+}. Sarcophagine (sar) chelator is ideal for labelling receptor-targeted biomolecules with [^{64}Cu]Cu^{2+}. Desferrioxamine-B (dfo) chelator, has been widely used to incorporate [^{89}Zr]Zr^{4+} into antibodies.

Purpose: We aim to (i) develop new bifunctional chelators of sar and dfo, derivatized with dibromomaleimides (dm), that enable site-specific and highly stable attachment of molecular cargoes to reduced, solvent-accessible, interstrand native disulfide groups; and (ii) demonstrate proof-of-principle of these new platforms in vitro and in vivo, using HER2-targeted trastuzumab, which is commonly used to treat breast cancer, and is employed here as a model antibody.

Methods: The new sar-dm and dfo-dm derivatives were chemically synthesised and attached to trastuzumab via reaction with reduced interstrand disulfide groups of the antibody. Both sar- and dfo-dm-trastuzumab conjugates were then radiolabeled with [^{64}Cu]Cu^{2+} and [^{89}Zr]Zr^{4+}, to yield [^{64}Cu]Cu-sar-dm-trastuzumab and [^{89}Zr]Zr-dfo-dm-trastuzumab respectively. The stability of these new radiolabeled immunoconjugates was assessed in serum. Cell uptake and *in vivo* PET imaging and biodistribution studies were undertaken with [^{64}Cu]Cu-sar-dm-trastuzumab.

Results: Both [^{64}Cu]Cu-sar-dm-trastuzumab and [^{89}Zr]Zr-dfo-dm-trastuzumab could be radiolabeled in near quantitative radiochemical yield (>99%). Both exhibited high stability in serum. *In vivo* PET imaging and biodistribution analyses showed that [^{64}Cu]Cu-sar-dm-trastuzumab possesses high stability in biological milieu and retains affinity and specificity for the HER2 receptor.

Conclusion: Our new chelator platforms can be easily applied to enable stable, site-specific radiolabelling of antibodies with PET isotopes, enabling tracking of antibodies with PET imaging.

79. Assessing in vitro functions of [^{89}Zr]Zr-oxine labelled Natural Killer cells and in vivo tracking with PET imaging

Truc Pham[a], Alicia Chenoweth[b], Gabriel Osborn[b], Sophia N Karagiannis[b], Michelle Ma[a]
[a]*Department of Imaging Chemistry and Biology, School of Bioengineering and Imaging Sciences, King's College London, London, United Kingdom.*
[b]*Cancer Antibody Discovery & Immunotherapy Group, St. John's Institute of Dermatology, School of Basic & Medical Biosciences, King's College London, London, United Kingdom*

Aims: To evaluate the *in vitro* functions of [^{89}Zr]Zr-oxine labelled Natural Killer (NK) cells and track them *in vivo* with PET imaging.

Methods: NK cells were isolated from healthy human volunteers and expanded *ex vivo*. [^{89}Zr]Zr-oxine was synthesised using a kit (F. Man *et al.*, 2020, 90-91:31-40 *Nucl. Med. Bio.*). Various *in vitro* functions of [^{89}Zr]Zr-oxine labelled NK were assessed including viability, proliferation, migration, antibody-dependent cellular cytotoxicity (ADCC) using trastuzumab against HER2 over-expressing cancer cell lines. Flow cytometry was used to monitor NK markers. PET-CTimaging was used to track ^{89}Zr-labelled NK *in vivo*.

Results: [^{89}Zr]Zr-oxine was reproducibly synthesised with good yields (92.1±3.5%, n=10), and used to radiolabel NK cells with moderate labelling efficiencies (39.4±6.6%, n=23). The radiolabelling didn't affect NK cells viability and characteristic marker CD16/CD56 expressions. Though ADCC assays showed donor-dependant responses, overall ^{89}Zr-labelled NK exhibited comparable ADCC functions to those of non-radiolabelled cells. Cell migration assay suggested that ^{89}Zr-labelled NK cells presented basic responses to stimuli, typical to NK cells. PET-CTimaging showed that NK cells migrated from lung at 24h to liver and spleen at 72h post-injection. *Ex vivo* flows cytometric analyses of these mouse tissues detected huCD45^{+} human leukocytes, which were further confirmed as human CD56^{+}CD16^{+} NK.

Conclusion: Ex vivo expanded NK cells can be radiolabelled with [^{89}Zr]Zr-oxine while maintaining their basic cellular and cytotoxic functions. Preliminary data showed that ^{89}Zr-labelled NK can be tracked *in vivo* using PET imaging, prompting further research to track NK kinetics including tumour infiltration in the presence of therapeutic antibodies in animal models of cancer.

80. Diphosphine bifunctional chelators: [^{99m}Tc]Tc-DP-PSMAt tracers for PSMA imaging in prostate cancer

Ingebjørg N. Hungnes[a], Truc T. Pham[a], Charlotte Rivas[a], George Firth[a], James A. Jarvis[a], Jennifer D. Young[a], Philip J. Blower[a], Paul G. Pringle[b], Michelle T. Ma[a]

[a]*King's College London, London, United Kingdom.*
[b]*Bristol University, Bristol, United Kingdom*

Receptor-targeted, molecular imaging with [^{99m}Tc]Tc-peptides have demonstrated clinical utility in the management of cancer. A challenge in the development of [^{99m}Tc]Tc-peptides is designing suitable chelators that allow one-step, kit-based radiolabelling of peptides.

We have developed a diphosphine (DP) platform for preparation of dimeric [^{99m}Tc]Tc-dipeptide tracers. Two diphosphines, 2,3-bis(diphenylphosphino)maleic anhydride (DP1) and 2,3-bis(di-*p*-tolylphosphino)maleic anhydride (DP2), were each reacted with a PSMA-targeted dipeptide (PSMAt) to form the conjugates, DP1-PSMAt and DP2-PSMAt. Each DP-PSMAt conjugate was incorporated into lyophilised kits and radiolabelled with [^{99m}Tc]Tc-pertechnetate in saline. Leaving the reconstituted kit at ambient temperature for 5 min yielded [^{99m}Tc]Tc-DP1-PSMAt in >75% radiochemical yield (RCY), and [^{99m}Tc]Tc-DP2-PSMAt in >80% RCY; heating the reaction at 100 °C for 5 min yielded [^{99m}Tc]Tc-DP1-PSMAt in >80% RCY, and [^{99m}Tc]Tc-DP2-PSMAt in >85% RCY. Biologically compatible solutions of each tracer in >95% radiochemical purity was obtained within a total of 30 min by HPLC purification.

Both [^{99m}Tc]Tc-DP1-PSMAt and [^{99m}Tc]Tc-DP2-PSMAt exhibited specific affinity to PSMA receptors in cell uptake studies, were hydrophilic, and showed high serum stability. Pre-clinical imaging and biodistribution studies in mice showed that both tracers had specific uptake in PSMA-expressing DU145-PSMA tumours, with low uptake in non-target organs, and were excreted *via* a renal pathway. HPLC examination of urine showed that both tracers were excreted intact.

PSMA-targeting conjugates, DP1-PSMAt and DP2-PSMAt, are readily radiolabelled with [^{99m}Tc]pertechnetate in 5 min using single-step kits, with tracers of >95% radiochemical purity obtainable in <30 min. The resulting PSMA-targeted tracers allow SPECT imaging of PSMA expression *in vivo*.

81. Towards imaging cisplatin resistance with ^{64}Cu PET

Fahad Al-salemee, Joanna Bartnicka, George Firth, Jana Kim, Timothy Witney, Philip Blower, Cinzia Imberti
School of Biomedical Engineering and Imaging Sciences, King's College London, London, United Kingdom

Background: Cisplatin efficacy is often limited by the development of resistance. Copper transporters (CTR1, ATP7A, ATP7B) have been proposed to mediate cisplatin transport. We investigated the novel application of unchelated ^{64}Cu(II) PET imaging as a predictor of cisplatin accumulation in tumours in vivo.

Methods: Two variants of the human ovarian carcinoma cell line A2780, cisplatin-sensitive (WT) and cisplatin-resistant (CisR), were used. Accumulation of [^{64}Cu]CuCl2 and cisplatin was compared between the two cell lines over 120 minutes via gamma counting and ICP-MS, respectively. PET-CTimaging of xenograft-bearing (WT or CisR) female Balb/c mice intravenously injected with pH-neutral [^{64}Cu]CuCl2 (2-4 MBq/animal) was done over 2 hours post injection.

Results: ^{64}Cu accumulation was significantly lower in CisR than WT cells (1.2±0.4 vs. 4.1±0.3 Bq/10^3 cells at 120 minutes)(n=3, p<0.001). The same was true for cisplatin (0.105±0.022 vs. 0.299±0.067 ng Pt/10^3 cells at 120 minutes)(n=3, p=0.009). On PET-CTimaging, CisR xenografts accumulated significantly less ^{64}Cu than WT xenografts over 2 hours post injection (2.96±0.34 vs. 6.12±0.54 and 2.99±0.32 vs. 6.95±0.73 %ID/g at 60 and 120 minutes, respectively) (n=4, p<0.001 for both time points).

Conclusion: ^{64}Cu accumulation correlated with cisplatin accumulation in vitro and with sensitivity/resistance to cisplatin in vitro in A2780 cells and in vivo in A2780 xenografts. These results show promise for ^{64}Cu PET imaging as a novel marker of tumour sensitivity/resistance to cisplatin.

82. Potential role of quantitative SPECT-CT in post-therapeutic assessment of patients with neuroectodermal tumours: a retrospective, single-centre, case series study

Laura May Davis[a], Alexandra Dudek[a], April-Louise Smith[a], Catherine Scott[a], John Dickson[a], Jamshed Bomanji[a], Stefan Vöö[a,b]
[a]*Institute of Nuclear Medicine, University College London Hospital, London, United Kingdom.*
[b]*Biomedical Research Centre, NIHR, University College London Hospital, London, United Kingdom*

Background: [I123/131]metaiodobenzylguanidine (MIBG) is an already established theragnostic approach in diagnosis and therapy of neuroectodermal tumours (NET), including pheochromocytoma, paraganglioma and neuroblastoma. Despite advances in imaging, the interpretation of pre-/post-therapeutic scans remains purely qualitative with limited predictability of patient's response to treatment and prognostication.

The current study aims to determine the role of quantitative SPECT-CT (qSPECT-CT) in NET patients' treatment response assessment.

Methods: All patients with histologically proven, MIBG-positive NET, who were referred to radionuclide MIBG therapy and had clinical 1-year follow-up in the period 2018-2021 were identified in the clinical records. Only those patients with equivocal/stable disease on post-therapy MIBG scans were included in the study. qSPECT-CT was performed on pre-/post-therapy MIBG images and used to quantify the change in maximum standard uptake value (SUVmax) within the global tumoral burden. Clinical outcome data was collected.

Results: 6 NET patients were included in the study. Average lesion volume 68 ml. All patients have equivocal/stable disease based on visual/qualitative interpretation of the pre-/post-therapy therapy images. However, qSPECT-CT showed that average SUVmax in responders was significantly higher than non-responders (median SUVmax:19 in responders; SUVmax 7.5 in non-responders ($P < 0.05$)).

Conclusion: Quantitative SPECT-CT proves to be a useful tool for response assessment following MIBG therapy in cases where standard qualitative image interpretation is equivocal or cannot depict metabolic change. Future research with a more complete dataset would allow pre- and post-therapy imaging parameters to be compared with a view to developing a scoring system that accounts for both changes in lesion size and avidity.

83. Experience of performing [^{177}Lu]Lu-PSMA radionuclide therapy in an outpatient setting

Nathaniel Scott[a], Matthew Patterson[a], Anne-Marie Stapleton[a,b], Anita Harte[a], Yong Du[a,c]
[a]*GenesisCare, Windsor, United Kingdom.*
[b]*Royal Surrey County Hospital NHS Foundation Trust, Guildford, United Kingdom.*
[c]*The Royal Marsden NHS Foundation Trust Foundation Trust, London, United Kingdom*

[^{177}Lu]Lu-PSMA radionuclide therapy is an emerging treatment option for men with metastatic castration-resistant prostate cancer (mCRPC). This work presents our experiences in setting up and running an outpatient [^{177}Lu]Lu-PSMA therapy service.

Methods: Genesis Care introduced the UK's first [^{177}Lu]Lu-PSMA non-trial outpatient service in 2019. Treatment eligibility criteria include: PSMA-expressing mCRPC (confirmed by a [^{68}Ga]Ga-PSMA PET-CTscan); a performance score ≤ 2; and no significant kidney, liver or bone marrow dysfunction. Treatments are performed in dual-purpose PET-CTuptake rooms with the radiopharmaceutical administered via IV injection, alongside an IV saline infusion and oral fluids. Planar whole-body scans performed ~1 hour post injection verify successful treatment delivery. Patients are discharged with radiation restrictions once their external dose rate is <25 μSv/hr at 1 metre and following a 10% reduction from their baseline reading.

Results: Between May 2019 and December 2021, 327 treatment cycles were administered over 104 individual patients using [^{177}Lu]Lu-PSMA. The median treatment time was 3 hours and the maximum number of patients treated in a single day was 4. The treatment procedure has been optimised to ensure safe treatment delivery and maximise patient throughput.

Conclusion: We have shown that performing [^{177}Lu]Lu-PSMA treatment in an outpatient setting is both safe and viable. This has helped to minimise costs and improve patient experience compared to traditional inpatient radionuclide therapies. To ensure a safe and effective service, input is required from a wide-ranging multidisciplinary team. Future service development will look to optimise post-therapy imaging to enable patient specific dosimetry to be performed.

84. Performance analysis of the Mediso nanoScan PET-CT system with zirconium-89 and vanadium-48 at low activities

Katherine Wilson[a,b], Stephen Paisey[c], Andrew Fenwick[d]
[a]*Singleton Hospital, Swansea, United Kingdom.*
[b]*Swansea University, Swansea, United Kingdom.*
[c]*Cardiff University, Cardiff, United Kingdom.*
[d]*National Physical Laboratory, London, United Kingdom*

Preclinical PET image quality using non-conventional radioisotopes zirconium-89 and vanadium-48 was evaluated. For zirconium-89, the purpose was to ascertain whether it would be feasible to reduce the dose administered to subjects without an inadmissible reduction in image quality. The objective of investigating vanadium-48 was to undertake a qualitative analysis of image quality at low activities.

Method: Syringes were filled with [^{89}Zr]Cl_4 and scanned seven times over the course of 22 days using the Mediso nanoScan PET-CTsystem. Activity ranged from 5.44 MBq to 6.60 kBq. A NEMA NU-4 image quality phantom was filled and similarly scanned as it decayed to 47.3 kBq.

A vanadium-48 dilution series simulated a decay over six half-lives. The activity range was 8 MBq to 14 kBq. A microDerenzo phantom was filled with 7 MBq to give an indication of the spatial resolution.

Results: Between 5.4 MBq and 30 kBq, all reconstructed zirconium-89 data deviated less than 3% from their expected activity. Recovery coefficients for cylinders of diameter 5 mm to 2 mm and spill over ratios for water and air were in statistical agreement with the manufacturer's

tolerance. The lowest measured activity for which the uniformity was permissible (< 15%) was 1.63 MBq.

Objects as small as 1 mm in diameter were resolvable in the vanadium-48 phantom. Activity deviation for the vanadium-48 dilution series was below 10% for all activities above 1.05 MBq.

This work showed that further studies would be warranted in the use of and dose minimisation of these radioisotopes.

85. Assessing the improvement in lesion detectability on the Siemens Biograph Vision PET – a phantom study using a Channelised Hotelling Observer

Christopher Oldfield[a], Ian Armstrong[b], Peter Julyan[a], Bal Sanghera[c]
[a]*The Christie, Manchester, United Kingdom.*
[b]*Manchester University NHS Foundation Trust, Manchester, United Kingdom.*
[c]*Mount Vernon, London, United Kingdom*

The Siemens Biograph Vision uses silicon photomultipliers (SiPMs) in place of photo-multiplier tubes and has the best timing resolution of any commercially available system. It provides superior timing and spatial resolution to the previous generation Siemens Biograph mCT. This work compared the performance of these two systems for lesion detectability using a modified NEMA IQ phantom filled at 4:1 with long-lived germanium-68 and a numerical observer.

The phantom was scanned on both systems. Choices in number of reconstruction updates (5-72), use of OSEM, OSEM+ToF, and OSEM+ToF+PSF, and post reconstruction smoothing (0-5 mm) were investigated using a Channelised Hotelling Observer (CHO). List-mode acquisitions were split into 50 frames of 90 seconds. For each reconstruction the CHO was given a subsample of the image volume from the phantom background and one containing the spherical insert. The area under a receiver operator characteristic curve (AUC) and associated confidence intervals were calculated for each set of reconstruction parameters.

The CHO produced AUC values of up to 0.83 for the 5 mm insert on the Vision – using OSEM +ToF+PSF with 3 iterations of 5 subsets and a 5 mm smoothing filter. For all images of this insert produced by the mCT the AUC was consistent with 0.5 – providing no discrimination.

This work has demonstrated that the Vision provides significant improvement in lesion detectability. The results have helped to modify clinical protocols at Manchester Foundation Trust – reducing reconstruction updates and acquisition time.

86. Building and validating a full gamma camera model in Geant4 for research applications

Gregory James, Joseph O'Brien, Bill Thomson
Sandwell and West Birmingham Hospitals NHS Trust, Birmingham, United Kingdom

Aim: Monte Carlo codes are helpful in modelling radiation transport through matter. Given the growing popularity of Geant4 and its flexibility for medical physics applications, the aim of this work was to build and validate a full gamma camera model in Geant4 for research applications.

Method: The Geant4 code was setup to record the total energy deposited by each photon in the NaI crystal as well as the (x,y,z) coordinates of the final interaction position. These data were then binned to produce an energy spectrum and image. The Geant4 gamma camera model was tested against a GE Discovery gamma camera for key performance indicators including statistical noise texture, energy spectrum, image quality, sensitivity and spatial resolution. These were tested for three radionuclides: technetium-99m, iodine-123 and indium-111.

Results: Chi-square testing concluded that the noise texture in a simulated flood image followed a Poisson distribution (all $p>0.05$). Energy spectrum data was not significantly different from real data in the photopeak region(s) however systematic differences were observed at low energies (<50 keV). Sensitivity was with 2% of real data and spatial resolution was within 2mm FWHM for a range of collimators and distances.

Conclusion: An accurate gamma camera model has been built and validated using Geant4. Validation showed some disagreement between the simulated Compton continuum and real data, however the energy spectrum around the photopeak(s) is sufficiently accurate. This allows specific research applications to be easily explored using varying imaging conditions.

87. Quantitative imaging using customised 3D printed phantoms

Jessica Johnson[a], Kathryn Adamson[a], Christopher Bunton[a], Silke Heyse[b]
[a]*Guy's and St Thomas' NHS Foundation Trust, London, United Kingdom.*
[b]*Brunel University, London, United Kingdom*

Purpose of the study: Design 3D-printed phantoms to provide information about the accuracy of SUV measurements in SPECT-CT in 2 different scenarios.

Methods: A Jaszczak phantom was modified to produce 2 different phantoms. Firstly, two 3D-printed fillable

spheres (100 ml and 200 ml volume) were constructed and fitted similar to the IEC NEMA phantom. Secondly, a clinically realistic 3D printed liver, based on patient CT data, with a refillable tumour was constructed. Design considerations allowed the spheres and liver to be interchangeable within the Jaszczak phantom.

The spheres were filled with technetium-99m with an activity concentration higher than the phantom background, with a known SUV of 12.45 and 12.86 for the 100ml and 200ml sphere respectively. The tumour was filled with an activity concentration higher than the liver with an SUV of 7.78.

SPECT-CT images were acquired and reconstructed on a Siemens Symbia Intevo Bold SPECT-CT system, calibrated for xSPECT Broad Quantification. Quantitative analysis was performed using 2 SUV metrics-SUV_{max}, and the average SUV for a VOI outlining the 50% isocontour for the sphere ($SUV_{50,meas}$).

Results: For the 100 ml and 200 ml spheres, the $SUV_{50,meas}$ overestimated the true values by 3.0% and 1.1% respectively, and the SUVmax overestimated by 32.8% and 24.7% respectively. For the tumour, $SUV_{50,meas}$ underestimated by 0.7%, and the SUV_{max} overestimated by 16%.

Conclusion: The $SUV_{50,meas}$ was the most accurate metric, giving results close to the true values. However, the variation in measured and true SUV values for both metrics highlights the need to exercise caution when using SPECT-CT SUVs.

88. Assessing the potential extent of spatial dependence of the Partial Volume Effect in SPECT

Rebecca Gillen
Department of Clinical Physics and Bioengineering, Glasgow, United Kingdom. Department of Nuclear Medicine, North-East Sector, Glasgow, United Kingdom. Institute of Nuclear Medicine, University College London, London, United Kingdom. Marine, Medical and Nuclear Department National Physical Laboratory, Teddington, United Kingdom

Aims: The spatial dependence of the partial volume effect (PVE) in SPECT imaging has been explored in simulation work (Gillen R. et al. 2019, 46(Suppl 1):S771 EJNMMI), demonstrating a potentially significant variation in quantification (up to 47%). A previous study observed up to 35% spatial variation in the activity concentration recovery, used for PVE correction, and noted that the variation in clinical images is likely underestimated (Armstrong IS. 2018, 40:287-293. Nucl. Med. Comms.). The current work aims to systematically assess the spatial dependence of the PVE in practice.

Methods: A NEMA phantom (filled with [^{99m}Tc], sphere-to-background ratio (SBR) 10:1) was positioned on the imaging couch with one sphere at CT isocentre. The phantom was then repositioned such that the sphere originally at isocentre was nearer the detectors. Poorer spatial resolution, i.e., increased PVE, was expected for the central sphere compared with the same sphere positioned nearer the detectors. Reconstructions were performed with a range of parameters. Sphere volumes were segmented using the A50 threshold, and the SBR calculated for each sphere in both positions.

Results: In both sphere sizes examined to date, the SBR was lower with the sphere positioned at isocentre compared with off-centre (10-32%, sphere size dependent) – as expected, if reconstructed without collimator modelling. With collimator modelling, the SBR was 20% lower in the smaller sphere but 7% higher for the larger sphere. Further investigation is ongoing.

Conclusions: This work demonstrates that the extent of the PVE depends on position by 7-32%, depending on the reconstruction parameters used.

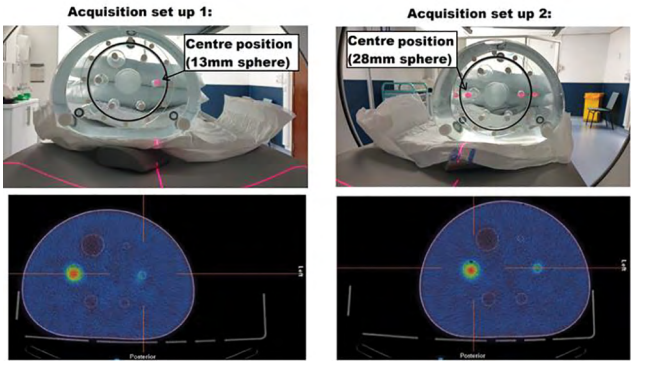

89. Optimising Vulval SLN SPECT-CT images with a Gaussian Filter

Joseph O'Brien, Dr Alp Notghi, Dr Bill Thomson, Dr Gregory James
Sandwell & West Birmingham Hospitals, Birmingham, United Kingdom

Aim: To determine if a Gaussian filter (GF) improves visualisation of vulval SLN studies over the standard Butterworth filter (BF).

Introduction: SPECT-CT of vulval SLN studies produces nodal counts that are significantly lower than injection site counts, requiring the reporter to use an extreme window in order to see the nodes. At this window level, negative count 'ring artefacts' associated with a BF during reconstruction are present around hot nodes and injection site, causing distraction. GF's do not create such

artefacts, but their use needs to be tested to ensure node detectability is retained.

Method: 25 patients acquired on a GE Discovery-NM/CT670 or Infinia-Hawkeye4, between Jan2020-Jan2022 were examined retrospectively. Using a GE Xeleris 4DR, an experienced physicist compared the original report to the images produced by default processing (resolution recovery with CTAC, 4x10 iterations, Butterworth PF=10, CF=0.50 cycles/cm). They reprocessed with a GF (FWHM x,y,z=1.5mm), and compared the number of nodes per side between the different filters.

Results: Comparing BF images and the original report, the same number of nodes per side were counted in 22/25 patients. In 3/25, there was a tendency to count one more equivocal node. Comparing GF vs BF images, the same number of nodes per side was counted in 23/25 cases, with 2/25 cases showing a potential extra node with GF. GF images appeared sharper.

Conclusion: Application of GF retained node sensitivity and can be used instead of BF to avoid distracting ring artefacts. This provides improved quality images to the reporter and surgeon.

90. PETiTe: Trial of Fast-track PET Scheduling ahead of biopsy in Lung Cancer

Goncalo Ferreira[a,b], Ana Matos[a,b], Alexander Small[a,b], Mary Dempsey[a,b], David Colville[c], Joris Van Der Horst[d]
[a]*West of Scotland PET Centre, Gartnavel General Hospital, Glasgow, United Kingdom.*
[b]*Department of Clinical Physics & Bioengineering, NHS Greater Glasgow & Clyde, Glasgow, United Kingdom.*
[c]*Diagnostic Imaging Services, NHS, Glasgow, United Kingdom.*
[d]*Consultant Respiratory Physician, NHS Greater Glasgow & Clyde, Glasgow, United Kingdom*

Introduction: Lung Cancer accounts for one of the highest cancer mortality rates in Scotland with overall survival below other European countries. One of the main factors is delay in diagnosis and staging in which PET-CTplays an important role. Due to average 14 day wait for a PET-CTin Glasgow, a pilot project, PETiTE, was implemented to prioritise patients suitable for curative treatment with early-stage peripheral lung cancer or possible mediastinal involvement.

Methods: Five "fast track" slots/week were allocated to those patients deemed to benefit most from early access to treatment to undergo CT, PET-CTand EBUS within one week. Provision of this project required robust communication/training of respiratory staff to ensure necessary information regarding PET appointment was relayed to the patient at clinic. Cut off times for referral were agreed so that PET appointments were fully utilised.

Results: To date, approximately 250 lung cancer patients have received "fast tracked" PET/CT. Early data demonstrated improvement with 80% completing diagnostic pathway in less than 31days, referral to treatment time reduced by 9 days and 60% fewer repeat invasive tests performed.

Conclusion: Collaboration between the PET department and Respiratory team has resulted in improvement in lung cancer pathway for selected patients and reduction in repeat procedures. As a result, expansion to the other sites in West of Scotland is planned with the aim to achieve the target Scottish National Optimal Lung Cancer Pathway of diagnosis within 21days and treatment within 42days for this patient group.

91. First Experience of PSMA PET-CT Imaging in the West of Scotland

Carolina Rodrigues[a,b], Ana Matos[a,b], David Colville[c], Sandy Small[a,b]
[a]*West of Scotland PET Centre, Gartnavel General Hospital, NHS Greater Glasgow and Clyde, Glasgow, United Kingdom.*
[b]*Department of Clinical Physics & Bioengineering, NHS Greater Glasgow and Clyde, Glasgow, United Kingdom.*
[c]*Diagnostic Imaging Services, NHS Greater Glasgow and Clyde, Glasgow, United Kingdom*

Introduction/Aim: In recent years, PSMA PET has been shown to be superior in the identification of recurrent Prostate Cancer and there was a demand to have this service available in Scotland. We aim to describe the initial setup of the first department to deliver PSMA service in Scotland.

Methods: Firstly, all patients were selected using strict referral criteria modified from the Scottish PSMA guidelines. Due to several factors including production limitations and expected throughput [^{68}Ga]Ga-PSMA was not a viable option for our clinical service and a decision was made to investigate [^{18}F]PSMA-1007. Initially this was sourced commercially, and an assessment of local production capability was performed by our Radiopharmacy Production Unit. Service setup was based on an extensive review of literature, international guidelines and experience from other departments across UK.

Results/Discussion: Between January 2021 and January 2022, 114 patients underwent [^{18}F]PSMA-1007 PET-CT scan. PET-CT imaging was performed on GE 710 Discovery and Siemens Vision 600 scanners with a low dose unenhanced CT, from mid-femur to eyes, 90 (± 10) min post-injection of [18F]PSMA-1007 with a recommended activity of 250 (±25) MBq. As part of patient preparation, during the uptake period oral hydration with 500 ml water was encouraged.

Review of patients scanned using commercially supplied [^{18}F]PSMA-1007 at regional MDT demonstrated good quality imaging and local production has also been successful providing adequate quantity of tracer for a high-volume service.

Conclusion: [^{18}F]PSMA-1007 is a viable option for Prostate Cancer imaging in a high-volume service with local production facilities.

92. Application of [^{68}Ga]PSMA PET-CT in Diagnosis and Management of Prostate Cancer Patients

Habibollah Dadgar
Nuclear Medicine and Molecular imaging, RAZAVI hospital, Mashhad, Islamic Republic of Iran

Purpose: PSMA PET-CT imaging has recently been introduced as a novel procedure in managing PC. The aim of this study was to evaluate the efficacy of [^{68}Ga] PSMA PET-CT in managing PC patients and to compare the detection rate of PET-CT and bone scans (BSs) in detecting bone metastasis.

Results: We evaluated 415 patients aged 41-99 (68.25 ± 9.59). Of these patients, 344 (82.9 %) had at least one localized lesion. The detection rates were 48.3 %, 52.6 %, 74.4 %, 79.6 %, and 93.9 % for a PSA value of < 0.2 ng/ml, ≥ 0.2-< 0.5 ng/ml, ≥ 0.5-< 1 ng/ml, ≥ 1-< 2 ng/ml, and ≥ 2 ng/ml, respectively ($p < 0.05$). The detection rates increased significantly with higher GSs; the rates were 68.3 % (28/41), 74.5 % (73/98), 93.9 % (46/49), and 91 % (61/67) for a GS of < 7, 7, 8, and > 8, respectively ($p < 0.05$). An ideal cut-off value of > 1.16 ng/ml was obtained for PSA value, which equates to specificity of 75 % and sensitivity of 77 %. In comparing BSs and PET/CT, a region-based analysis showed the superiority of PET-CT over BSs for all regions expect the skull ($p < 0.05$). PET-CT detected 258 suspicious regions, 255 of which were metastatic and three of which were equivocal. BSs detected only 223 suspicious regions, 203 of which were metastatic and 20 of which were equivocal.

Conclusions: [^{68}Ga]PSMA PET-CT showed a high detection rate for lesions in PC patients. PSA level, GS, and a PSA doubling time of less than 6 months were shown to be the affective variables.

93. Comparison of [^{68}Ga]-PSMA and [^{18}F]FDG PET-CT for evaluation of advanced Hepatocellular Carcinoma (HCC)

Shamim Ahmed Shamim, Naresh Kumar, Geetanjali Arora, Shivanand Gamanagatti, Dr. Shalimar CS Bal,
All India Institute of Medical Sciences, New Delhi, India

Purpose of study: PSMA receptors are located in the endothelium and have proven their correlation with VEGF expression in highly vascular tumours. Few case reports have documented radiotracer uptake in HCC. [^{18}F]FDG PET-CT is useful for staging, restaging & response evaluation after therapy for HCC. We planned the present study to see the additional role of [^{68}Ga]-PSMA in HCC and compare it with [^{18}F]FDG PET-CT.

Methods used: Confirmed cases of HCC were prospectively included in the study. Images were acquired at 60- & 30-mins post-injection after injecting 10mCi of [^{18}F] FDG and 3-5mCi of [^{68}Ga]-PSMA, respectively. Images were analysed visually & quantitatively.

Results: 34 patients (30 male, 4 female) with mean age 53.91± 11.14 years. On [^{18}F]FDG PET/CT, 28 out of 34 patients were positive, single lesion seen in 17 patients while 11 patients had multifocal liver lesions. On [^{68}Ga]-PSMA scan, tracer uptake was seen in 32 of 34 patients with single lesion in 18 patients and multifocal lesions in remaining 14 patients. Of 17 patients with single lesion on FDG scan, 14 showed concordant single lesion on PSMA while 3 patients showed additional liver lesions. Of the 11 patients with multifocal lesions on FDG, 2 patients showed single lesion, 8 showed multifocal lesions and 1 patient showed no tracer uptake in PSMA PET/CT.

Conclusion: [^{68}Ga]-PSMA may be an additional modality for diagnostic workup of HCC with an added advantage of being used as theragnostic marker in patients with limited therapeutic options, expressing PSMA.

94. Initial Experience with [^{99m}Tc]Tc-MIP-1404 SPECT-CT Imaging of Prostate Cancer Patients

Sergejs Magers, Nitasha Singh, Maryam Jessop, Helen Cripps, Eleonora Manca, Ashok Nikapota, Angus Robinson, Sabina Dizdarevic
University Hospitals Sussex NHS Foundation Trust, Brighton, United Kingdom

Aim: [^{99m}Tc]Tc-MIP-1404, a radiopharmaceutical that detects prostate-specific membrane antigen (PSMA) expressing cells, has recently become available in the United Kingdom. Outcomes of imaging the first cohort of patients in the United Kingdom are shared to demonstrate its clinical utility.

Method: Case series of nine patients referred to our department for [^{99m}Tc]Tc-MIP-1404 SPECT-CT following conventional imaging.

Results: Seven patients with biopsy-confirmed prostate cancer, one with radiologically & biochemically diagnosed prostate cancer and one with high-grade prostatic intraepithelial neoplasia (PIN) underwent [^{99m}Tc]

Tc-MIP-1404 SPECT-CT from September to December 2021. Median serum PSA level was 38.1 µg/l (range 2.97-634 µg/l) at the time of referral. In two cases metastatic disease was excluded, whilst in two other cases osseous metastases were corroborated and visceral metastases excluded enabling ^{223}Ra-dichloride therapy consideration. Local prostate cancer recurrence was demonstrated in two cases. Two cases of PSMA-positive inguinal lymphadenopathy required further investigation – one was positive for prostate cancer on core biopsy, the second remains indeterminate. [^{99m}Tc]Tc-MIP-1404 SPECT-CT was particularly helpful in differentiating presumed metastatic lesions in a case of metachronous prostate cancer and neuroendocrine tumour. Furthermore, absence of metastatic disease was confirmed in the patient with high-grade PIN.

Conclusion: [^{99m}Tc]Tc-MIP-1404 SPECT-CT provides valuable diagnostic information enabling appropriate further clinical management of prostate cancer patients. Its full impact on patient care, however, will be further determined based on continued research based on evolving evidence.

95. Insights from the first [^{18}F]PSMA-1007 PET-CT imaging service in Scotland – detection rate and factors predicting disease detection

Anna Coad, Hesham Dyab, Louise Hartley, Dave Colville
West of Scotland PET centre, Glasgow, United Kingdom

Background & Method: [^{18}F]PSMA-1007 PET-CT is a highly promising new method of imaging prostate cancer, out-performing conventional prostate cancer imaging methods for detection rate after biochemical recurrence. The West of Scotland PET Centre is the first PET centre in Scotland to offer this technique, performing [^{18}F] PSMA-1007 PET-CT since January 2021. The first 99 patients imaged with [18F]PSMA-1007 PET-CT were reviewed and outcomes compared with those in the literature.

Results: Of 99 patients, 96 were referred for biochemical recurrence (BCR) following radical prostatectomy or radiotherapy, and 3 for initial evaluation prior to treatment. In the biochemical recurrence group [^{18}F]PSMA-1007 PET-CT was positive in 67% (n = 64). Positive results were subdivided into local recurrence (n = 36, 56%), pelvic nodes (n = 36, 56%), extra-pelvic nodes (n = 8, 13%) and extra-nodal metastases (n = 8, 13%).

Median PSA for the BCR group was 0.4 (range 0.2-20.3). Detection rate for patients with PSA levels ≥0.5 ng/ml was significantly higher than for those with PSA level <0.5 ng/ml (91% vs 45%, p<0.0001). The value of the pre-operative Gleason score in predicting positivity was less stark. A moderately elevated detection rate was seen in patients with Gleason scores of 8 or 9, compared to those with Gleason scores of 6 or 7 (70% vs 64%, p>0.05).

Conclusion: In our patient cohort, [^{18}F]PSMA-1007 PET-CT yielded a detection rate of 67% in patients with biochemical recurrence of prostate cancer. PSA levels were a strong predictor of positive detection rate, as reflected in the published literature.

96. Insights from the first [^{18}F]PSMA-1007 PET-CT imaging service in Scotland – incidental PSMA-avid lesions

Hesham Dyab, Anna Coad, Louise Hartley, Dave Colville
West of Scotland PET centre, Glasgow, United Kingdom

The emergence of [^{18}F]PSMA-1007 PET-CT has changed imaging of prostate cancer, allowing localisation of disease which would previously have been undetectable on traditional imaging modalities. A new tracer, however, presents new pitfalls. PSMA uptake is seen in other tumours, both benign and malignant, as well as in relation to neovascularisation and inflammation. The importance of correctly interpreting the nature of these lesions is self-evident and there is a growing body of case reports in the literature for reference. In this case series, taken from the first 99 patients to undergo [^{18}F]PSMA-1007 PET-CT imaging in Scotland, we present cases of four such PSMA-avid lesions which are not related to prostate cancer - multinodular thyroid goitre, vestibular schwannoma, splenic and hepatic haemangiomata and a presumed pancreatic neuroendocrine tumour.

97. [^{18}F]FDG PET-CT in Assessment of Active Cardiac Sarcoid: Review of Departmental Practice

Pardeep Vasudev, Abbas Hiba, Charis Lois, Sara Moeen, Marko Berovic, Sachin Kamat, Mohamed Halim, Nicola Mulholland
King's College Hospital NHS Foundation Trust, London, United Kingdom

Aim: Review our PET-CT cardiac sarcoidosis service in relation to referral indications, outcomes and adequacy of dietary suppression.

Methodology: Retrospective review of whole body [^{18}F] FDG PET-CT scans including cardiac acquisition with an indication involving sarcoidosis performed between January 2019 and December 2021(36 months). Demographics, previous sarcoid or cardiac history, CMR result, diabetes status and outcome were recorded. Analysis was performed using SPSS software.

Results: Total number N= 98 studies were reviewed. Median patient age was 56.5 years (range 26-83), 80% were males and 14.3% were diabetics (n=14). In the referral indication, 51 mentioned a history of sarcoid, 30 had previous cardiac arrhythmias and 36 had late Gadolinium enhancement on CMR.

84/98 (85.7%) had adequate dietary suppression, including 12/14 diabetics. Of the remaining 84 studies, 65.4% (n=55) were considered negative for active sarcoidosis, 11.9% (n=10) had both cardiac and extra-cardiac disease, 17.8% (n=15) had extra-cardiac sarcoid only and 4 were suspicious for possible isolated cardiac involvement.

On further review of clinical records of these four cases, one patient had subsequently confirmed arrythmogenic left ventricular cardiomyopathy (ALVC), one had autoimmune myocarditis, one had negative CMR and was considered not to have sarcoidosis on clinical basis and one had likely inadequate cardiac suppression with a subsequent negative study after four months without treatment.

Conclusion: The majority of cases had good cardiac glucose metabolism suppression including the relatively small diabetic cohort. Interestingly, despite varied cardiac referral indications, no confirmed cases of isolated cardiac sarcoid were identified.

98. Role of [^{18}F]FDG PET scan in evaluating the extent of viability using quantitative method in addition to routine visual method, and its impact on management and clinical outcome

Shreya Dang, Melvika Pereira, Natasha Singh, Divya Shivdasani, Debdip Roy, Rachita Rungta
P.D. Hinduja National Hospital and Medical Research Centre, Mumbai, India

Purpose: Coronary artery disease(CAD) is the leading cause of left ventricular dysfunction(LVD). Infarcted viable myocardium can restore its function-contractility post-revascularisation. Hence, we assess role of [^{18}F]FDG PET scan in evaluating viability extent using visual and quantitative method, its impact on management and clinical outcome.

Materials and Methods: Retrospective study(2011-2021) included 51 LVD patients,ejection fraction(EF)<=35%, with moderate-large perfusion defects(>10% of total LV volume). PET findings categorised them as predominantly viable, and predominantly scarred myocardium(quantitative-threshold 50%). Patients underwent revascularisation or medical management, and outcome was followed-up based on EF change>=5% post-intervention(>=6months) and cardiac event-free survival.

Results: Of 51 patients, 26(50.9%) had predominantly viable myocardium. 18/26(69.7%) underwent revascularisation and most(94.4%) showed improved/stable EF. Of 8/26(30.7%) kept on medical management, 7(87.5%) had EF fall/cardiac events. 25/51 patients(49.1%) had predominantly scarred myocardium, where all 6 patients(24%) on medical management showed improved/stable EF. 19/25(76%) patients' post-revascularisation showed improved EF in 11(57.9%) which can be attributed to presence of additional viable areas(at least 7% of total LV volume or viability up to 30% of affected myocardium) or ischemic areas. 8/19 patients(42.1%) showed fall in EF/cardiac events post-revascularisation.

Conclusion: [^{18}F]FDG PET scan is pivotal in determining myocardial viability in LVD with moderate-large perfusion defect. Extent of PET-determined viable myocardium is a good prognostic factor in determining clinical outcome post-intervention in terms of LVEF improvement/cardiac events. Predominantly scarred myocardium can benefit post-revascularisation if additional viable/ischemic areas are present.

Posters

P01. Implementation of Whole-Body Bone SPECT-CT imaging

Rita Cabral[a], Glenn Woolley[a,b], Graham Wright[a], Gerard Avery[a]
[a]*Hull University Teaching Hospitals, Hull, United Kingdom.*
[b]*University of Hull, Hull, United Kingdom*

P02. A rare association of two different sclerosing skeletal diseases: DISH and SAPHO syndrome

Jonathan Adlam[a], Alexis Corrigan[a], Ramya Balachandar[b]
[a]*Maidstone and Tunbridge Wells NHS Trust, Maidstone, United Kingdom.*
[b]*Medway Maritime Hospital, Medway, United Kingdom*

P03. Use of qualitative FDG PET reporting criteria in suspected polymyalgia rheumatica – an audit of clinical practice

Sundus Mohamed, Krishanth Ganesan, Scarsbrook Andrew, Sarah Mackie
Leeds Teaching hospital, Leeds, United Kingdom

P04. ^{18}F-Choline PET-CT performance in primary hyperparathyroidism

Alex McClement, Tamir Ali, Andrew McQueen, Peter Truran, John Robinson, George Petrides

Newcastle upon Tyne Hospitals NHS Foundation Trust, Newcastle upon Tyne, United Kingdom

P05. Cushing's Syndrome secondary to an ectopic ACTH-producing lesion in the maxillary sinus – a case report

Marianne Kimura, Mathuri Sakthithasan, Julian Kabala, Randeep Kulshrestha
Bristol and Weston University Hospitals NHS Trust, Bristol, United Kingdom

P06. Can HIDA scans with similar findings have completely different interpretations?

Mohamed El-Sayed, Poonam Parekh, Michael Wilson, James Cullis, Simon Hughes
University Hospitals Birmingham NHS Foundation Trust, Birmingham, United Kingdom

P07. Case studies: incidental findings of a bowel perforation and gastric outlet obstruction on two separate [^{18}F]FDG PET-CT studies

Suzannah Patel[a], Kelly Kilby[a], Bruno Ferreira[a], Chun Lap Pang[a,b]
[a]*Paul Strickland Scanner Centre, Northwood, United Kingdom.*
[b]*Northwick Park Hospital, Harrow, United Kingdom*

P08. Role of ^{18}F- FDG PET-CT scan in evaluation of tuberculosis - pulmonary and unusual extrapulmonary involvement: A pulmonary case series

Rachita Rungta, Melvika Pereira, Natasha Singh, Divya Shivadasani, Debdip Roy, Shreya Dang
P.D.Hinduja National Hospital, Mumbai, India

P09. Improving skills of interpretation of ^{67}Gallium skull base otitis externa/osteomyelitis by correlating with prior high-resolution CT and MR IAMs and 3D anatomical slices

Randeep Kulshrestha, Nirav Kaneria, Ayah Nawwar, Julian Kabala
University Hospitals Bristol & Weston NHS Foundation Trust, Bristol, United Kingdom

P10. Assessment of Inter-operator Variability for Infection Imaging of Patients Following Knee Joint Replacement

James McDermott[a], Sarah Williams[a,b,c], Rebecca Gillen[a,b,d], Carolyn Paterson[a,b], Gillian Ainslie-McLaren[a,b], Alison Bolster[a,b,c]
[a]*Department of Clinical Physics and Bioengineering, NHS Greater Glasgow and Clyde, Glasgow, United Kingdom.*
[b]*Department of Nuclear Medicine, North-East Sector, NHS Greater Glasgow and Clyde, Glasgow, United Kingdom.*
[c]*College of Medical, Veterinary and Life Sciences, University of Glasgow, Glasgow, United Kingdom.*
[d]*Institute of Nuclear Medicine, University College London, London, United Kingdom*

P11. Cross-centre collaboration during the coronavirus pandemic: nuclear medicine investigation of hepatopulmonary syndrome

Afsara A Ahmmed[a], Randeep Kulshrestha[b]
[a]*North West School of Radiology, Manchester, United Kingdom.*
[b]*University Hospitals Bristol and Weston NHS Foundation Trust, Bristol, United Kingdom*

P12. The value of [^{18}F]FDG PET-CT in early diagnosis of autoimmune anti-LGI1 limbic encephalitis

Isabelle Farlam, Sergejs Magers, Nitasha Singh, Eleonora Manca, James Hunter, Sabina Dizdarevic
University Hospitals Sussex NHS Foundation Trust, Brighton, United Kingdom

P13. Multi-modality molecular imaging can aid the probable clinical diagnosis of chronic traumatic encephalopathy (CTE)

Benjamin Becarevic[a,b], Sergejs Magers[b], Nitasha Singh[b], Nicolas Eftychiou[b], Maryam Jessop[b], James Hunter[c], Malgorzata Raczek[d]
[a]*Brighton College, Brighton, United Kingdom.*
[b]*University Hospital Sussex NHS Foundation Trust, Brighton, United Kingdom.*
[c]*Clinical Imaging Sciences Centre Brighton and Sussex Medical School, Brighton, United Kingdom.*
[d]*Centre for Dementia Studies Clinical Imaging Sciences Centre Brighton Sussex Medical School, Brighton, United Kingdom*

P14. [^{123}I]FP-CIT referral patterns for Movement Disorder or Dementia with Lewy Bodies with reference to the COVID pandemic

Alice Nicol, Paul Smith, David Brown, Ravi Jampana
Queen Elizabeth University Hospital, Glasgow, United Kingdom

P15. Usefulness of dynamic brain PET image acquisition in pre-surgical epilepsy work up

Mary-Frances Dempsey, Ana Matos, Sandy Small, Sai Han, Natasha Fullerton, Alice Nicol
NHSGGC, Glasgow, United Kingdom

P16. "Audit of local departmental practice for DaTSCAN against guidelines: How consistent are we at performing DaTSCAN?"

Asifa Javed, Alp Notghi, Bill Thompson, Joseph O'Brien, Gregory James
Sandwell and West Birmingham NHS Trust, Birmingham, United Kingdom

P17. Evaluation of Appropriate Use Criteria for bone scintigraphy in breast cancer patients

Amir Zarei, Alexander Lory, Ahmed Osman, Sriram Vaidyanathan, Fahmid Chowdhury, Andrew Scarsbrook, Chirag Patel
Leeds Teaching Hospitals NHS Trust, Leeds, United Kingdom

P18. The value of [^{68}Ga]Ga-PSMA PET-CT in patients with biochemical recurrence of prostate cancer

Ivan Rogic, Anja Tea Golubic, Margareta Dobrenic, Marijan Zuvic, Tea Smitran, Drazen Huic
Department of Nuclear Medicine and Radiation Protection, University Hospital Centre Zagreb, School of Medicine, Zagreb, Croatia

P19. Accuracy and sensitivity of ^{18}F-PSMA PET-CT versus [^{11}C]choline PET-CT in the evaluation of prostate cancer patients

Mathuri Sakthithasan, Matt Spurr, Marrianne Kimura, Randeep Kulshrestha, Julian Kabala, Amarnath Challapalli
Bristol Royal Infirmary, Bristol, United Kingdom.

P20. Equivocal Radiotracer Uptake on ^{18}F-PSMA-1007 PET-CT in Patients with Prostate Cancer

Mathuri Sakthithasan, Mathew Spurr, Marrianne Kimura, Randeep Kulshresthra, Julian Kabala, Amarnath Challapalli
Bristol Royal Infirmary, Bristol, United Kingdom.

P21. Detection rates at different PSA levels of ^{18}F-PSMA PET-CT in the evaluation of prostate cancer patients with suspected recurrence

Mathuri Sakthithasan, Marrianne Kimura, Matthew Spurr, Randeep Kulshrestha, Amarnath Challapalli
Bristol Royal Infirmary, Bristol, United Kingdom.

P22. Great Expectations - comparing our clinical experience of ^{18}F-PSMA PET-CT comparing with previously published performance

Alvin Gardner[a], Amarjot Chander[b], Prakash Manoharan[b], Peter Julyan[b], Thomas Westwood[b]
[a]*University of Manchester, Manchester, United Kingdom.*
[b]*The Christie NHS Foundation Trust, Manchester, United Kingdom*

P23. Pictorial review of incidental prostate findings on routine [^{18}F]FDG PET-CT

Meedya Sharifpour, Anver Kamil
University Hospitals of Leicester, Leicester, United Kingdom

P24. Should the lower limbs be routinely included in [^{18}F] FDG PET-CT scans of patients with malignant melanoma?

Sivasankari Babu, Amarjot Chander, Prakash Manoharan, Peter Julyan, Thomas Westwood
The Christie NHS Foundation Trust, Manchester, United Kingdom

P25. Scoring Systems in FDG PET-CT Scan Interpretation

Maha AlRasheedi[a], Sai Han[b]
[a]*Institute of Cancer Sciences, University of Glasgow, West of Scotland PET Centre, Gartnavel General Hospital, Glasgow, Glasgow, United Kingdom.*
[b]*West of Scotland PET Centre, Gartnavel General Hospital, Glasgow, Glasgow, United Kingdom*

P26. A comparative evaluation of mediastinal nodal SUVmax and SUV ratios from ^{18}F-FDG PET-CT to predict nodal metastases in non-small-cell lung cancer (NSCLC)

Maha AlRasheedi[a], Sai Han[b], Matt Neilson[c], Fraser Hendry[b], Ahmed Alkarn[d], John D Maclay[d], Hing Y. Leung[e]
[a]*Institute of Cancer Sciences, University of Glasgow, West of Scotland PET Centre, Gartnavel General Hospital, Glasgow, Glasgow, United Kingdom.*
[b]*West of Scotland PET Centre, Gartnavel General Hospital, Glasgow, Glasgow, United Kingdom.*

[c]*Cancer Research UK Beatson Institute, Glasgow, Glasgow, United Kingdom.*
[d]*Respiratory Medicine, Glasgow Royal Infirmary, Glasgow, Glasgow, United Kingdom.*
[e]*Institute of Cancer Sciences, Cancer Research UK Beatson Institute, Glasgow, Glasgow, United Kingdom*

P27. Deviation of Metastasis Due to Hydropneumothorax Mimicking a New Lesion on PET-CT

Farzana Ali[a], Jan-Henning Schierz[b]
[a]*Stony Brook University, Stony Brook, NY, USA.*
[b]*Municipal Hospital and Academic Teaching Hospital of the Technical University Dresden, Dresden, Germany*

P28. Does the Delay Between Radionuclide Lymphoscintigraphy and Sentinel Node Biopsy Influence Outcome in Patients With Breast Carcinoma?

Luciana Calovi Motschenbacher, Brent Drake, Thomas Grüning
University Hospitals Plymouth NHS Trust, Plymouth, United Kingdom

P29. Streamlined Imaging Pathway In Prostate Cancer Restaging; Using The CT in SPECT-CT

Lucia Chen, Hassan Ahmed, Peter Ostler, Barnaby Barrass, Kai Low
Bedfordshire Hospitals NHS Foundation Trust, Luton, United Kingdom

P30. Pathological uptake of [^{111}In]Octreotide in Somatostatin Receptor Scintigraphy - can we safely reduce the field of view?

Charlotte Thompson, Stewart Redman, David Little
Royal United Hospitals, Bath, Bath, United Kingdom

P31. Octreotide avid lymph nodes – an important false positive in an era of COVID-19 vaccination

Amanda Isherwood, Ged Avery
Hull Royal Infirmary, Hull, United Kingdom

P32. Investigation of adrenal uptake on [^{99m}Tc]EDDA/HYNIC-TOC (Tektrotyd) SPECT-CT imaging

Caitlin Reilly, Alice Nicol, Jen Dennis, Ian McLaughlin, John Morrison
NHS Greater Glasgow & Clyde, Glasgow, United Kingdom

P33. Paediatric [^{123}I]I-mIBG - back to basics

Faraz Arfeen, Sabrina Alam, Banu Sathya Murthi, Rakesh Sajjan
Manchester University NHS Foundation Trust, Manchester, United Kingdom

P34. Review of Local Imaging Protocol Results for Sentinel Lymph Node Biopsy (SLNB) For Staging Oral Squamous Cell Carcinoma

Jen Dennis, Christopher Laurins, Alice Nicol
Department of Nuclear Medicine and DCPB Queen Elizabeth University Hospital, Glasgow, United Kingdom

P35. The accuracy of clinical assessment and Kaposi-Stemmer sign in the diagnosis of lymphoedema compared to lymphoscintigraphy

Amir Zarei, Reshma Koshy, Chirag Patel, Fahmid Chowdhury, Andrew Scarsbrook, Sriram Vaidyanathan
Leeds Teaching Hospitals NHS Trust, Leeds, United Kingdom

P36. A Case of Unusually Large Kidneys

Sergejs Magers, Nitasha Singh, Sabina Dizdarevic
University Hospitals Sussex NHS Foundation Trust, Brighton, United Kingdom

P37. Planar and SPECT [^{99}mTc]Tc-DMSA in children at a paediatric tertiary centre

Tricia Yeoh, Giulia Magro, Katharine Orr
Royal Hospital for Children, Glasgow, United Kingdom

P38. PET-CT Assessment for Large Vessel Vasculitis: A Single Centre Experience and Pictorial Review

Ruth Maybin[a], Euan Carter[a], Shona Olson[a], Dana Kidder[b]
[a]*NHS Grampian, Aberdeen, United Kingdom.*
[b]*University of Aberdeen, Aberdeen, United Kingdom*

P39. The case of the missing [^{177}Lu]Lu-PSMA-617. When you get that sinking feeling…

Anne-Marie Stapleton, James Scuffham, Vineet Prakash
Royal Surrey NHS Foundation Trust, Guildford, United Kingdom

P40. Single time point dosimetry following [^{177}Lu] Lu-PSMA using xSPECT Quant

Sofia Michopoulou[a], Timothy Melhuish[a], Gemma Lewis[a], Anna Chilcott[a], Francis Sundram[b], Zia Saad[b], Liane Armstrong[b], Nadine Duffin[b], Julian Williams[b], Matthew Guy[a]
[a]*Imaging Physics, University Hospital Southampton NHS Foundation Trust, Southampton, United Kingdom.*
[b]*Nuclear Medicine, University Hospital Southampton NHS Foundation Trust, Southampton, United Kingdom*

P41. Challenging radioiodine therapy of a patient with significant learning disability: A case study

Richard Fernandez, Peter Croasdale, Kerry Harwood, David Gallacher, Amy Eccles
Guy's & St Thomas' NHS Foundation Trust, London, United Kingdom

P42. Using quantification of bone scans and assessment of blood markers to identify prognostic and response markers in radium therapy

James Gray, James Scuffham, Ralf Clauss, Manu Shastry, Vineet Prakash
Royal Surrey NHS Foundation Trust, Guildford, United Kingdom

P43. Experiences as the First UK Centre to Provide ^{166}Ho Microsphere Treatment

Christopher Oldfield[a], Nat Gunson[a], Ben Shaw[a], Michael Gornall[a], Jill Tipping[a], Steve Jeans[a], Pippa Lane[b]
[a]*The Christie, Manchester, United Kingdom.*
[b]*Terumo Corporation, Surrey, United Kingdom*

P44. Comparison of Local Patient Outcomes to the Phase III Clinical Trial, ALSYMPCA, for Patients with Metastatic Castration-Resistant Prostate Cancer being treated with Radium-223 [^{223}Ra] Therapy (Xifigo)

Kieran Hamilton, Andrew Bussey, Mark Richardson, Adam Baker
James Cook University Hospital, Middlesbrough, United Kingdom

P45. Referral Rates and Overall Survival of Patients Receiving ^{223}Ra Therapy for mCRCP at the Beatson West of Scotland Cancer Centre

Iain Kerr, Colin Brown, Gail Buchanan
Gartnavel General Hospital, Glasgow, United Kingdom

P46. Implications and management of radioactive waste containing ^{177}Lu/^{177m}Lu

Mariq Weatherley, Dr Matthew Aldridge
Maidstone and Tunbridge Wells NHS Trust, Maidstone, United Kingdom

P47. [^{226}Ra] Source Containment

Emma Doran[a], Sarah Williams[a,b,c], Rebecca Gillen[a,b,d], Alison Bolster[a,b,c]
[a]*Department of Clinical Physics and Bioengineering, Glasgow, United Kingdom.*
[b]*Department of Nuclear Medicine, Glasgow North East Sector, Glasgow, United Kingdom.*
[c]*College of Medical, Veterinary and Life Sciences, University of Glasgow, Glasgow, United Kingdom.*
[d]*Institute of Nuclear Medicine, University College London, London, United Kingdom*

P48. Is there a Role for Learning from Excellence as a Tool in Radiation Safety Learning?

Alice Nicol, Ross Williamson
NHS GGC, South & Clyde, Glasgow, United Kingdom

P49. Clinical Evaluation of Bayesian Penalized Likely Hood Reconstruction (GE Q.Clear) and OSEM Reconstruction Algorithms on Adrenal Assessment with [^{18}F]FDG-PETCT

Meedya Sharifpour, Anver Kamil
University Hospitals of Leicester, Leicester, United Kingdom

P50. Investigating the Effect of Step and Shoot Continuous Acquisition on SPECT Image Quality

Jasmine Davies[a,b], Gordon Ellul[a], Liviu Stanisor[a], Claire Hooker[a], John Dickson[b]
[a]*East Kent Hospitals University NHS Foundation Trust, Canterbury, United Kingdom.*
[b]*University College London, London, United Kingdom*

P51. Quantitative imaging following [^{177}Lu]Lu-DOTA-TATE therapy using Siemens xSPECT Broad Quant

Jessica Johnson, Kathryn Adamson
Guy's and St Thomas' Hospitals NHS Foundation Trust, London, United Kingdom

P52. Feasibility of Quantification of ^{177}Lu on a Cadmium Zinc Telluride Gamma Camera

Anna Chilcott[a,b], James Scuffham[a]
[a]*Royal Surrey NHS Foundation Trust, Guildford, United Kingdom.*
[b]*University Hospital Southampton NHS Foundation Trust, Southampton, United Kingdom*

P53. Characterisation of SPECT-CT system for Dead-Time in post-therapy imaging of ^{177}Lu

Lara Bonney[a], Daniel McGowan[a,b], Lawrence Hutton[a], William Turner[a]
[a]*Oxford University Hospitals NHS Foundation Trust, Oxford, United Kingdom.*
[b]*University of Oxford, Oxford, United Kingdom*

P54. To optimise CT image quality for larger patients in PET-CT Imaging

Sorcha Curry, Manil Subesinghe, John Joemon, Jane MacKewn
King's College London, London, United Kingdom

P55. Initial Experience using the HaNNA Mannikin phantom – A training tool for gamma probe use in Sentinel Lymph Node Biopsy Procedures

James Hubber, Ruby Callister, Anton Paramithas
St George's University Hospitals NHS Foundation Trust, London, United Kingdom

P56. Performance Testing of the GE StarGuide CZT SPECT-CT System

Catherine Humphreys, Christine Turner, Cate Gascoigne, Katherine-Ann Wilson, Rachel Bidder, Andy Irwin
Swansea Bay University Health Board, Swansea, United Kingdom

P57. Anatomy specific CT DRLs for SPECT-CT

Tom Sanderson, Robert Harding
Nottingham University Hospitals NHS Trust, Nottingham, United Kingdom

P58. Improving patient compliance in nuclear medicine procedures and reducing DNA (did not attend) rate: A single centre district hospital experience

Frederico Golebski[a,b], Bernadith Marimon[a,b], Mustafa Hassan[a], Stefan Voo[b,a,c]
[a]*Whittington Health NHS Trust, London, United Kingdom.*
[b]*Institute of Nuclear Medicine, University College London Hospitals NHS Foundation Trust, London, United Kingdom.*
[c]*Biomedical Research Centre, NIHR, UCLH, London, United Kingdom*

P59. The adaptation of our practice during the COVID-19 pandemic

Ieva Petrulyte, Armidita Jacob, Sofia Pereira, Joemon John, Giorgio Testanera
King's College London, London, United Kingdom

P60. Optimising workflow processes for GFR clinics for improved compliance with post-pandemic cancer targets

Mariq Weatherley, Dr Matthew Aldridge
Maidstone and Tunbridge Wells NHS Trust, Maidstone, United Kingdom

P61. Carer & Comforters Audit

Aimee Ellis, Liana Bates, Caitlin Reilly, Alice Nicol
Department of Nuclear Medicine & DCPB, Glasgow, United Kingdom

P62. Personal comparison of Dose Exposure before and during pregnancy in a PET-CT Department

Sulamita Aragao, Sofia Pereira, Sorcha Curry
King's College London, London, United Kingdom

P63. Radioactive Isotope Permeability of Routinely used PPE in Nuclear Medicine

Iain Kerr, Clare McKeown, Alastair Gemmel, Jill Davidson
NHS Greater Glasgow & Clyde, Glasgow, United Kingdom

P64. Experience of [^{177}Lu]Lu-DOTA-TATE therapy patient transfer to High Dependency Unit

Anita Kaur, Caitlin Reilly, Ross Williamson, Jonathan Dixon, Alice Nicol
Department of Nuclear Medicine, DCPB, NHS GGC, Glasgow, United Kingdom

P65. The role of the Radionuclide Nurse Case Manager

Liane Armstrong
University Hospital Southampton, Southampton, United Kingdom

P66. Myocardial perfusion imaging: a comparison of the incidence of subdiaphragmatic interference in MPS 2-day SPECT-CT and Rb-82 PET

Niamh Bickford, Joe Purden
Swansea University, Swansea, United Kingdom

P67. Reducing Scan Acquisition Time for ^{18}F-PSMA PET-CT

Andrea Dimarucut, Deborah Pencharz
The Royal Free Hospital, London, United Kingdom

P68. Assessing PET-CT image quality following change in diabetic fasting protocol

Mariana Pinto, William Murphy, Karen Mullin
Royal Belfast Hospitals, Belfast, United Kingdom

P69. Is 1 second per projection SPECT-CT sufficient as an adjunct for problem solving in planar bone scintigraphy? A case series utilising a new technique

Amanda Isherwood, Rita Cabral, Ged Avery
Castle Hill Hospital, Hull, United Kingdom

P70. Quality Control for Radioactivity Management using IsoStock

Martin Anslow, Lois Collins
East Kent Hospitals University Foundation Trust, Canterbury, United Kingdom

P71. Red Blood cell labelling with kit-produced [^{68}Ga]Ga(oxinate)$_3$ from [^{68}Ga]GaCl$_3$ generator eluate

Amaia Carrascal-Miniño[a], Francis Man[b], Rafael T. M. de Rosales[a]
[a]*Imaging Chemistry & Biology, King's College London, London, United Kingdom.*
[b]*Institute of Pharmaceutical Science, King's College London, London, United Kingdom*